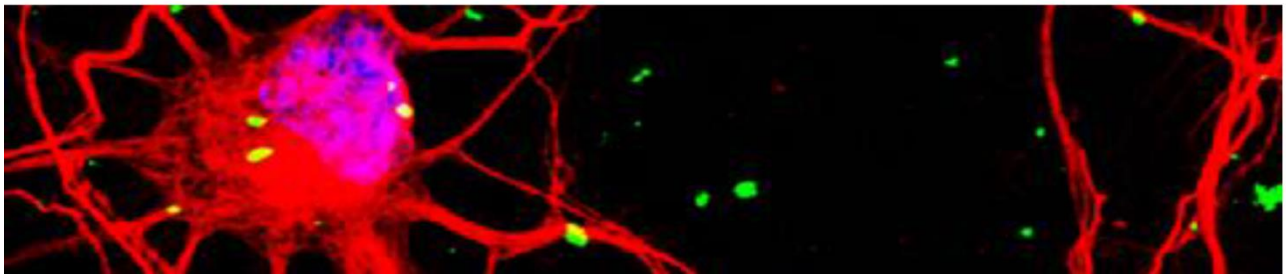

Corso di Dottorato in Neuroscienze

Curriculum Neuroscienze e Neurotecnologie

Ciclo XXXIV

Functional interaction between BDNF and Kidins220: a study in primary mouse astrocytes and in an adult conditional knock-out mouse model

Author

Albini Martina

Supervisors

Prof. Fabio Benfenati

Prof. Fabrizia Cesca

ISTITUTO ITALIANO DI TECNOLOGIA

UNIVERSITÀ DEGLI STUDI DI GENOVA

Index

1. Abstract

Neurotrophins are a family of growth factors known for their pleiotropic effects on neuronal survival, maturation and plasticity. Brain-derived neurotrophic factor (BDNF) is the most expressed in the brain. The activation of specific BDNF downstream pathways hinges on BDNF binding to its receptor TrkB. Kidins220 is a scaffold protein that interacts with neurotrophin receptors and is directly involved in the activation of neurotrophin signaling. It is also required for neuron differentiation, survival and plasticity. This protein has been linked to several diseases including psychiatric and neurodegenerative pathologies and for this reason, several KO animal models have been generated. So far none of them was viable after birth, making it impossible to investigate the role of this protein in postnatal/adult brain development.

Astrocytes are fundamental in maintaining nervous system homeostasis. They are capable of perceiving a wide variety of extracellular cues and transducing them via the activation of specific intracellular signaling pathways into responses that may be protective or disruptive toward neighboring neurons. Moreover, astrocytes are key regulators of neuronal circuit formation and synaptic transmission. Several aspects of astrocyte physiology are controlled by neurotrophins. However, the role of Kidins220 in astrocytes, as well as in the adult brain remains largely unknown. Thus, in this thesis we aimed to deeply understand the role of Kidins220 using both *in vivo* and *in vitro* models.

First we compared the signaling competence of embryonic and postnatal primary cortical astrocytes exposed to BDNF, and observed a shift from a kinase-based response in embryonic cells to a predominantly Ca^{2+}-based response in postnatal cultures. We demonstrated that Kidins220 ablation is accompanied by a decreased expression of both BDNF receptor TrkB isoforms. We also described the role of Kidins220 in BDNF-induced signaling in astrocytes, showing that it contributes to both kinase and Ca^{2+}-activated pathways. To evaluate the effect of Kidins220 ablation in the adult brain we used a floxed line that expresses only the full-length isoform, which we crossed with mice expressing Cre under the CamKII promoter, leading to a conditional knockout (cKO) line where Kidins220 is absent only in the excitatory neurons of the forebrain, starting at the second postnatal week. In this animal model, we have observed altered dendritic arborization and spine number in the cortico-hippocampal regions. The deletion of Kidins220 also leads to

behavioral changes, such as reduced anxiety-like traits due to to alterations in TrkB-BDNF signaling.

Our data increase the knowledge of the complex role played by Kidins220 both in astrocytes and in adult brains, reveal a previously unidentified role of this protein in astrocytes, controlling the response to BDNF and to Ca^{2+} dynamics during development. Finally, our data confirm the fundamental role of Kidins220 in adult mice, where its ablation leads to both behavioral and biochemical impairments.

2. Introduction

2.1. Brain-Derived Neurotrophic Factor (BDNF)

Neurotrophins

The neurotrophins are a well-characterized family of trophic factors for neural cells. It is composed by nerve growth factor (NGF), brain-derived growth factor (BDNF), neurotrophin-3 (NT-3) and neurotrophin-4 (NT-4 or NT4/5).NGF was discovered and characterized in 1953 [1], followed by BDNF, discovered in 1982 as a trophic factor for sensory neurons [2]. Thanks to the similarity in the nucleotide sequence of NGF and BDNF [3], NT-3 and NT-4/5, other two members of the neurotrophin family, were subsequently discovered [4-7].

Physiologically, neurotrophins exist as non-covalently associated dimers of about 27 kDa. Each subunit is formed by two pairs of antiparallel β-strands stabilized by three disulphide bonds. All neurotrophins are synthetized as proneurotrophins, which can be stored in secretory vesicles where they can be cut by proteases producing the mature neurotrophins [8], or can be directly secreted and processed by proteases such as plasmin and matrix metalloproteinases in the extracellular environment [9].

a. BDNF expression and function

BDNF is the neurotrophin with the highest expression in the brain, where it plays a critical role in regulation of synaptic physiology. It was first described for its role in the survival of target cells, however we know that BDNF's main function is the regulation of synaptic plasticity memory, cognition and complex behaviors. BDNF deficits are linked to the development of many neurodegenerative and psychiatric diseases such as Alzheimer' disease, Huntington's disease and depression [10-13].

The main BDNF source are neurons. During development the *bdnf* gene is more expressed in the nervous system and its expression levels increase further in postnatal brain [14, 15]. The higher expression of BDNF mRNA and protein can be found in the cortex, hippocampus, septum, amygdala and hypothalamus in the central nervous system (CNS) and in the dorsal root ganglia (DRGs) in the peripheral nervous system (PNS).

Synaptic activity regulates BDNF synthesis, maturation and degradation. The BDNF mRNA can be targeted to dendrites in an activity dependent manner [16] *Bdnf* mRNA has been found also in other tissues such heart and lung and lower levels in the thymus, liver,

spleen, and muscle [17]. The 3'-UTR, instead, has been shown to confer activity-regulated stability in cortical neurons using a luciferase reporter gene, and elements mediating this effect have been mapped in the 3'-UTR [18].

As all the other neurotrophins, BDNF is initially synthetized as a pro-neurotrophin and can be secreted by vesicles in both a constitutive and regulated way. The secretion of mature BDNF is induced by neuron depolarization and high frequency stimulation (HFS), which induces long-term potentiation (LTP). Interestingly, also the secretion of pro-BDNF is regulated in hippocampal neurons.

A polymorphism in the human *bdnf* gene, on the Val66Met, localized in the prodomain, has been described and studied in order to increase the knowledge about BNDF physiology, in particular the mechanisms leading BDNF to the regulated secretory pathway. Interestingly, this polymorphism induces a strong decrease of the amount of BDNF secreted in response to cell depolarization [19].

b. BDNF receptors

Once released into the extracellular space and bound to specific receptors, proneurotrophins and their corresponding mature forms activate specific signaling pathways. The main classes of receptors are tropomyosin-related kinase (Trk) and p75 neurotrophin receptor ($p75^{NTR}$) [20] (**Figure 1**). Trk receptors belong to a class of receptors with tyrosine kinase activity; they primarily mediate neuronal growth and survival signals. Each neurotrophin demonstrates binding specificity for a different class of receptors: TrkA for NGF, TrkB for BDNF and NT-4 and TrkC for NT-3. Neurotrophins play a wide range of different biological functions according to the set of receptors present on the target cell. The actions performed by Trks are multiple as, for example, the regulation of synaptic function, cell proliferation and survival, dendritic and axonal growth, the regulation of cell channels and retrograde signaling [21, 22]. The extracellular structure of Trk receptors differs from the other tyrosine kinase receptors; they have a great homology in the intracellular regions whereas the extracellular portion is quite variable. The latter is the one that determines the specificity of binding with the ligand [23]. Adjacent to the signal sequence that is cut in the maturation process, there are three leucine-rich domains, consisting of 24 residues (LRR1-3) flanked by two cysteine clusters (C1 and C2). Alongside these structures there are two immunoglobulin-like domains (Ig1 and Ig2), which are followed by a single transmembrane

domain and a cytoplasmic domain containing the tyrosine kinase domain [24]. Three windings of the β-hairpins demonstrate very low similarity in the neurotrophin family. In fact, they represent three of the five variable regions in neurotrophins and play a key role in the neurotrophin-receptor interface.

After the binding with the specific neurotrophin, the subunits of the receptors form dimers triggering the catalytic activity of their intracellular tyrosine kinase domains. In the autoregulatory loop of these domains there are three important tyrosine (Tyr) residues. Their phosphorylation increases the activation of the kinase activity that starts the downstream signaling cascades inside the cell. For example, when Tyr (515) in the intracellular domain is phosphorylated, it recruits Shc, fibroblast growth factor receptor substrate 2 (Frs2), and other adaptors, which induce the activation of Ras and PI3 kinase, while phosphorylation of Tyr (816) recruits PLCγ. The tyrosine kinase domain is surrounded by other Tyr residues, which are also sites of phosphorylation, and once phosphorylated they will act as docking sites for signaling proteins.

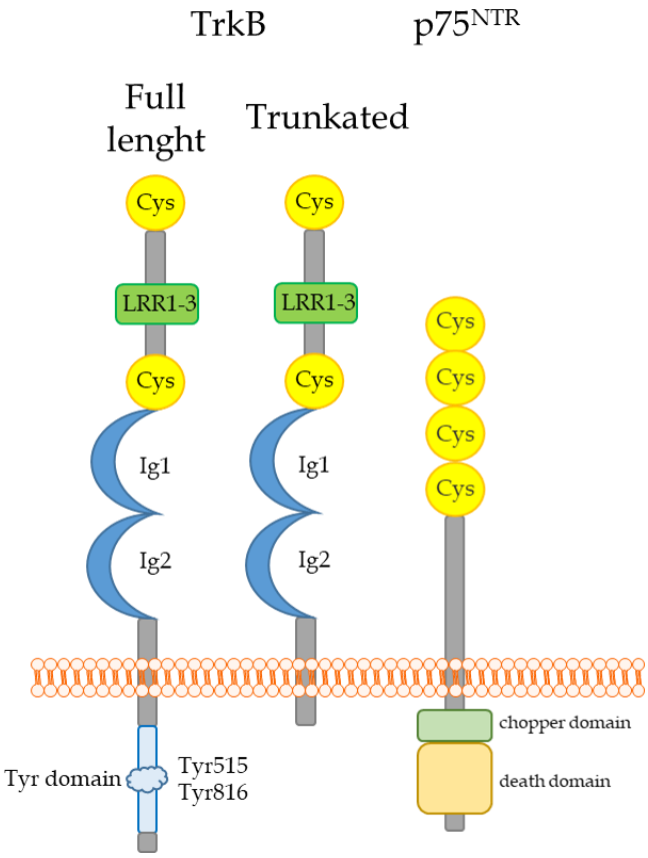

Figure 1 Schematic representation of Trks and p75^{NTR} receptors. Each neurotrophin binds a specific Trk receptor (NGF to TrkA, BDNF and NT-4 to TrkB, and NT-3 to TrkC). All the Trk receptors present a phosphorylation site in the intracellular domain. All four neurotrophins can also bind to p75^{NTR} that can form a complex with all three Trks.

The TrkB receptor is expressed both in CNS and PNS, but it has been found also in heart, ovary, and spleen. TrkB presents also another isoform that almost entirely lacks the intracellular portion, including the tyrosine kinase domain. This truncated isoform (TrkB-T) was initially considered as a dominant negative regulator because it can sequester free neurotrophins, but it now is accepted that TrkB-T has also other functions. In fact it has been observed that upon BDNF binding, TrkB-T induces the release of Ca^{2+} from intracellular stores in glial cells [25]. Moreover, knock-out (KO) mice for TrkB-T show decrease dendritic complexity, an impairment that has been associated with increased anxiety [26].

Once bound to the neurotrophin, the neo-formed receptor-ligand complexes are internalized [27-31] and are enzymatically active. Once formed, the complexes may be degraded, recycled or retrogradely transported along axons in structures called signaling endosomes, which contains also activated components of the PI3K, MAPK, and PLCγ pathways [29, 31, 32]. This because Trk signaling mediates several cell processes for which protein synthesis is necessary and the signaling molecules need to reach the cell nucleus to modulate the gene expression. It has been also reported that axons regulate spatially and temporally the introduction of new proteins thought the induction of axonal mRNA translation. Consequently, axons can mediate the mRNA transport with some ribonucleoproteins without protein synthesis [33]. The binding between the neurotrophins and their receptors can also induce this process.

Trk receptors binding affinity and specificity are modulated by the presence of another key receptor, the pan-neurotrophin receptor $p75^{NTR}$. It is a receptor common to all of the four neurotrophins; it acts as a coreceptor for multiple ligands and displays a wide range of distinct biological activities: it inhibits axonal growth of neurons, it induces the process of myelination of the axons of DRGs, it modulates synaptic plasticity, and it induces axonal retraction and activates the process of apoptosis [34]. In 1991 the formation of the TrkA/$p75^{NTR}$ receptor complex was observed for the first time [35] and in the following years it was further characterized [24, 36], highlighting that this interaction is mediated by the cysteine-rich domains present in the extracellular part of the receptor [37]; in this way $p75^{NTR}$ increases the receptors' affinity for mature neurotrophins, promoting cell survival [38, 39]. The intracellular domain of $p75^{NTR}$ is similar to tumor necrosis factor receptors (TNFRs) and Apo1 antigen [40-42]. These two families of receptors are known as inducers

of cell apoptosis. For this reason, the intracellular domain of p75^{NTR} was called "death domain" even if the receptor can promote both apoptosis and cell survival. This duality depends on the type of ligand (pro vs mature neurotrophins) as well as on the co-receptors that are co-expressed on cell membranes. Indeed, p75^{NTR} can interact with Trk receptors or it may have an opposite effect and induce cell death when associated with Sortilin [36, 43, 44].

c. BDNF signaling

Different signaling pathways are activated, leading to completely different fates, depending on the receptor involved. The binding of neurotrophins induces Trk dimerization and the consequent autophosphorylation on tyrosine residues present in the cytoplasmic tail. This modification allows the recruitment of the different components of signaling and the activation of the intracellular cascades, allowing the formation of binding sites for adapter proteins specific for the activation of different pathways.

Signaling pathways activated by Trks

The main signaling pathways activated by Trks are Ras-Raf-MAPK, PI3-kinase Akt and PLC-γ-Ca^{2+} **(Figure 2)**.

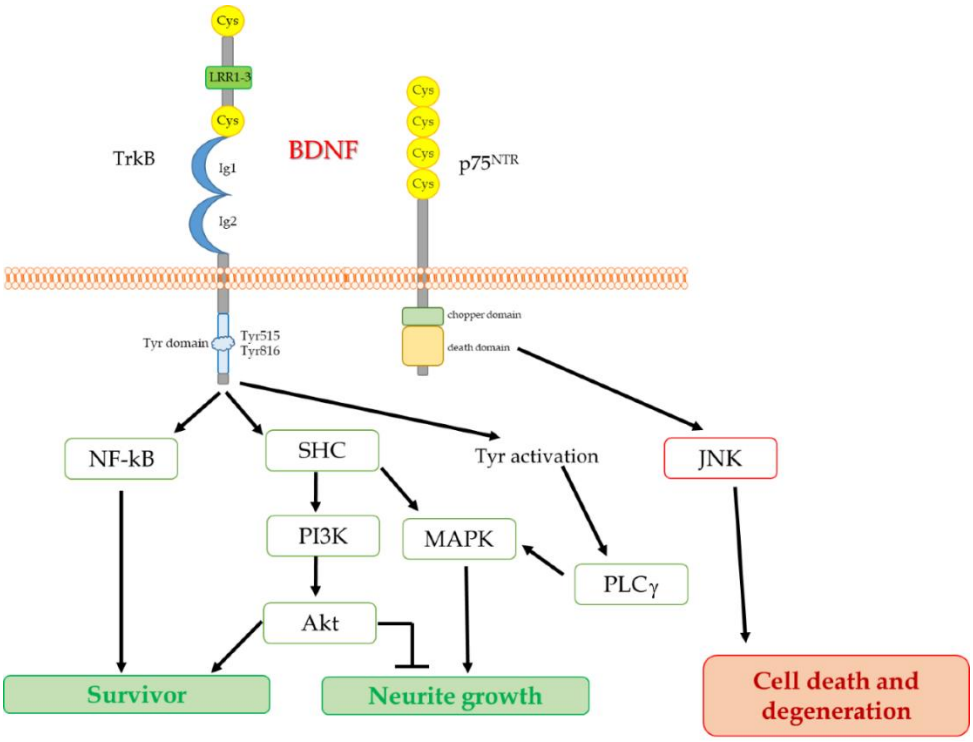

Figure 2 Schematic representation of neurotrophin receptors and their signaling upon pro and mature neurotrophin binding. Once secreted, mature neurotrophins can bind two different receptors, Trks and p75^{NTR}. Through them they promote neuronal survival and maturation. The neurotrophin precursors (proNT) can bind the p75^{NTR} and the sortilin receptors inducing pro apoptotic signaling. Modified from [45].

MAPKs (Mitogen Activated-Protein Kinases) are a protein family involved in signal transduction from the cell membrane to the nucleus that include ERK 1/2 (extracellular signal-regulated kinase, the first to be discovered), JNK (c-Jun N-terminal kinases), p38, ERK5 and ERK7. Many of the signaling cascades activated by neurotrophin binding to Trks lead to activation of Ras that will directly activate ERK1/2, which can activate the MAPK specific targets thought the phosphorylation of two specific residues. This phosphorylation induces only a transient activation of MAPK signaling, but it can be prolonged by recruiting some other proteins that act as adaptors.

Another important protein activated upon Trk phosphorylation in a Ras dependent way is Akt, also known as protein kinase B (PKB). It is involved in many cellular processes, such as activation of transcription, cell proliferation and migration, glucose metabolism and apoptosis. Akt is a downstream signaling protein of PI3-kinase, which is responsible for production of P3-phosphorylated phosphoinositides. The production of P3-phosphorylated phosphoinositides on the cell membrane allows the translocation of Akt from the cytosol to the membrane where it undergoes a multistep activation. Once activated, Akt translocates to the nucleus were it phosphorylates its substrates. Among all its substrates, Akt can act on proteins involved in the apoptotic process. One of those proteins is Bad, a pro-apoptotic protein whose phosphorylation is requested in order inhibit its action. Another substrate is IκB, which is a NFκB inhibitor. Through Akt, I_KB can be degraded and in this way, NFκB it is free to translocate in the nucleus where it can promote transcription of genes involved in neuronal survival. Interestingly, both Trk receptors and $p75^{NTR}$ promote NFκB activation. PI3-kinase-Akt signaling regulates also the cytoskeleton throughout the recruitment and activation of small G-proteins. The localized activation of PI3-kinase drives cell mobility. This pathway also regulates growth cone steering in response to neurotrophin gradients, axon diameter and branching.

It has been proposed that binding of neurotrophins to $p75^{NTR}$ increases its binding affinity to Trks, reinforces signaling through AKT and MAPKs, and promotes survival through activation of NF-κB.

Biological functions of BDNF-TrkB signaling

It is known that neurotrophins promote cell survival and that BDNF is the most expressed in the CNS together with its receptor TrkB. In TrkB KO mice, some populations of PNS

neurons are absent. In contrast, in the brain neuronal loss is not so strong [46-48]. Similar observations have been made using genetic alteration of the BDNF levels in the brain. Using some conditional KO (cKO) models [49-52] where the BDNF ablation happened only after birth, a marked decrease in dendritic complexity and spine density were observed. The elimination of TrkB at later stages of development caused progressive loss of cortical and striatal neurons. BDNF-TrkB may promote survival in pathological states and administration of exogenous BDNF may reduce the death of cortical neurons [46].

Other studies demonstrated that TrkB mediates BDNF role in late phases of LTP; the reduction of BDNF levels impairs the induction of L-LTP in rat hippocampal slices. The BDNF-TrkB signaling acts in different way according to the modality by which BDNF is administered on the receptors; the effects obtained from the activation of the pathway are also different. Acute application of BDNF induces the strong and transient (declines after 2 h) activation of TrkB and its downstream signaling molecules promoting neurite elongation and spine head enlargement. Instead, if BDNF is gradually applied, the kinetic of TrkB activation is slower (it takes 1 h to reach the maximum activation) but it is maintained for 8 h further supporting dendritic branching and filopodia-like spines.

BDNF-TrkB signaling plays a crucial role also in the regulation of cytoskeleton. The molecular mechanisms involved include the induction of MAPK to regulate microtubule dynamics, playing an important role in dendritic spine formation and maintenance, which is fundamental for the regulation of synaptic plasticity, the downregulation of RhoA activator and the activity of the multi-scaffold protein Kidins220 [53]. BDNF plays also a critical role in long-term memory through TrkB, indeed overexpression of TrkB-T impairs long-term spatial memory [54] while overexpression of the full-length isoform improves memory and learning [55].

BDNF-TrkB signaling in pathology

Alteration in BNDF/TrkB signaling has been observed in many human pathologies [56]. Nowadays, there is increasing evidence linking neurotrophin deficits with neuropsychiatric disorders suggesting that both the development and maturation of neuronal circuitry may be involved in the development of these disorders. There is also increasing evidence for the involvement of BDNF in anxiety [57]. Moreover, a haploinsufficiency of BDNF have been connected to autism, attention deficit and bipolar disorders. BDNF and NT-3 have been

connected also to the development of schizophrenia. Given the fundamental importance of BNDF/TrkB signaling for the development of GABAergic interneurons, and the decrease of TrkB and BDNF mRNA levels in the prefrontal cortex of schizophrenic patients, a contribution of GABAergic deficits to this disorder should be considered.

Signaling pathways activated by p75^{NTR}

As shown in **Figure 2,** p75^{NTR} can induce two opposite pathways depending on its coreceptor. An increasing body of evidence indicates that p75^{NTR} induces apoptosis through the activation of c-Jun N-terminal kinases (JNK). In this case, p75^{NTR} is cut and its ICD domain (intracellular domain) recruits proteins such as NADE, NRAGE, NRIF (NADE, p75^{NTR}-associated cell death executor; NRAGE, neurotrophin receptor-interacting MAGE homologue; NRIF, neurotrophin receptor-interacting factor)[45, 58]. The signal transduction pathway linked to JNK-3 (c-Jun N-terminal kinase 3), which is the most expressed in the nervous system, is then activated, promoting cell cycle arrest and activation of the apoptotic process (**Figure 2)** [32 , 33]. p75^{NTR} also triggers cell survival in a Trk-dependent manner, increasing by 100-fold the affinity of Trk receptors to their binding partners by the interaction between their transmembrane regions [35, 59].

The p75^{NTR} death domain also interacts with IRAK (interleukin-1 receptor-associated kinase) and TRAF6 (TNF receptor-associated factor 6) proteins, inducing in this way the activation of NF-κB. These protein interactions allow the ubiquitination of the IκB protein, phosphorylated by the IKK kinase, the consequent degradation of IκB within the proteasome, and the subsequent translocation of NF-κB into the nucleus with ensuing activation of pro-survival genes [60].

2.2. Kidins220

a. Kidins220 structure and interaction

Kidins220 (Kinase D-interacting substrate of 220kDa) / ARMS (Ankyrin repeat-rich membrane spanning), hereby referred to as Kidins220, was identified as the first physiological Kinase D substrate in neural cells [61] and as a novel downstream target of neurotrophin and ephrin receptor tyrosine kinases [62]. Kidins220 is a transmembrane scaffold protein ubiquitously expressed with a higher presence in the nervous system [61, 62]. Its sequence is highly conserved across species [62], which allows the study of Kidins220 with animal models. Its sequence presents, starting from the N-terminal: 11 ankyrin repeats,

4 transmembrane domains, a poly-proline stretch domain, a Sterile-α Motif (SAM), a Kinesin-Interacting domain (KIM) and a PDZ domain at the C-terminal (**Figure 3**) [61].

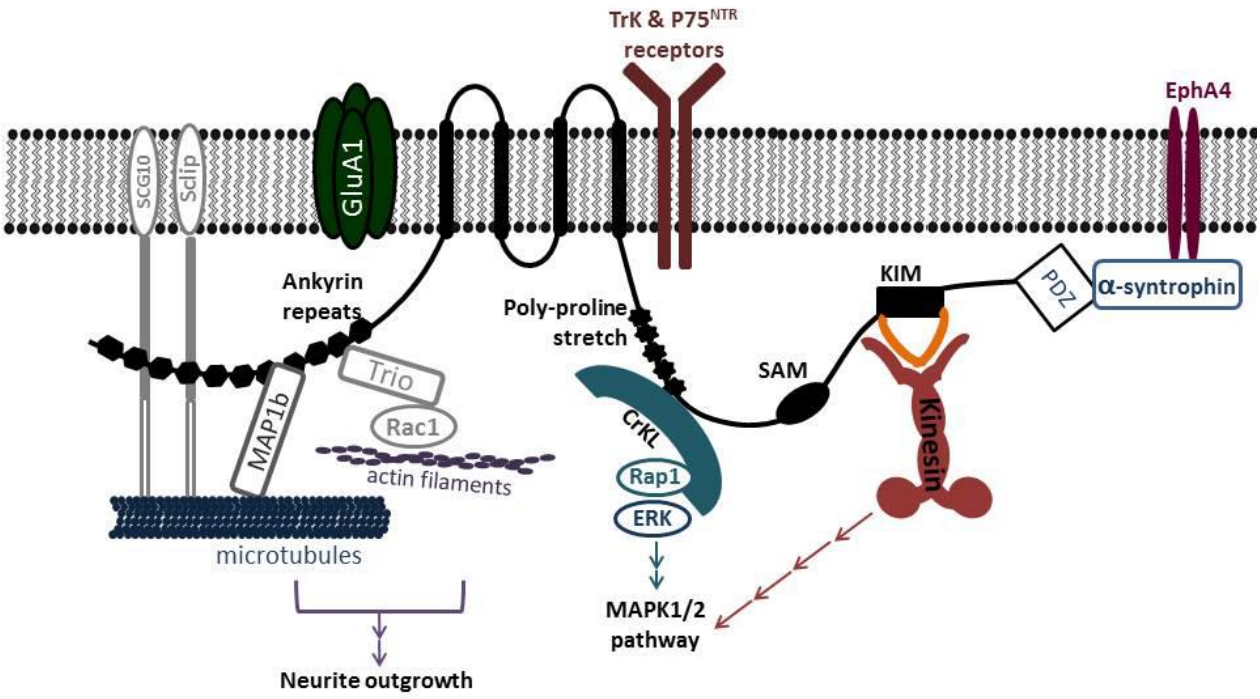

Figure 3. Kidins220 and its interacting proteins. (modified from [63])

An ankyrin repeat consists of 30-34 amino acid residues. Their function is to mediate protein-protein interactions [64]. Through this region Kidins220 interacts with:

- Trio, which mediates cytoskeletal remodeling. This protein allows Kidins220 to promote neurite outgrowth by activating GTPases [65].
- MAP1b (microtubule associated protein 1b), which acts directly on microtubules to stabilize them. MAP1b also anchors AMPA (α-amino-3-hydroxy-5-methyl-4-isoxazolepropionic acid) receptors to microtubules and, in this way, controls their intracellular trafficking. Through its interaction with Kidins220, MAP1b regulates early axonal outgrowth and influences microtubule dynamics to induce neuronal polarity [66].
- SCG10 (superior cervical ganglion 10) and Sclip (Scgn10 like-protein). They interact with Kidins220 in the perinuclear region and the growth cones, facilitating the early stages of neural differentiation [66].

Kidins220 transmembrane domains allow the interaction with Trks [62] and the GluA1 subunit of AMPA receptors, modulating neuronal activity [67].

Kidins220 effect on Trk activity is different depending on which neurotrophin is involved and, consequently, on which Trk is recruited. In fact, upon NGF stimulation Kidins220 binds the TrkA receptor and the disruption of this interaction results in aborted NGF-dependent signal transduction critical for neurite outgrowth [68]. Upon BDNF binding, TrkB associates with the transmembrane domain of Kidins220 and phosphorylates a specific residue (Tyr1096) in its cytoplasmic C-terminal tail, promoting downstream signaling (see below) [62, 68]. The interaction between Kidins220 and TrkC has been reported [68] but the functional consequences of Kidins220-TrkC interaction are still not described.

The poly-proline stretch domain, located in the C-terminus of Kidins220, is known to interact with the adaptor protein CrkL (Crk-like protein) via its SH3 (SRC Homology 3) domain. Interestingly, when Tyr1096 is phosphorylated by Trk, CrkL binds to Kidins220 through its SH2 domain. This switch in the binding allows the release of the SH3 domain of CrkL in order to recruit Rap1 and trigger MAPK sustained activation [69]. In fact, Kidins220 is one of the few proteins specifically required for sustained MAPK signaling activation [65]. This sustained activation leads to neurite outgrowth and the eventual cell cycle arrest. Other proteins contribute to transient MAPK signaling resulting in cell proliferation [70].

The SAM domain present in the C-terminal of Kidins220, is one of the most conserved protein interaction domains across species [62] but it is still unknown if any protein interacts with Kidins220 through this domain. The KIM domain mediates the intracellular trafficking of Kidins220 through a direct binding to KLC-1 (Kinesin light chain-1) and KLC-2, which are both subunits of the molecular motor Kinesin-1 [71]. KIM overexpression reduces NGF-dependent differentiation of PC12 cells, thus suggesting that Kidins220 transport by Kinesin-1 plays a role in the NGF-triggered sustained activation of the MAPK pathway, and subsequent cell differentiation [72].

The PDZ domain is a structural domain consisting of 80-90 amino acid residues localized in signaling proteins. By its PDZ-binding motif, Kidins220 interacts with various proteins:

- α-and β-syntrophin are scaffold proteins of the sarcolemma of the skeletal muscle, in the neuromuscular junction [73].

- Pdzm3 is a protein involved in early neurogenesis. PDZM 3 and KIDINS220 genes show overlapping expression domains in the posterior brain, ventral retina and motor neurons of zebrafish [74].
- S-SCAM (synaptic scaffolding molecule) forms a tetrameric complex with Trk receptors, Kidins220 and the Rap1 activator through the PDZ domain present in S-SCAM and the PDZ-binding sequence of Kidins220. In this way the complex induces the sustained ERK stimulation [71]. Out of the 6 PDZ domains contained in S-SCAM, PDZ5 binds directly to NMDAR subunits, whereas PDZ4 mediates the interaction with Kidins220. Consequently, S-SCAM might also participate in the association of Kidins220 and the NMDARs. In fact, the overactivation of NMDARs induces a dramatic downregulation of Kidins220 both *in vitro* and *in vivo* [75].
- SNX27 (sortin nexin 27) is a protein involved in the retrograde transport of endosomes, which specifically binds and directs sorting of PDZ-containing transmembrane proteins, preventing the entry into the lysosomal pathway. This protein interacts with Kidins220 preventing its degradation [76].
- $p75^{NTR}$ is a neurotrophin receptor with the potential to dimerize with monomers of any of the three Trks and it interacts with Kidins220 through its C- terminal tail.

Kidins220 and $p75^{NTR}$ expression overlaps in adult most notably in the olfactory bulb, Purkinje cells of the cerebellum, and motor neurons of the spinal cord [62]. A common feature of Kidins220, $p75^{NTR}$, TrkA and Eph receptors is that they all contain putative C-terminal PDZ-binding motifs. It is possible that these proteins are localized to the same subcellular compartment by these motifs, and this co-localization may contribute to signaling events both in the development and in the adulthood.

Kidins220 expression is modulated across development: in mouse, the highest protein expression occurs at birth and decreases over the first month, after which it remains constant [66]. Kidins220 is expressed in the entire mouse brain, with a prominent concentration in the cortex, principally in cell bodies and dendritic projections of layer 5 pyramidal neurons, and in the hippocampus, in the somas of the neurons of all areas and in the dendrites of dentate gyrus neurons [77].

b. Kidins220 isoforms

Kidins220 mRNA undergoes alternative splicing, which is subjected to spatio-temporal regulation throughout development resulting in several different Kidins220 isoforms. In 2015 Schmieg and colleagues [78] for the first time described a number of isoforms providing an explanation to for the diverse functions and localization of this protein. They found 6 isoforms in the central region and 3 isoforms at the C-terminal region of the Kidins220 protein in mice, and 3 isoforms in the central region and 3 at the C-terminal region in humans (**Figure 4**). The reduced number of splice isoforms found in humans is due to the fact that exons 27 and 28 are undetectable in the human genome [79].

All the mouse and human isoforms, with the exception of the mouse m3 isoform, have been detected in brain tissue. Two alternative terminal exons (ATE) in mice were also discovered: ATE C1, encoding a small portion of exon 32 and exon 33, and ATE C2 encoding solely exon 33. The authors observed isoforms m4 and m6 from DIV (days *in vitro*) 1 to DIV 7 in primary hippocampal, cortical and motor neurons, while from DIV 11 cultured cells expressed also isoforms m1 and m3. Interestingly, motor neurons expressed the highest variety of isoforms (all of them with the exception of m2) but lacked any ATE splicing. ATE C1 and C2 expression increased from E 13.5 until P9. While ATE C1 expression decreased until undetectable levels in adult brain, ATE C2 remained present.

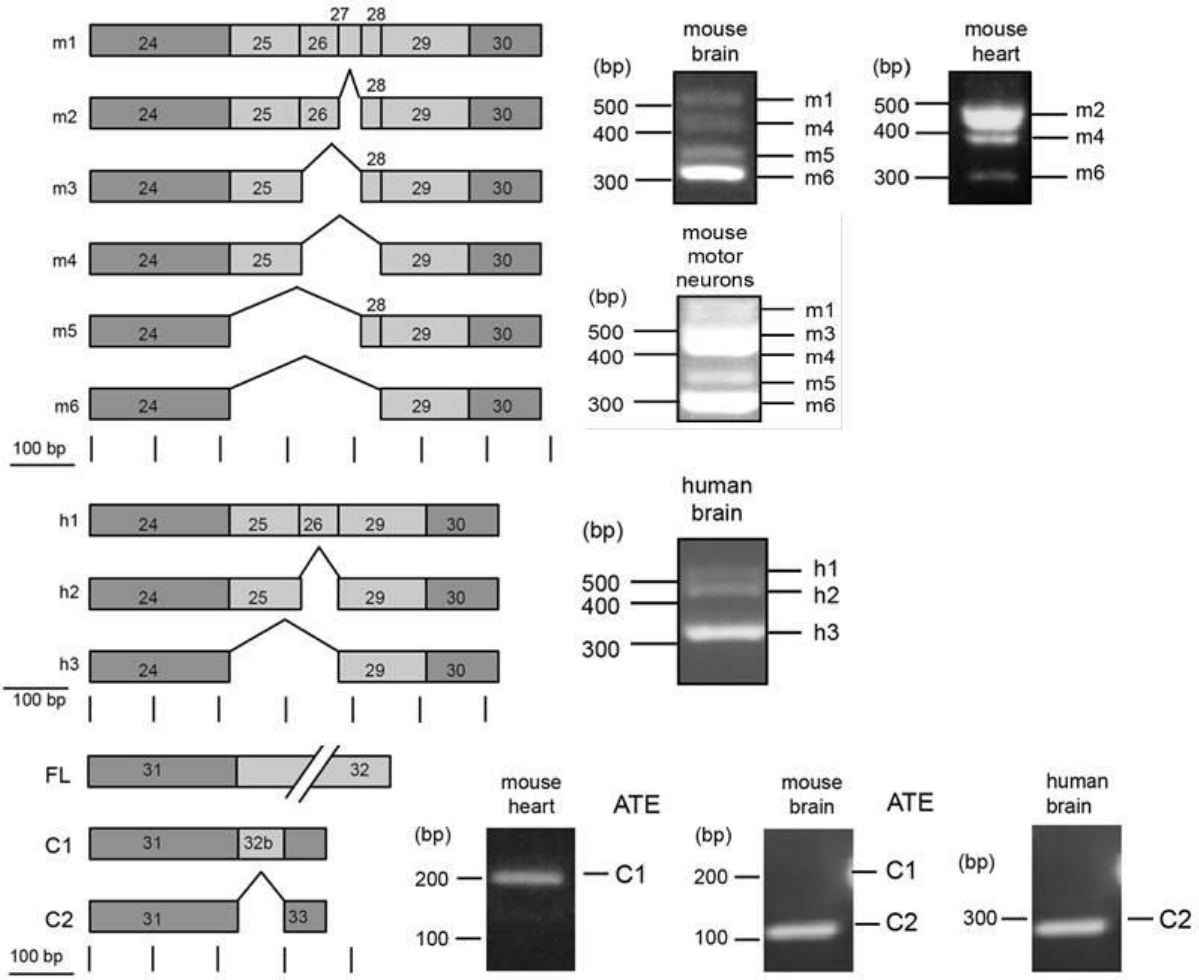

Figure 4. Schematic representation of Kidins220 alternatively spliced isoforms [78]. The first 6 isoforms in the upper panel are found in mouse tissue (m), while the subsequent three are found in human tissue (h). At the bottom the splicing isoforms of the carboxy-terminal, present in mouse and human, are represented. On the right, representative PCR products for the isoforms detected in different adult mouse and human tissues.

It was proposed that the fine tuning of neurotrophin signaling function could be achieved by varying the levels of the different ATE isoforms. Furthermore, the fast appearance of isoform m1 upon BDNF stimulation in cortical and hippocampal neurons suggests that neurotrophins might influence Kidins220 function by controlling the expression of its multiple isoforms.

2.3. Kidins220 and neurotrophins

Kidins220 was initially identified as an interactor of $p75^{NTR}$ [62]. In the same study the researchers also confirmed that Kidins220 binds TrkA. Today it is well established that

Kidins220 binds all Trks and $p75^{NTR}$ receptors creating a ternary complex which activates and sustains the downstream signaling [80].

Nervous system development and functionality is controlled by several growth factors that bind specific membrane receptors. Some of these receptors, such as the neurotrophin receptors, act through a common set of signaling molecules so, in order to achieve the specificity necessary for the correct biological response, something else should play an important role. Due to its properties of multi-scaffold protein, and the described ability of binding the neurotrophin receptors, Kidins220 seems the perfect candidate for achieving the required specificity.

Kidins220 is expressed in central regions of the nervous system (i.e., hippocampus), where TrkA is not present and TrkB is really abundant. A study demonstrated that Kidins220 is phosphorylated by TrkB upon BDNF treatment and the kinetics of Kidins220 phosphorylation occurs simultaneously with the autophosphorylation of the receptors [68]. Trks and Kidins220 interacts through their transmembrane motifs, and it has been hypothesized that Kidins220 coordinates a rapid Trk signal transduction through its multiple protein interaction domains. In particular, Kidins220 can sustain MAPK activation [68]. Mutations in the Kidins220 polyproline region cause decreased neurotrophin-induced MAPK phosphorylation and decreased NGF-dependent neurite outgrowth in PC12 cells, affecting only the sustained MAPK activation but not the transient MAPK phosphorylation neither Akt phosphorylation, which remain unaltered. Indeed, Trks phosphorylate Kidins220 on the residue that is critical in the sustained MAPK activation [68].

The sustained activation of MAPK signaling is also mediated in an independent way by the formation of a tetrameric complex in late endosomes composed by Kidins220, TrkA, the S-SCAM protein and the nucleotide exchange factors PDZ-GEF1 [71]. This Kidins220-dependent sustained signaling is also important for the activation of NF-κB.

2.4. Kidins220 and pathology

Alteration in Kidins220 protein levels has been linked to several types of cancers [81]. The overexpression of Kidins220 promotes melanoma formation by suppressing MAPK-mediated stress-induced cell death, and it correlated with reduced patients' survival [82]. Kidins220 is also involved in the development of neuroblastoma, a tumor originating from the neural crest. Kidins220 promotes the survival of neuroblastoma cell lines by mediating

NGF-induced MAPK signaling [83]. Among others, a genetic screening described an intragenic break point in the human KIDINS220 gene related to pediatric high-grade glioma (pHGG) [84].

Increased expression of Kidins220 is also associated with the development of Alzheimer's disease (AD). AD is characterized by three main pathophysiological characteristics: extracellular senile plaques containing (Aβ), intracellular neurofibrillary tangles (NFT) and hyper-phosphorylated forms of the microtubule-associated protein (MAP) Tau [85]. The accumulation of Kidins220 in AD was strongly associated with the accumulation of Tau [86].

Several studies have related Kidins220 expression with Autism Spectrum Disorders (ASD), which are characterized by two key diagnostic elements: persistent deficits in verbal and non-verbal social communication and social interaction across multiple contexts and restricted, repetitive patterns of behavior, interests, or activities. Kidins220 is overexpressed (2.16-fold change) in the blood transcriptome performed on 170 ASD patients and 115 controls. The Kidins220 gene was one of the 12 genes with an average fold change bigger than 1.5. Moreover, impairment in neurotrophin signaling pathways is known to be present in ASD patients, including the MAPK, PI3K and PLC pathway. The research on this psychiatric disorder involving animal models is focusing on distinguishable subgroups of biological defects known to be present in groups of ASD patients. Considering the types of social deficits in communication and interaction common in ASD, social behavior tests have been developed. For the evaluation of repetitive behaviors and motor stereotypes, behavioral tests relevant to anxiety, cognitive impairment, hyperactivity and sensory reactivity are used [87], like, among others, the open field, elevated plus maze and fear conditioning.

Schizophrenia is a neurodevelopmental psychiatric disorder. Genetic and epigenetic variants are both crucial risk factors to be considered in the diagnosis of this disorder [88]. Kidins220 has been related to schizophrenia via genetic studies. In 2015 Kranz and colleagues [89] found 5 carriers of variations in the KIDINS220 gene out of a group of 48 cases, identifying 2 rare missense polymorphisms and 1 novel missense mutation in the KIDINS220 gene. The novel missense mutation was located in the poly-proline stretch, the region that leads to sustained MAPK activation. It is still not known to what extent these sequence variations affect the physiological interactions of Kidins220 and the downstream

pathways. Moreover, 50% of the identified missense coding variants were found in the NGF-TrkA-Kidins220 pathway. Another study reported the phenotypes of subsets of cases with missense coding polymorphisms or novel mutations in four different genes. KIDINS220 was one of those genes considered potentially relevant for psychosis. A significant overlap of biological pathways between ASD and schizophrenia has been established by various studies [90]. Among these common pathways, the small GTPase family and MAPK signaling are particularly relevant as they contain many genes associated to neurodevelopmental disorders and have been implicated in synapse plasticity and behavior [91]. Given the scaffold nature of Kidins220 it could be possible that it plays a critical role in the signaling pathways shared between these two disorders.

Kidins220 has been recently related to the SINO, a new syndrome characterized by Spastic paraplegia, Intellectual disability, Nystagmus and Obesity. In 2016 for the first time, SINO was described in three unrelated pediatric patients (between 1 and 3 years old) carrying a de novo nonsense variant in the KIDINS220 gene [79]. These de novo variants encode truncated isoforms of Kidins220, which resemble isoforms that are not normally expressed in the developing embryo or present in motor neurons. This indicates that the disruption of the Kidins220 isoforms repertoire possibly caused the neurological phenotype found in these patients. In particular, the C-terminal region of Kidins220, which is not present or altered in the pathogenic variants, contains the KIM and PDZ domains, which are crucial for protein interactions and transport. Remarkably, the three patients showed dilated lateral and third brain ventricles. This alteration has been found in Kidins220 mutant mice as reported in [92, 93] confirming that the scaffold protein must be involved in ventriculomegaly/ hydrocephalus.

The pathophysiology of obesity may be related to the involvement of Kidins220 in neurotrophin signaling, since neurotrophins, and especially BDNF, have been largely related to the control of body weight [94]. Moreover, a new KIDINS220 mutation has been recently found and linked to alteration in the adipocyte differentiation [95].

Since 2016 several new mutations in the KIDINS220 gene have been discovered. [96]. They varied in the location and type of mutation, mode of inheritance and set of symptoms, including their lethality (**Figure 5**).

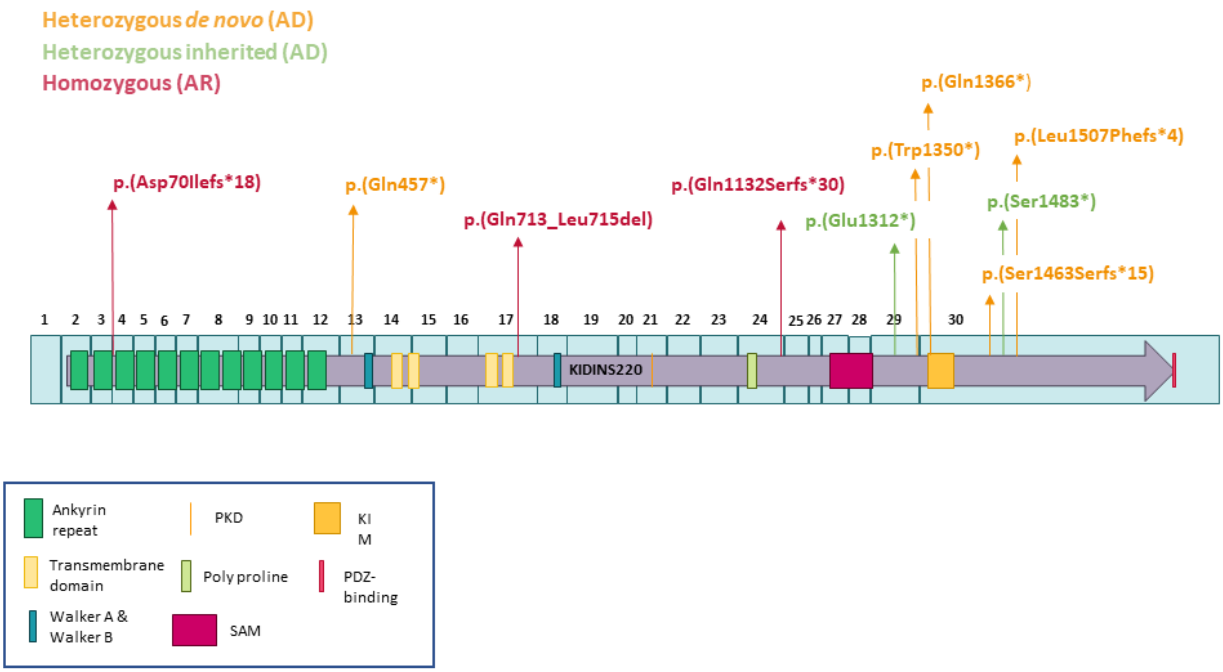

Figure 5 Schematic representation of Kidins220 mutation found in SINO patients and their localization along the gene. Image kindly provided by Ms A. Krawczun-Rygmaczewska.

2.5. Astrocytes

a. General

Astrocytes are neuroglia intercalated between nerve cells in the CNS. They represent around 50% of the total cells present in the brain. Astrocytes play a key role in numerous functions within the central nervous system (CNS) [97]. Based on their morphology they are divided into fibrous and protoplasmic astrocytes. The main biochemical feature of fibrous astrocytes is the presence, in the cell body and in the extensions, of thick fibrillar structures consisting of filaments of GFAP (the acid fibrillar glial protein), while in protoplasmic astrocytes such filaments are less abundant [98].

The morphological structure of astrocytes has two functional poles: one that allows the absorption of energetic substrates, the other that controls the composition of the perineural interstitial fluid and therefore, indirectly, neuronal activity. They also offer trophic support to neurons as energy storage, by absorbing glucose, storing it in the form of glycogen granules, which can be metabolized to lactate and transferred to neurons where it can be transformed into pyruvate and finally used to produce ATP [99]. In this way they support the metabolic activity of neurons [100].

They are also as a defense against oxidative/nitrosative stress and have a key role in neurogenesis acting on synapse formation and elimination [101] Astrocytes are able to

control several ions (i.e., Ca^{2+}, K^{+}), glutamate and water homeostasis expressing several different channels and neurotransmitter receptors [98, 102]. Among these are also calcium channels. Even if these cells are not electrical active, the expression of voltage gated Ca^{2+} channels in astrocytes has been reported in cultured astrocytes and in situ at least at the molecular level [103, 104]. Ca^{2+} is a universal second messenger that regulates the most important activities of all eukaryotic cells. In the CNS, Ca^{2+} participates in the transmission of information by regulating synaptic activity [105]. The activation of Ca^{2+} channels in astrocytes causes an influx of Ca^{2+} that leads to an increase in its intracellular concentration. A transient increases in cytosolic Ca^{2+} levels promote the release of signal molecules capable of regulating neuronal function. This mechanism is crucial in the modulation of synaptic potency [106]. The astroglia processes that modify cytosolic Ca^{2+} is still not clearly defined but the neuronal release of neurotransmitters seems to have an important role [102].

b. Astrocytes and BDNF

Astrocytes also synthesize, release and re-uptake trophic factors such as neurotrophins. The idea that astrocytes produce and secrete NGF goes back to the early years of neurotrophin research. In the following years, much effort was put into identifying the factor(s) that would induce astrocytes to produce and secrete not only NGF, but also other neurotrophins. In 1992, it was reported for the first time that astrocytes also produce BDNF [107]. In the following years, a growing body of literature supported that astrocytes are able to produce, bind, internalize and release BDNF [108] and that its expression is increased by specific stimuli [107]. Subsequently, this ability of astrocytes was investigated in greater depth [109]. Importantly, the capacity of astrocytes to respond to BDNF stimuli seems to vary depending on the different brain areas involved. In fact, recently Saba et al have demonstrated that, upon BDNF stimulation, cortical and striatal astrocytes can respond to the neurotrophin, modifying the expression of GLAST differently in the two brain areas [110].

It is known that astrocytes express mainly one of the TrkB isoforms, the truncated one (TrkB-T). There are also some reports that demonstrated the weak presence of the full-length receptor in cultured astrocytes [111]. Since its discovery, TrkB-T was shown to have a different expression pattern from the full-length receptor within the brain. Early experimental evidence showed the induction of TrkB-T in glial cells suggesting its possible

function could be to guide axon regrowth and synaptic reorganization [112]. Importantly, the expression of both TrkB isoforms were mediated by intracellular cAMP, indicating that the same stimuli are able to induce astroglia production and secretion of BDNF and TrkB expression in astrocytes [103]. The scientific community does not agree about the astrocytes' ability to induce the activation of the signaling pathways downstream of BDNF. Some studies demonstrated that astrocytes activate the MAPK pathway and the intracellular Ca^{2+} transients in response to BDNF similarly to what is observed in neurons. Initially the latter ability was attributed to the expression of full-length TrkB [113] but in 2003 Rose and colleagues demonstrated that there could also be the participation of TrkB-T [25].

c. Kidins220 in astrocytes

Several groups have shown that astrocytes are actively involved in the alterations of CNS function observed in various acute and chronic neurological diseases, including neurodegenerative diseases such as Alzheimer's disease. As reported above (**paragraph 2.4**) an altered expression of Kidins220 has been found in several pathologies and its role has been comprehensively addressed in neurons. Presently its function in astroglial cells is just beginning to be investigated.

As already clearly described, Kidins220 is expressed ubiquitously, with a higher presence in the nervous system [61, 62]. It has an important function supporting BDNF signaling and its subsequent involvement in Ca^{2+} dynamics through PLCγ activation, an important role in Ca^{2+} homeostasis and, consequently, in neuronal function and in the modulation of synaptic efficacy. It is important to deeply investigate the physiological functions of this protein in glial cells. What it is known about Kidins220 and astrocytes has been described for the first time by Jaudon and colleagues [114]. A follow up of the mentioned evidence on the role of Kidins220 in mediating neurotrophic signaling in astrocytes, is one of the aims of this thesis.

2.6. Animal models

In order to study Kidins220 role in a more physiological system, several animal models have been assessed.

The first KO model was described in 2009. Kidins220 KO mice were generated in Dr. Chao's laboratory using the Cre/lox system [77]. In this model the Kidins220 gene was removed through the action of the Cre enzyme driven by the actin promoter, which is

ubiquitously expressed and active from embryogenesis. This model generated Het and WT but not full KO mice. This ablation in fact was lethal since early embryonic stage. Het mice showed approximately 70% of the physiological amount of the protein compared with the WT littermates. They displayed decreased dendritic complexity accompanied by a reduction in spine stability. The authors observed reduced spatial memory with cell death in the cortex in female mice [77].

In 2011 another full Kidins220 KO mouse line was generated and described in Dr. Schiavo's laboratory [115]. Also in this case, the Cre/lox system was used but the enzyme was expressed under the phosphoglycerate kinase (PGK) promoter. Kidins220$^{+/-}$ animals were viable and fertile. They expressed comparable amount of protein as WT mice, and did not show any overt behavioral phenotype. In this case the homozygous ablation was lethal during the last stages of the pregnancy. At E18 the fetal brains were smaller and their hearts showed dilated and congested atria as well as disorganized ventricular walls. Kidins220 KO embryos exhibited extensive cell death in both the CNS and PNS. Moreover, Kidins220$^{-/-}$ primary neurons displayed an impaired response to BDNF, leading to deficiencies in cell survival, axonal/dendritic differentiation as well as in the BDNF-induced potentiation of EPSCs [115, 116].

In 2012 another approach was used in order to study the impact of Kidins220 ablation on brain development [117]. In this case the authors knocked out the scaffold protein by in utero electroporation at E14. Using this approach, the authors observed impaired dendritic branching *in vivo* and a significant decrease in complexity of the dendritic arbors *in vitro*. They also confirmed that those defects were directly link to Kidins220 important role in the mediation of BDNF signaling. In fact, they observed that those impairment were due to reduced activation of the PI3K/Akt signaling pathway.

Even if several different approaches have been tried, none of them permitted the study of Kidins220 ablation in adult animals. For this reason, a cKO mouse model has been generated in our laboratory. This model was generated using the same approach used for the first two KO lines (the Cre/lox system) but in this case the enzyme was put under the CamKII promoter to achieve the KO of the protein two weeks after birth and only in the excitatory neurons of the forebrain. It is worth highlighting that the Kidins220$^{lox/lox}$ mice needed to obtain the cKO, express only the full-length isoform of Kidins220. This is due to the insertion

of a CDNA cassette downstream of exon 16, lacking the possibility of alternative splicing [116]. Recently it has been becoming increasingly evident that the different isoforms of Kidins220 have different roles in different brain areas and neuronal subpopulations. This calls for a better understanding of the consequences of their absence. Therefore, the characterization of the cKO and Kidins220lox/lox models described above is one of the aims of this project.

In 2020 a new animal model was generated in order to better understand Kidins220 role in neuronal plasticity. Li and colleagues [118] knocked down Kidins220 gene in *C. elegans* using the RNA interfering technique, highlighting that Kidins220 plays a fundamental role in the age-related decline of high-activity neuron plasticity. Even if this new approach and its results are very interesting, it is important to consider that this model it is not fully able to recapitulate the role of Kidins220 in mammalian systems due to the absence of the classical neurotrophins in nematodes.

2.7. State of the art

As reported in the first paragraph of this thesis (**paragraph 2.2a**), Kidins220 is ubiquitously expressed. Almost all the information we have about Kidins220 come from *in vivo* models that unfortunately are lethal at the embryonic level and from *in vitro* experiments performed on neurons. For this reason, we wondered (i) whether Kidins220 plays a role also glial cells and (ii) what is the role of Kidins220 in the postnatal/adult brain. In the next paragraphs I summarize the results that had been already obtained when I joined the laboratory, which constitute the basis of my experimental work.

a. Astrocytic Kidins220 is directly involved in astrocyte [Ca^{2+}] dynamics and its ablation impacts on neuron development *in vitro*

Data from Jaudon et al. [114] demonstrated that Kidins220 absence in embryonic astrocytes manifests altered Ca^{2+} dynamics. Kidins220 is involved also in the ion signaling associated with the stored-operated Ca^{2+} entry (SOCE), impairing astrocytes maturation (**Figure 6A-B**). They also observed an increased expression of the Ca^{2+}-channel transient receptor potential vanilloid-type 4 (TRPV4), both at the mRNA and protein levels (**Figure 6C-D**). Moreover, when wild-type neurons were co-cultured with KO astrocytes an impairment in neuronal development was observed. This impairment was reflected also on the neuron excitability (**Figure 6E**). Interestingly, this was also observed when neurons were cultured with the conditional medium derived from those astrocytes (**Figure 6F**), highlighting an impairment in gliotransmitter secretion and/or constitutive secretion necessary for proper neuronal development.

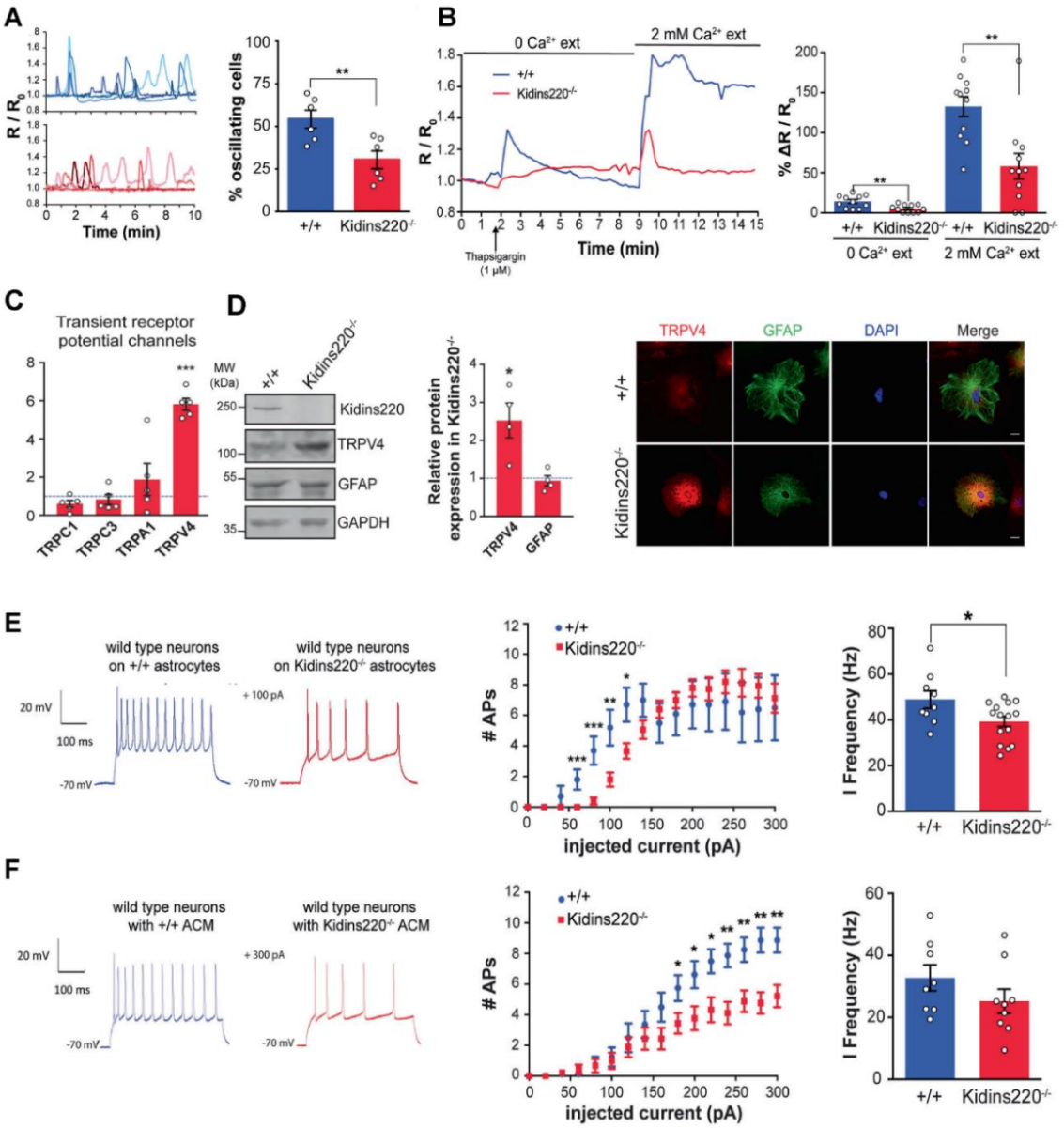

Figure 6. Background results about the effect of Kidins220 ablation in embryonic astrocytes. **A.** Removal of Kidins220 in astrocytes leads to a reduction of the number of cells showing spontaneous Ca^{2+} oscillations. Thapsigargin-induced intracellular [Ca2+]i responses in wild-type and Kidins220$^{-/-}$ astrocytes. **B-D.** Defect in Ca^{2+} dependent signaling are accompanied by changes in the expression of several proteins involved in Ca^{2+} dynamics (i.e., TRPV4 channels). Representative traces (*left*) and quantification of fluorescence intensity (*right*) of thapsigargin (1 µM)-treated wildtype or Kidins220$^{-/-}$ astrocytes, in the presence or absence of 2 mM external Ca^{2+} (B), mRNA expression profile of Ca^{2+} signaling proteins in Kidins220$^{-/-}$ astrocyte cultures (C), TPRV4 protein expression was analyzed by western blot analysis (*left*) and by immunofluorescence staining followed by confocal analysis (*right*) (D). **E-F.** Kidins220 expression in astrocytes is required for proper neuronal maturation. Firing properties of wild-type neurons grown on either wild-type or Kidins220$^{-/-}$ astrocytes (E) or in astrocyte-conditioned medium (ACM) from either wild-type (+/+) or Kidins220$^{-/-}$ astrocytes (F) for 14 DIV. From [114].

b. Ablation of Kidins220 *in vivo* affects brain morphology and mouse behavior

In order to investigate Kidins220 role in an *in vivo* model that survives birth, in our laboratory a cKO model was generated. In this mouse model the knockout of Kidins220 was

cell type and time specific. In fact, the ablation was driven by the CamKII promoter, which is active only in the excitatory neurons of the forebrain starting from the second postnatal week.

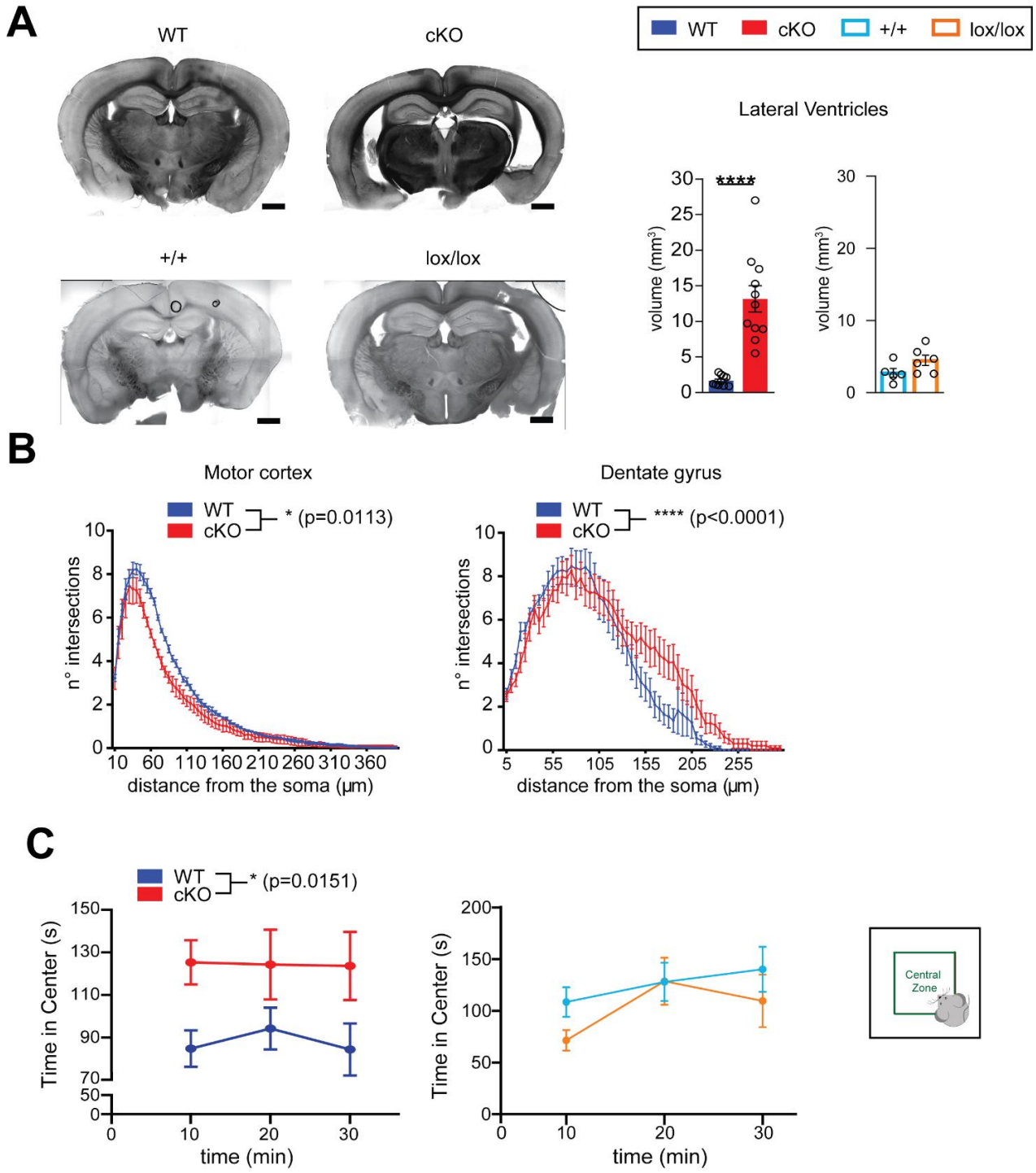

Figure 7. Effects of Kidins220 postnatal ablation on mouse brain morphology and behavior. **A.** Quantification of lateral ventricle volume for WT, cKO (*upper*), +/+ and lox/lox animals (*lower*). Lateral ventricles are enlarged in Kidins220 cKO animals. Scale bars: 1mm. **B.** Sholl analysis shows a reduced dendritic arborization in the motor cortex, and increased arborization in the granule cells of the hippocampus of cKO mice. **C.** Quantification of the time spent by WT and cKO mice (left), +/+ and lox/lox mice (middle) in the central zone. On the right a schematic representation of the open field test is presented.

Background data obtained in the laboratory before I joined the group had described WT (+/+; Cre/+), cKO (lox/lox, Cre/+), +/+ and lox/lox mice showing that, even if mice of all genotypes had a comparable physical development for the first 3 months, Kidins220 removal induced several defects. In fact an enlargement of brain ventricles had been observed in both cKO and Kidins220lox/lox mice (**Figure 7A**), and also altered neuronal morphology in those areas were the scaffold protein is known to be most expressed, such as the cortex and the dentate gyrus of the hippocampus of cKO animals (**Figure 7B**). Moreover, some behavioral experiments were performed, highlighting a reduced anxiety in cKO mice (**Figure 7C**) but not in the lox/lox.

Due to the differences observed in the control groups another question needed an answer: does the presence of the Cre enzyme in the genome have any effect on behaviour? Data already produced in our laboratory showed that the controls bearing the Cre enzyme were hyperactive but less anxious compared to the wild type mice [93], underlying how important it is to choose the correct controls for all the experiments.

3. Aim of the thesis

Neurotrophins are important proteins that play a fundamental role in neuronal physiology. Among all of them, BDNF is the one with the highest expression in the brain. Its action depends on the binding of specific receptors, i.e., Trks and $p75^{NTR}$ and the consequent activation of the downstream pathways. The proteins recruited upon BDNF receptor activation are several and have different effects on neuronal physiology including, but not limited to, neuronal survival, synaptic plasticity, and higher functions as memory, cognition and complex behaviors. Kidins220 is a scaffold protein that interacts with neurotrophin receptors and, among other functions, is directly involved in the activation of neurotrophin signaling.

Despite the available literature, the role of Kidins220 in astrocytes, in their response to BDNF, and the physiological role of this scaffold protein at different stages of astroglia maturation are still open questions. Moreover, Kidins220 has been identified as an important risk factor in several psychiatric diseases as well as in SINO syndrome, but until now it has not been possible to investigate the role of this protein in the postnatal / adult brain development. Building on the preliminary results and these still open questions, the aim of my thesis was to characterize the physiological role of Kidins220 in primary astrocytes *in vitro* and *in vivo* in a conditional knock-out mouse line where Kidins220 is postnatally ablated.

In order to achieve my goal I first focused my attention on *in vitro* astrocytes. In these cells I evaluated how Kidins220 ablation affects BDNF response, its receptors and their downstream pathways using different biochemical techniques. I also tested if Kidins220 absence has any effects on calcium dynamics depending on the developmental stage of the astrocytes through the use of calcium imaging.

Using the conditional knock-out mouse model I evaluated the consequences of Kidins220 ablation in the adult central nervous system. In particular, I looked into whether the lack of Kidins220 affects BDNF levels, its receptors and the downstream pathway using different biochemical techniques. Since the role of BDNF and Kidins220 in dendritic maturation is known, I also investigated if there are impairments in dendritic maturation stemming from the scaffold protein's absence in an adult mouse brain, taking advantage of Golgi-Cox

staining. Finally, I also wondered whether the behavioral defects observed in these mice can be rescued through the chronic administration of a BDNF mimetic.

4. Materials and Methods

4.1. Animal models

In the present study a number of transgenic mouse lines were used, which were all on the C57BL/6 background.

In vitro experiments

For the *in vitro* experiments we used both embryonic and postnatal primary mouse astrocytes. The embryonic primary astrocytes were obtained at E18.5 from crosses of Kidins220$^{+/-}$ mice [116, 119]. The Kidins220$^{+/-}$ mice are heterozygous; they were mated overnight and separated in the morning. The development of the embryos was timed from the detection of a vaginal plug, which was considered day 0.5. The embryos obtained were:

- C57BL/6 wild type (abbreviated as +/+),
- C57BL/6 full knock out for Kidins220 gene (abbreviated as Kidins220$^{-/-}$),
- C57BL/6 heterozygous for Kidins220 gene (abbreviated as Kidins220$^{+/-}$. Cells obtained from these embryos were not used for the experiments).

Postnatal cultures were prepared from P0-P1 pups obtained from crosses of Kidins220$^{+/lox}$ mice. In this case the pups used were:

- C57BL/6 wild type (abbreviated as Kidins220$^{+/+}$),
- C57BL/6 with lox site (abbreviated as Kidins220$^{lox/lox}$).

In these cultures, the excision of Kidins220 was obtained by infection with lentiviruses expressing the Cre recombinase (see **paragraph 4.3**).

In vivo experiments

In order to analyze the role of Kidins220 in the adult mouse brain, a new conditional KO (cKO) mice line was generated by crossing the Kidins220$^{lox/lox}$ animals with transgenic mice that express the Cre recombinase under the control of the CaMKII promoter. This promoter was selected because it drives the expression of Cre only in forebrain excitatory neurons starting from the second postnatal week, thus circumventing the developmental defects in the nervous and cardiovascular systems of full KO embryos[115]. The Kidins220$^{lox/lox}$ mice line was obtained from Dr. G. Schiavo (UCL London, UK) and the CaMKII-Cre mice line was bought from Jackson Laboratories (Maine, USA) [#B6.Cg-Tg(Camk2a- Cre)T29-1Stl/J]. The Kidins220 cKO line was established as an essential tool to investigate any abnormalities arising in the adult brain due to the lack of Kidins220, as well as to understand the role of

Kidins220 in the formation and maintenance of the cortico-hippocampal circuits. A 4-step crossing plan was designed to obtain the cKO animals, as shown in **Figure 8.**

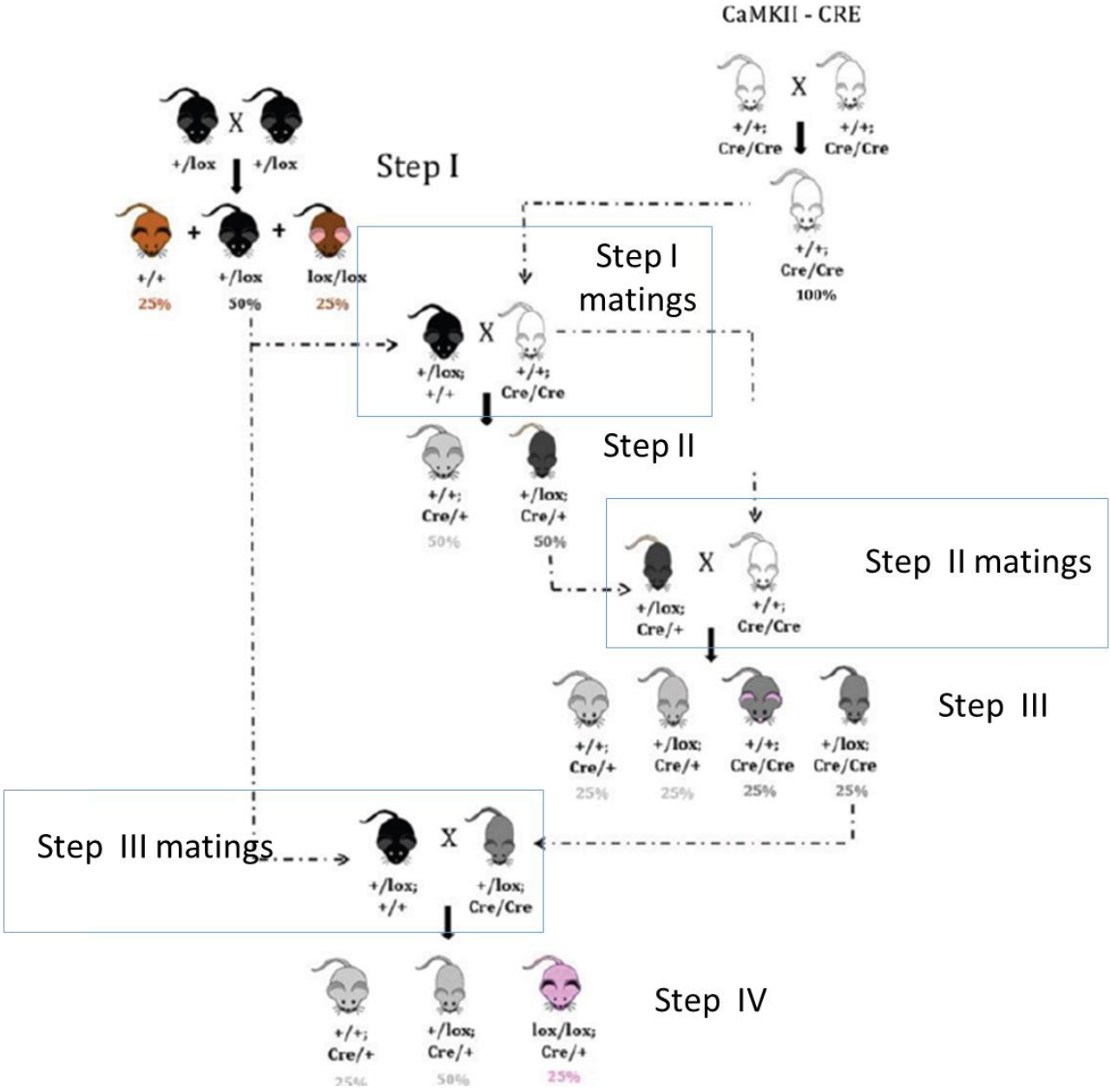

Figure 8 Crossing plan. The diagram illustrates the steps necessary to obtain Kidins220 cKO mice.

For the *in vivo* behavioral experiments the animals were:

- C57BL/6 wild type (abbreviated as +/+),
- C57BL/6 with the Kidins220 gene flanked by lox sites (lox/lox),
- C57BL/6 wild type for Kidins220 but bearing one allele for the Cre enzyme ($Kidins^{+/+;\,+/Cre}$ abbreviated as WT),
- C57BL/6 with the Kidins220 gene flanked by lox sites and one allele for the Cre

enzyme (Kidins$^{lox/lox;\ +/Cre}$ abbreviated as cKO).

The lox/lox mice only express the Kidins220 long isoform. WT mice on the other hand, present all the Kidins220 isoforms but are heterozygous for the Cre allele. Finally, cKO mice express only the long isoform and one allele for the Cre enzyme.

All procedures were approved by the Italian Ministry of Health and strictly adhere to the recommendations in the Guide for the Care and Use of Laboratory Animals of the National Institutes of Health.

a. Genotyping of animals

All animals were individually genotyped with the polymerase-chain reaction (PCR) technique. Genomic DNA was isolated from tail or ear snips of young mouse pups (E18.5 or P0 for the *in vitro* experiments and three week old for the *in vivo* experiments) for determining their genotype.

I. DNA extraction and quantification

This tissue was lysed rapidly by incubating it in 50 mM (NaOH) at 98◦C for 50 min. After this process, Tris HCl buffer (0.1 M, pH 8.0) was added to the sample, which then was centrifuged at 16,000 g for 5 min at 4°C. At the end of this process the DNA was used for the PCR and/or quantified for the quantitative PCR (qPCR) analysis.

II. Genotyping PCR

Genotyping PCRs for lox/lox and CaMKII-Cre animals were performed using primers specific for the floxed allele, for the Cre allele and for the tissue specific activation of the Cre enzyme.

The PCR mix was obtained by adding the specific primers, at the concentrations reported in **Table 1**, to the GoTaq Green PCR Master Mix (#M712, Promega), which contains Taq DNA Polymerase, colored dyes, $MgCl_2$ and dNTPs**.**

Genomic DNA amplified by the PCRs was run on a 2% agarose gel prepared by dissolving 2% agarose (#C OB-8100-01, Eppendorf) in Tris Acetate-EDTA (TAE) Buffer (#T9650, Sigma- Aldrich) and SyberSafe (#EMR440001, EuroClone) at a final concentration of 0.1 µg/mL. The PCR samples were loaded directly into the agarose gel and electrophoresed at 80 V in TAE Buffer.

III. Genotyping qPCR

In order to determine if the Cre transgene was expressed in heterozygosity or

homozygosity, qPCR was performed on 20 ng of genomic DNA. The mix was an TaqManR Universal PCR Master Mix, no AmpEraseRUNG (#4324018, ThermoFisher Scientific) with a fluorophore-quencher combination (as recommended by the Jackson Laboratory). The primer concentrations are reported in **Table 1.**

In order to obtain the correct amount of the Cre transgene present in the animals, all the samples were compared with other well-known genotype samples (Wt. Het and cKO).

Primer		**Use concentration**	**Sequence 5′ to 3′**
Kidins220 Primers	Long	1 µM	GAGCACAGACTTCTCTTATGG
	Flox	1 µM	GCGTTTCTAGCATACACATG
	Splice	1 µM	CAGATGGCTGTGAACCACCGTTTAAAC
Cre Primers	Transgene Fw	1 µM	GCGGTCTGGCAGTAAAAACTATC
	Transgene Rv	1 µM	GTGAAACAGCATTGCTGTCACTT
	Internal Positive Control Fw	1 µM	CTAGGCCACAGAATTGAAAGATCT
	Internal Postitive Control Rv	1 µM	GTAGGTGGAAATTCTAGCATCATCC
Cre qRT-PCR Primers	Tg Probe	0.15 µM	AACATGCTTCATCGTCGGTCCGG
	IC Probe	0.15 µM	CCAATGGTCGGGCACTGCTCAA
	Transgene Fw	0.2 µM	GCGGTCTGGCAGTAAAAACTATC
	Transgene Rv	0.2 µM	GTGAAACAGCATTGCTGTCACTT
	Internal Positive Control Fw	0.4 µM	CACGTGGGCTCCAGCATT
	Internal Positive Control Rv	0.4 µM	TCACCAGTCATTTCTGCCTTTG

Table 1 Primers used for genotyping

4.2. Primary astrocyte cultures

E18.5 or P0-P1 cortices were dissected in ice-cold PBS, incubated with trypsin 0.25% and 1 mg/ml DNase I for 30 min at 37°C, and later mechanically dissociated. Cells were then re-suspended and plated on poly-D-lysine-coated flasks, in DMEM medium containing 10% Fetal Bovine Serum (FBS), 2 mM glutamine, 33 mM glucose and antibiotics (astrocyte culture medium) in a 5% CO_2 humidified incubator at 37 °C. After 24 h, the medium was removed and replaced with fresh culture medium. After one week, half of the medium was replaced with fresh culture medium. Embryonic and postnatal cultures were composed of about 90% astrocytes and were isolated from of neurons [114].

4.3. Lentivirus production and infection procedures

HEK293T cells were maintained in Iscove's Modified Dulbecco's Medium supplemented with 10% FBS, 2 mM glutamine, 100 U/ml penicillin and 0.1 mg/ml streptomycin in a 5% CO_2 humidified incubator at 37 °C. Cells were transfected with the Δ8.9 encapsidation plasmid, the VSVG envelope plasmid and the pLenti-PGK-Cre-EGFP or pLenti-PGK-ΔCre-EGFP plasmids [120] using the calcium phosphate method. The transfection medium was replaced by fresh medium after 16 h. Supernatants were collected 48 h after transfection, centrifuged to remove cell debris, passed through a 0.45 μm filter and ultracentrifuged for 2 h at 20,000 x g at 4°C. Viral pellets were re-suspended in PBS, aliquoted and stored at -80°C until use.

Confluent postnatal astrocyte cultures were trypsinized and seeded on 6-well plates or glass coverslips coated with poly-*D*-lysine for subsequent experiments. Cells were infected 3 days later with lentiviruses encoding catalytically dead (ΔCre) or active Cre recombinase with the lowest infectious dose capable of transducing ≥95% of cells and used for experiments 7 days after transduction.

4.4. Cell treatments

For the chronic stimulation of postnatal primary astrocytes, cultures were serum starved overnight three days after lentiviral infection. The following day they were treated with 1 ng/ml BDNF or left untreated. This treatment was repeated for the next two days. At the end of the 72 h of treatment, astrocytes were lysed for the following experiments.

4.5. Molecular techniques

For molecular analyses, RNA was extracted with the QIAzol lysis reagent (cat. N. 79306, Qiagen). The same extraction and retro-transcription protocol was used for cells and tissues.

a. qPCR

RNA was extracted from 500,000 cells. For the *in vivo* experiments, 8 different brain areas were analysed in order to map gene expression induced by external stimuli (social/non social odours) and depending on the genotypes.

I. RNA extraction, quantification and retrotranscription.

For RNA extraction, samples were lysed at room temperature (RT) in QIAzol lysis reagent (Qiagen) (0.5 ml Trizol per sample). Then, after 5 min of incubation at RT, 0.1 ml of chloroform was added. Homogenate samples were centrifuged at 10,000 rpm for 15 min at 4°C in order to obtain three separate phases (a lower red phenol-chloroform, an interphase and a colourless upper aqueous phase containing the RNA). The aqueous phase was carefully transferred to a new tube, 0.25 ml of isopropanol was added and then samples were centrifuged at 10,000 rpm for 10 min at 4°C to precipitate RNA. At this point 2 washes with 70% ethanol were performed. After a short drying time, the pellet was resuspended in 20 µl DEPC-treated water and RNA was quantified using the Nanodrop 2000 (ThermoScientific) and store at -80°C until use.

The corresponding cDNAs were prepared by reverse transcription of 1 µg of RNA using the SuperScript IV First-Strand Synthesis System (#18091050, Invitrogen) with an oligo-dT primer following the protocol of the kit.

The protocol followed is:

1st step	RNA	250 ng
	50 µM Oligo-dT	1 µl
	10 mM dNTP mix	1 µl
	DEPC water	up to 12.5 µl
2nd step	5X RT Buffer	5 µl
	0.1 M DTT	1 µl
	RNase OUT	0.25 µl
	Superscript IV	0.25 µl

PCR	
T°	**Time**
65°C	5 min
4°C	1 min
T°	**Time**
52°C	10 min
80°C	10 min
4°C	5 min

II. Primer setting

Primer setting was done in two steps. In the first step, different concentrations of each primer pair were tested (100; 150; 200 and 300 nM) on cDNA from a tissue where the gene of interest is expressed. The amplification and its specificity with the dissociation curve were tested.

The second part of the setting was performed using the determined concentration of the primers on a standard curve of cDNA. The R^2, that needs to be > 0.950, and the efficiency (95% > efficiency > 110%) were checked. The primers used are reported in **Table 2**.

III. qPCR

The resulting cDNAs were used as a template for RT-qPCR using a CFX96 Real-Time PCR Detection System (Biorad) with a SYBR Green master mix (# 79306 Qiagen). The relative quantification in gene expression was determined using the ΔΔCt method. Data were normalized to the housekeeping genes by the multiple internal control gene method with GeNorm algorithm [121].

For the *in vitro* experiments, we checked the expression of the main genes involved in astrocyte physiology:

- Inward rectifier potassium channel (Kir 4.1) NM_001039484.1
- Glutamate Transporter 1 (GLT-1) NM_001077514.4
- Aquaporin 4 (Aqp4) NM_009700.3
- Connexin 43 (Cnx43) NM_010288.3

The housekeeping genes used for the normalization were:

- Transferrin receptor protein 1 (TRFR), NM_011638.4
- TATA-box-binding protein (TBP), NM_013684.3
- Tubulin beta-2A (TUBB2) NM_009450.2

Sequences and concentrations of the primers used are reported in the following table:

Gene		Concentration (nM)	Sequence
Acq4	Forward	200	CTGTGGCAGCGAGATAATGG
	Reverse	200	GCCTTTCTGGGAACTCACAC
Cnx43	Forward	200	CTTTGACTTCAGCCTCCAAGG
	Reverse	200	GGGCACCTCTCTTTCACTTAAT
GLT-1	Forward	150	ACTGGCTGCTGGATAGAATGA
	Reverse	150	AATGGTGTCCAGCTCAGACT
Kir4.1	Forward	150	GCCCCGCGATTTATCAGAG
	Reverse	150	TCCATTCTCACATTGCTCCG
Housekeeping gene		**Concentration (nM)**	**Sequence**
	Reverse	200	CCTGCTTCACCACCTTCTTGA
TBP	Forward	150	ACTTCGTGCAAGAAATGCTGAAT
	Reverse	150	CAGTTGTCCGTGGCTCTCTTATT
TRFR	Forward	300	AGACCTTGCACTGTTTGGACATG
	Reverse	300	GGTGTGTATGGATCACCAGTTCCTA
TUBB2	Forward	200	CAAGGCTTTCCTGCACTGGT
	Reverse	200	AACTCCATCTCGTCCATGCC

Table 2 List of primers used for the qPCR experiments.

4.6. Biochemical analysis

a. Protein extraction and quantification

Astrocytes were first washed with ice-cold PBS and then lysed using RIPA buffer:

- Tris HCl pH 7.4 50 mM,
- NaCl 150 mM,
- EDTA 2 mM,
- NP-40 1%,
- SDS 0.1%
- Protease inhibitors 0.02%
- Phosphatase inhibitors 0.01%

Lysates were then centrifuged at 16,000 g for 15 min at 4°C. The supernatant was moved to a clean tube, lysates were then quantified and stored at -20 °C.

Animals' brains were dissected and different brain areas were isolated. These brain areas were lysed with a tissue weight (mg)/RIPA volume (µl) ratio of 1:30 in order to obtain a final concentration between 1.5 and 3 µg/µl. Lysates were then centrifuged at 16,000 g for 15 min at 4°C. Supernatant was moved to a clean tube and the process was repeated until no trace of pellet was found. Lysates were then quantified and stored at -20 °C.

Protein concentration was obtained using a spectrophotometer (TECAN InfiniteF500) and a commercial kit **(**Pierce BCA Protein Assay, #23228, ThermoScientific) based on a colorimetric detection method (BCA protein assay). The kit required the preparation of bovine serum albumin (BSA) standard curve starting from 2 mg/ml. Subsequent serial dilutions in the range of 125-2.000 µg/ml were prepared. The BCA working reagent (WR) was prepared mixing 50 parts of BCA Reagent A with 1 part of BCA Reagent B. 5 µl of standard curve and protein samples were plated into a 96-well plate and 100 µl of WR were added to each well. The plate was then covered and incubated at 37 °C for 30 min, after which the absorbance was read (O.D.=562 nm). The values obtained from the BSA samples at known concentrations were interpolated by a standard curve, which was used to calculate brain sample concentration. The Microsoft Excel software was used to create standard curves and execute calculations.

b. Western Blotting

I. Sample Preparation

In order to prepare the samples for the western blot, 20 µg of protein extract were mixed with Loading Buffer 5X (62.5 mM Tris HCl pH 6.8, 20% glycerol, 2% SDS, 0.1% bromophenol blue, 20% β-mercapto-ethanol). Samples were then heated at 99°C for 5 min in a Thermomixer Eppendorf Comfort in order to allow protein denaturation and disulphide bonds reduction.

II. SDS page and electrophoretic run

Samples (20 µg) were loaded in a polyacrylamide gel made by a running (25% 1.5 M Tris HCl pH 8.8, 6-12% Acrylamide, 0.1% SDS, 0.1% ammonium persulfate, 0.04-0.06% TEMED) and a stacking gel (12.5% 1 M Tris HCl pH 6.8, 5% Acrylamide, 0.1% SDS, 0.1% ammonium persulfate, 0.01% TEMED). Proteins were then separated during the electrophoretic run which took place inside an electrophoresis chamber (Bio Rad Mini Protean tetra vertical) filled up with running buffer (25 mM Tris HCl, 190 mM Glycine pH 8.3, 0.1% SDS). A constant current of 35 mA was applied to the chamber for about 1 h and 30 min at RT. To better follow the electrophoretic run and to precisely identify the different molecular weights, a molecular weight marker was always loaded in parallel to the samples **(**Precision Plus Protein™ Dual Color Standards, #1610374, BIO-RAD).

III. Western blotting

Proteins, which by the end of the electrophoretic run were separated based on their molecular weight, were transferred from the gel to a nitrocellulose membrane in an electrophoretic chamber filled with transfer buffer (25 mM Tris HCl, 190 mM glycine pH 8.3, 20% ethanol) at a constant voltage of 100 V for 2 h at 4 °C. Once the transfer was over, the membrane was blocked for 1 h using 5% BSA dissolved in TBS / 0.1%Tween (TBST: Tris 10 mM pH 7.5, NaCl 100 mM, Tween-20 0.1%) in order to block all non-specific binding sites. Membrane was then incubated overnight (O/N) at 4°C with primary antibodies (**Table 3**) dissolved in TBS/5% BSA.

The following day, the membrane was washed 4 times with TBST and incubated with the corresponding horseradish peroxidase (HRP)-conjugated secondary antibodies, diluted as described in **Table 3**, for 1 h at RT. The membrane was than thoroughly

washed in TBST and the highly sensitive ECL substrate (ECL^{tm} Western Blotting, #16923242, Amersham^{tm} GE Healthcare) was placed on the membrane for about 1 min. The membrane was then developed using the iBright1500 (ThermoFisher, #A44114). The exposure time varied between 3 and 5 min depending on the antibody. The intensity of the immunoreactive bands was quantified with the ImageJ software.

Antibodies	**Production Company**	**Product code**	**Dilution**	**Specie**
Kidins220	Abcam	GSC16	1:1500	Rabbit
TrkB	Millipore	07225	1:2000	Rabbit
p75^{NTR}	Promega	G323A	1:2000	Rabbit
pMAPK (Thr^{202}/Tyr^{204})	Cell signalling	4377	1:2000	Rabbit
MAPK	Millipore	06-182	1:2000	Rabbit
pAKT (Ser^{473})	Cell signalling	4058	1:1000	Rabbit
AKT	Cell signalling	9272	1:1000	Rabbit
pPLCγ (Tyr^{783})	Cell signalling	2821	1:500	Rabbit
PLCγ	Cell signalling	2822	1:1000	Rabbit
GAPDH	Cell signaling	14C10	1:10000	Rabbit
Calnexin	Enzo	ADISPA860	1:5000	Rabbit
Actin	Sigma	A2066	1:5000	Rabbit
HRP-conjugated goat anti-rabbit	ThermoFisher scientific	#31460	1:4000	

Table 3 List of antibodies used for the biochemical analysis

c. ELISA

A direct ELISA assay was performed in order to measure the amount of BDNF present in the various brain areas of our mice. For this analysis a kit was used (#D1248, R&D) following the protocol suggested from the R&D system company. Instead a home-made direct ELISA assay was performed in order to measure the amount of phosphorylated TrkB (pTrkB). All the procedures were performed at RT.

I. BDNF ELISA

Sample and plate preparation

We used the same samples for the western blot analysis. All the samples were diluted in PBS at the same concentration (1 µg/µl). For the standard curve, a serial dilution of the BDNF protein was prepared (1500 pg/ml to 23.4 pg/ml).

First, the capture antibody was diluted at the working concentration (2 µg/ml) in PBS and then a 96 multi-well plate (#3590, Corning incorporated Costar) was coated and left to incubate overnight. The next day, after 3 washes with PBS/0.05% Tween20 the plate was blocked with PBS/1%BSA for 90 min.

ELISA assay

The sample and the standard curve were plated and left for 2 h at RT in order to let the BDNF present in the sample to be captured by the coating antibody. Once this step was finished, the BDNF detection antibody diluted in PBS 1% BSA (working concentration 25 ng/ml) was plated and incubated for 2 h. After this, the streptavidin-HRP diluted in PBS 1% BSA was added and incubated for 20 min in the dark. After every step described above, 2 washes with PBS/0.05% Tween20 were performed in order to remove the excess antibodies that were not bound to the substrate. At the end of the streptavidin incubation, the substrate TMB One solution (3,3',5,5'-tetramethylbenzidine, #G7431, Promega) was plated and left in the dark for 20 min at RT inducing the colorimetric reaction. Then, the reaction was stopped by 2 N sulphuric acid. The plate was then read determining the optical density of each well immediately, using a spectrophotometer (TECAN InfiniteF500) set to 450 nm first and subsequently to 540 nm (the reading at the second wavelength was done in order to perform an accurate quantification of the BDNF present in the plate).

A standard curve interpolated over the values obtained from the samples at known concentrations was used to calculate BDNF sample concentrations. The Microsoft Excel software was used to create standard curves and execute calculations.

II. pTrkB ELISA

Sample and plate preparation

We tested the same samples used for the western blot analysis. All the samples were diluted in PBS at the same concentration (1 µg/µl). For the standard curve, lysates

from BDNF-stimulated DIV 14 cortical neurons were used. These cells were stimulated for 15 min with BDNF (50 ng/ml), washed with ice-cold PBS, lysed in RIPA buffer and quantified. The standard curve was prepared with serial dilutions of these lysates (range from 1000 ng/ml to 15.6 ng/ml).

First, the "capture" monoclonal anti-phosphotyrosine antibody (clone 4G10, #05-321, Millipore) was diluted at the working concentration of 3 µg/ml in carbonate/bicarbonate buffer (CB) pH 9.6, and then a 96 multi-well plate was coated and incubated overnight at 4°C with gentle agitation. The next day, after 3 washes with PBS/0.05% Tween20, the plate was blocked with PBS/1%BSA for 90 min.

ELISA assay

The samples and the standard curve were plated and left for 2 h at 37°C in order to allow all the phosphotyrosines present in the sample to be captured by the coating antibody. Once this step was finished, the polyclonal anti-TrkB (#07-225, Millipore) diluted in PBS/1%BSA (working concentration 1 µg/ml) was plated and left 2 h at RT for the incubation. In this way only pTrkB were detected. After this incubation, the plate was washed 4 times with PBS/0.05%Tween20 and the secondary anti-rabbit IgG coupled to horseradish peroxidase (#31460, Thermo Fisher Scientific) diluted in PBS/1%BSA (working concentration 0.02 µg/ml) was added and incubated 1 h at RT. After these last 4 washes, the TMB One solution was plated and left shaking in the dark for up to 10 min inducing the colorimetric reaction (forming a blue color). Then, the reaction was stopped by the 1 N hydrochloric acid inducing, upon acidification, a color change from blue to yellow. Within 30 min of stopping the reactions the plate was read determining the optical density of each well immediately, using a spectrophotometer (TECAN InfiniteF500) set to 450 nm.

The values obtained from the samples at known concentrations were interpolated by a standard curve, which was used to calculate the pTrkB sample concentration. The Microsoft Excel software was used to create standard curves and executed calculations.

d. Lactate assay

Lactate contents were measured using an L-Lactate assay kit (#MAK064, Sigma) according to the manufacturer's instructions. Culture medium was collected from confluent cultures,

filtered through a 30 kDa cut-off spin filter and stored at -80°C until processing. Reaction reagents were prepared following the instructions and mixed with 50 µL of the samples, incubated at RT for 30 min protected from light, and the OD at 570 nm was determined. Lactate concentration was normalized to the number of cells.

4.7. Immunohistochemistry

a. Immunocytochemistry and image analysis on astrocytes

Embryonic astrocytes were fixed in 4% paraformaldehyde (PFA) for 15 min, then washed in PBS. Cells were subsequently permeabilized with 0.2% Triton-X 100 in PBS for 10 min at RT and then incubated with primary antibodies diluted in PBS 1% BSA overnight at 4°C. After washes in PBS, cells were incubated for 1 h with fluorescent secondary antibodies diluted in PBS 1% BSA, washed, and coverslips were finally mounted with Mowiol. All the antibodies used are reported in **Table 4**.

Antibodies	**Production Company**	**Product code**	**Dilution**	**Specie**
pTrkB (Tyr^{516})	Cell Signaling	4619	1:250	Rabbit
GFAP	Synaptic System	173004	1:500	Guinea pig
Hoechst	Sigma-Aldrich	B2261	1:500	
Alexa Fluor 488	Thermo-Fisher Scientific	A11029	1:500	Goat anti rabbit
Alexa Fluor 647	Thermo-Fisher Scientific	A21450	1:500	Goat anti guinea pig

Table 4 List of the antibodies used for the immunohistochemistry analysis

Confocal stacks were acquired with a Leica SP8 using a 40X oil immersion objective (NA 1.40), with 1 µm between optical sections. Images were analyzed using the ImageJ software (NIH). The maximal fluorescence intensities of in-focus stacks were z-projected and the resulting images were automatically thresholded. Regions of interest (ROIs) were manually drawn around the extremities of all GFAP positive cells in the respective channel and fluorescence intensity was measured in the pTrkB channel. Quantification was performed on 18-20 fields per condition from three independent preparations. Data were reported as the average fluorescence intensity in all GFAP+ cells in the field.

b. Golgi Cox Staining

I. Sample preparation

For this type of analysis, a commercial kit (FD Rapid GolgiStaining™ Kit FD, #PK401A Neurotechnologies) was used. This kit contains all the different solutions required for the staining. 24 h before collecting the brains, the solution A+B was prepared. The brains were taken without perfusion, washed with milliQ water and placed inside 15 ml Falcon tubes filled with 5 ml of A+B solution. The following day the solution was changed with 5 ml of fresh one. Falcon tubes were covered with aluminium foil and samples were incubated in the dark for 10 days. At the end of this incubation, the brains were transferred into tubes containing 5 ml of solution C [5% potassium chromate (K_2CrO_4)] for 3-4 days, after which they were ready to be cut.

II. Brain sections

Brain sections were obtained using a vibratome. The vibratome bath was filled with homemade solution C. Section thickness was set to 120 µm. Sections were placed on gelatin-coated slides and left to dry in the dark O/N at RT.

III. Staining

Slices were washed twice with milliQ water for 4 min and incubated for 10 min in a solution made of 1 part of solution D, 1 part of solution E and 2 parts of milliQ water. Slides were then washed twice with milliQ water for 4 min and then dehydrated with increasing concentrations of ethanol (50% - 75% - 95% ethanol / H_2O), for 4 min each. Last, 4 washes with 100% ethanol were performed. After, sections were cleaned 3 times for 4 min using Xylene under the hood. Coverslips were then mounted on top of the slides using mowiol.

IV. Imaging of slices

Image acquisition was carried out using the brightfield setting on a Leica SP8 microscope. Golgi-stained slices were first imaged using a 10X air objective in order to get low-magnification pictures of the entire hippocampus. We then sequentially used 20X air and 40X oil-immersion objectives focusing on the granule cells of the dentate gyrus. Images of single neurons were captured using a 63X oil-immersion objective, acquiring z-stacks with a z-step of 1µm.

V. Analysis

For each animal brain, at least 3 slices were taken into consideration. In each slice at least 3 dentate gyrus neurons were chosen and for each one at least 3 dendrites were selected. Having set a distance of 20 μm from the cell body, spines were counted across a 30-40 μm length. Results are expressed as the average number of spines in a 10 μm-dendrite stretch.

4.8. Calcium imaging on astrocytes

Astrocytes at 7-8 DIV after lentivirus infection were loaded with 1 μg/ml Fura-2-AM (#F1221, ThermoFisher) in astrocyte culture medium for 30 min at 37 °C. Subsequently, cells were washed in recording buffer (10 mM HEPES pH 7.4, 150 mM NaCl, 3 mM KCl, 1 mM $MgCl_2$, 10 mM glucose and 2 mM $CaCl_2$) for 30 min at 37°C to allow hydrolysis of the esterified groups. Coverslips with cells were mounted on the imaging chamber and loaded with 0.45 ml of recording buffer. Fura-2-loaded cultures were observed with an inverted Leica 6000 microscope using a 63x oil immersion objective. For analyzing BDNF-evoked Ca^{2+} transients, 50 μl of BDNF solution (final concentration 20 ng/ml, as reported in [25] #B3795, Sigma) were manually added to the culture medium 15 s after the beginning of the recordings. Where indicated, cells were preincubated with 150 nM K-252a (tyrosine kinase blocker, #K1639, Sigma), 1 μM ANA-12 (TrkB receptor antagonist, #SML0209, Sigma), 10 μM U73122 (PLCγ inhibitor, #U6756, Sigma) or 10 μM U73343 (inactive analog, #U6881, Sigma) for 10 min before the beginning of the recordings. Samples were excited at 340 and 380 nm and images of fluorescence emission at 510 nm were acquired using a Hamamatsu-C9100-02-LNK00 camera. Calcium levels were estimated from background subtracted ratio images (340/380nm) of Fura-2-loaded astrocytes at the cell body level according to the equation of Grynkiewicz [122]:

$$\left[\mathrm{Ca}^{2+}\right] = K_d \times \frac{R - R_{\min}}{R_{\max} - R} \times \frac{F^{380}_{\max}}{F^{380}_{\min}},$$

where R is the measured 340/380 nm ratio; R_{min} and R_{max} are the ratios in the absence of Ca^{2+} or when Fura-2 is saturated by Ca^{2+}, and $F^{380}{}_{max}$ and $F^{380}{}_{min}$ are the fluorescence intensity of 380 nm excitation at 0 Ca^{2+} and at Ca^{2+} saturation. To determine the Kd in our system, in situ calibration was performed by using 1 μM of the Ca^{2+}-ionophore ionomycin

in recording buffer containing an increasing concentration of Ca^{2+}, ranging from 1 nM to 10 mM.

4.9. Rescue experiment

The protocol was performed following [123]. 7,8-dihydroxyflavone (DHF) (TCI, Tokyo Chemical industry Ltd., #D1916) was used in order to investigate the effect of a BDNF mimetic in our animal model.

The drinking solution was 0.2% sucrose in H_2O for both the vehicle (DMSO) and the treatment (DHF) groups. The DMSO and the DHF concentration in the drinking solution was 0.08%. The DHF was firstly suspended in DMSO at 100 mg/ml, aliquoted and stored at -20°C. The amount of DHF administered to the animals was 80 µg/ml. The DHF treatment was applied starting 3 weeks before the behavioral experiments. The treatment was maintained while the behavioral experiments were performed. Solution intake was monitored and bottles changed every 3 days. All the drinking bottles were covered with aluminium foil to avoid DMSO oxidation. Behavioral experiments were performed during the last week of treatment.

The mice tested were 3-5 months old. The animals were 2-3 per cage, in a climate-controlled animal facility (22◦C±2◦C), maintaining a 12 h light/dark cycle. Even though only cKO and WT and +/+ and lox/lox mice were tested, heterozygotes for both genotypes were kept in the cages to avoid changes in housing conditions. Food and water were available ad libitum. 1 h habituation in a third room was mandatory before performing all tests. Males and females were tested separately in all tests, cleaning the apparatus with 70% ethanol between different animals as well as different trials. Experimenters were blind to the mouse genotype during testing and behavioral scoring.

a. Open field

Basic locomotor activity was tested in the open field test by placing each animal in a large square empty open arena (45 cm X 45 cm X 45 cm) surrounded by non- transparent sides for 30 min under red light. The mice were situated in the center of the maze at the beginning of the test. An overhead camera recorded the animals and the video was stored, tracked and analyzed by the Stoelting ANY-maze software (U.S.A.). A square 20 cm X 20 cm zone was determined in the center of the arena (marked as the central zone). The Stoelting ANY-maze software (U.S.A.) calculated the total distance covered and the amount of time that the mice

spent in the central zone.

4.10. Statistical analysis

The statistical analysis is described in the figure legends. All data were tested for normality (D'Agostino & Pearson test for n>6 or the Shapiro-Wilk test for n≤6) and outliers (ROUT test). For comparing two groups, Student's t-test for normal data and Mann-Whitney test for non-parametric data or one-sample t-test were used.

When more than two groups were compared, 2 way RM-ANOVA test was performed with Sidak's *post-hoc* test or Tukey's post hoc multiple comparison test. Alpha levels for all tests were 0.05% (95% confidence intervals). Statistical significance was set at P value < 0.05, using the GraphPad Prism statistical software 9.1.0 as indicated in figure legends.

For all the experiments in this thesis the n was calculated setting the power of the test as ≤0,85 with the formula

$$n = 2\left[\left(z_{\frac{a}{2}} - z_b\right)\frac{\sigma}{d}\right]^2$$

where $z_{\frac{a}{2}}$ is 1.96 for type I error α=0.05, z_b -0.86 for type II error β=0.05, σ is the is the standard deviation (in %, calculated from preliminary data obtained from similar experiments or from data present in the literature) and d is the minimum difference between groups (in %) detectable in a single experiment.

5. Results

5.1. Investigating the role of Kidins220 in primary astrocytes

a. Kidins220 has an impact on the expression of the specific BDNF receptor TrkB but not on the main downstream proteins in embryonic astrocytes.

In order to identify the role of Kidins220 in the modulation of BDNF signaling in astrocytes, we compared expression of TrkB in wildtype (+/+) and Kidins220$^{-/-}$ primary astrocytes by using western blot analysis. Compared with wild-type cells, Kidins220$^{-/-}$ astrocytes displayed a significant reduction of both full-length (~40%) and truncated TrkB forms (~50%), while the ratio between these two isoforms remained unchanged (**Figure 9A**). We also verified the expression of the other BDNF receptor, p75^{NTR}. In this case no differences were detected in the expression of p75^{NTR} between the two genotypes (**Figure 9B**).We then evaluated the expression of the main downstream effectors of the BDNF-TrkB pathway, i.e., mitogen-activated protein kinases 1 and 2 (MAPK1 and 2) / extracellular regulated kinase ½ (Erk1/2), phospholipase C-gamma-1 (PLCG1, hereafter referred to as PLCγ) and Akt. Whereas total protein levels of MAPK1/2 and Akt1, 2 and 3 (hereafter referred to as Akt) were unaffected, we found a significant reduction of PLCγ in Kidins220$^{-/-}$ astrocytes (**Figure 9C**). It is known that the main TrkB isoform expressed by astrocytes is the truncated one. There has been some indication that primary astrocytes also express full length neurotrophin receptors under physiological conditions and/or upon specific stimuli [113, 124, 125]. In our culturing conditions, primary glial cultures are predominantly represented by astrocytes – with only a small percentage of microglial cells [114]. We wanted to confirm that the observed activation of signaling pathways is, indeed, ascribable to astrocytes. Thus, we performed immunostaining experiments using antibodies specifically recognizing TrkB phosphorylated at Tyr516, i.e., the site required to be phosphorylated to activate MAPK, as well as antibodies against GFAP. Indeed, stimulation with BDNF increased fluorescence intensity of pTrkB in GFAP-positive cells, confirming that full-length TrkB activation occurred in astrocytes (**Figure 9D**). Together these results show that, similar to its function in neurons [68, 116], Kidins220 is a crucial regulator of BDNF-dependent TrkB signaling also in astrocytes.

For each figure, the contribution of the Candidate and of other Colleagues is indicated. If not specified, all experiments were performed by the Candidate.

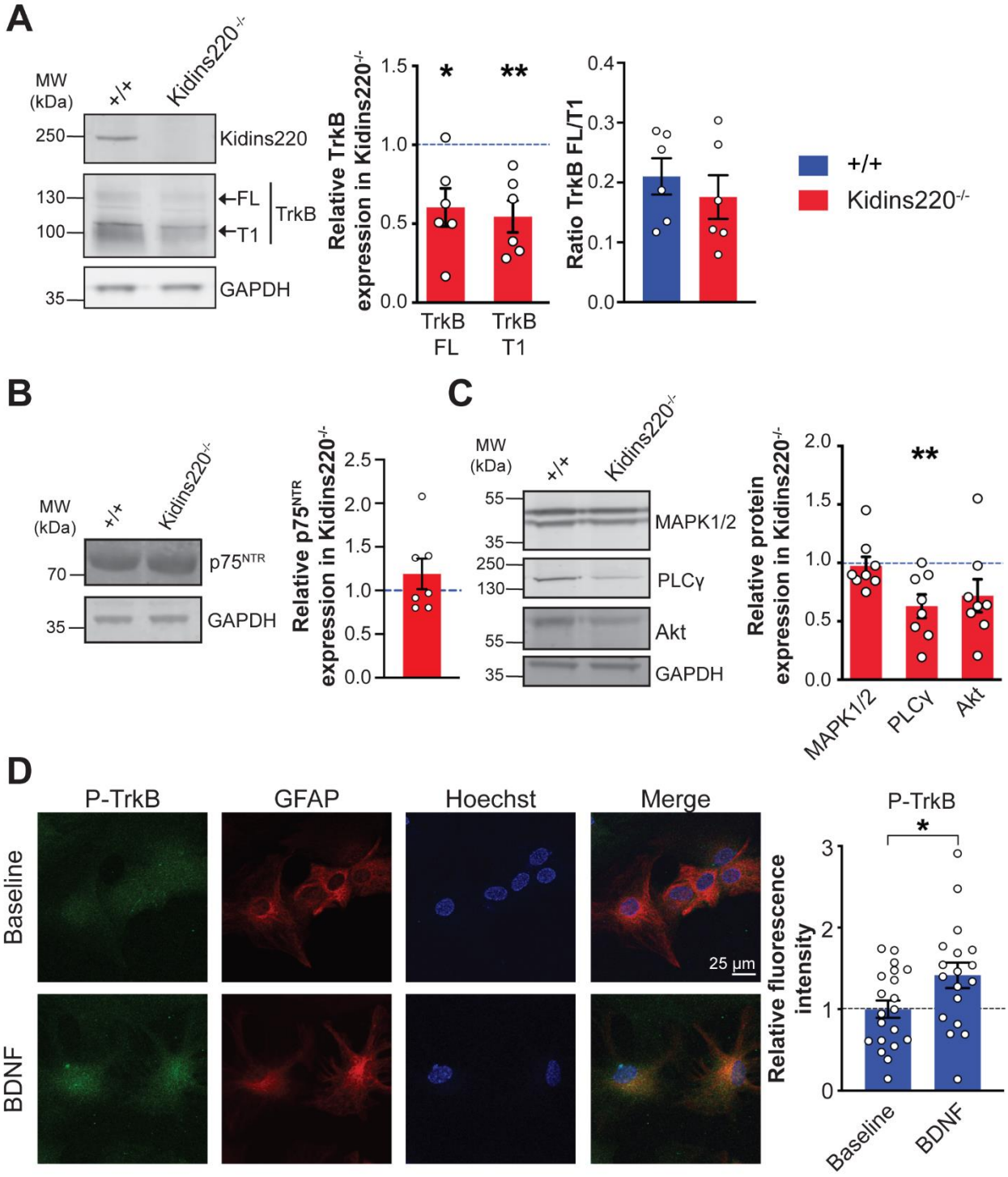

Figure 9 TrkB expression and signaling are reduced in Kidins220$^{-/-}$ embryonic astrocytes. (A,B,C) Protein extracts from wild-type (+/+) and Kidins220$^{-/-}$ embryonic astrocyte cultures at 15 DIV were analyzed by western blotting using anti-Kidins220 and anti-TrkB antibodies (A); anti-p75NTR antibodies (B); anti-MAPK1/2, anti-PLCγ and anti-Akt antibodies (C). Representative immunoblots are shown on the left; quantification of immunoreactive bands is plotted on the right. The intensity of bands from Kidins220$^{-/-}$ samples was normalized to that of corresponding wild-type samples within the same nitrocellulose membrane. *P<0.05, **P<0.01, one sample Student's t-test; wild-type and Kidins220$^{-/-}$ cultures were n=6 (A), n=7 (B), and n=8 (C). (D) Left: Representative confocal images of wild-type astrocytes treated with BDNF (1 ng/ml for 5 min) or not treated, stained with anti-pTrkB (Tyr516, green), anti- GFAP (red)

antibodies and Hoechst to visualize nuclei. Scale bar: 25 µm. Right: Quantification of pTrkB fluorescence intensity in GFAP-positive cells. *P<0.05, unpaired Student's t-test, n=20 (not treated) and 18 (BDNF-treated) cells from three independent preparations. Data show the average pTrkB fluorescence intensity of all GFAP-positive cells within each field. Values are expressed as means ± S.E.M.

Contribution: Experiments in panels A-C were performed by Dr. Jaudon; experiments in panel B-D were performed by Ms. Albini.

b. BDNF induces the activation of intracellular signaling pathways mediated by full-length TrkB and Kidins220 in embryonic astrocytes

We then asked whether ablation of Kidins220 in these cells affects the response to BDNF and TrkB-mediated signaling. At 15 DIV, astrocytes were treated with 50 ng/ml BDNF for 5 or 30 min and levels of phosphorylated forms of MAPK1/2, PLCγ and Akt (P-MAPK, P-PLCγ and P-AKT, respectively) were quantified by western blotting using phospho-specific antibodies (**Figure 10A**). The basal levels of phosphorylated MAPK1/2 and Akt were unchanged in Kidins220$^{-/-}$ astrocytes while we detected a significant reduction of the basal PLCγ phosphorylation levels. Treating the astrocytes with BDNF (50 ng/ml) we observed a reduction of P-MAPK1/2 in Kidins220$^{-/-}$ astrocytes that reached statistical significance at 30 min. Instead the percent increase in PLCγ phosphorylation induced by BDNF was similar between wild-type and Kidins220$^{-/-}$ astrocytes. We also tried to prolong the treatment with BDNF up to 2 h. This did not increase the levels of pMAPK and pAkt in wild-type or Kidins220$^{-/-}$ astrocytes; moreover, in knock-out (KO) samples, levels of pMAPK and pAKT dropped to even lower levels compared with those in wild-type cells exposed to BDNF for 2 h (**Figure 10B**). This indicates that the absence of Kidins220 affects the magnitude of the BDNF response and not its kinetics. A similar trend was observed when BDNF was used at lower concentration (1 ng/ml). However, in this case, the fold increase of MAPK phosphorylation was reduced compared to that when 50 ng/ml BDNF were used for stimulation (**Figure 10C**). Of note, we were unable to detect reliable phosphorylation of PLCγ under these experimental conditions (not shown).

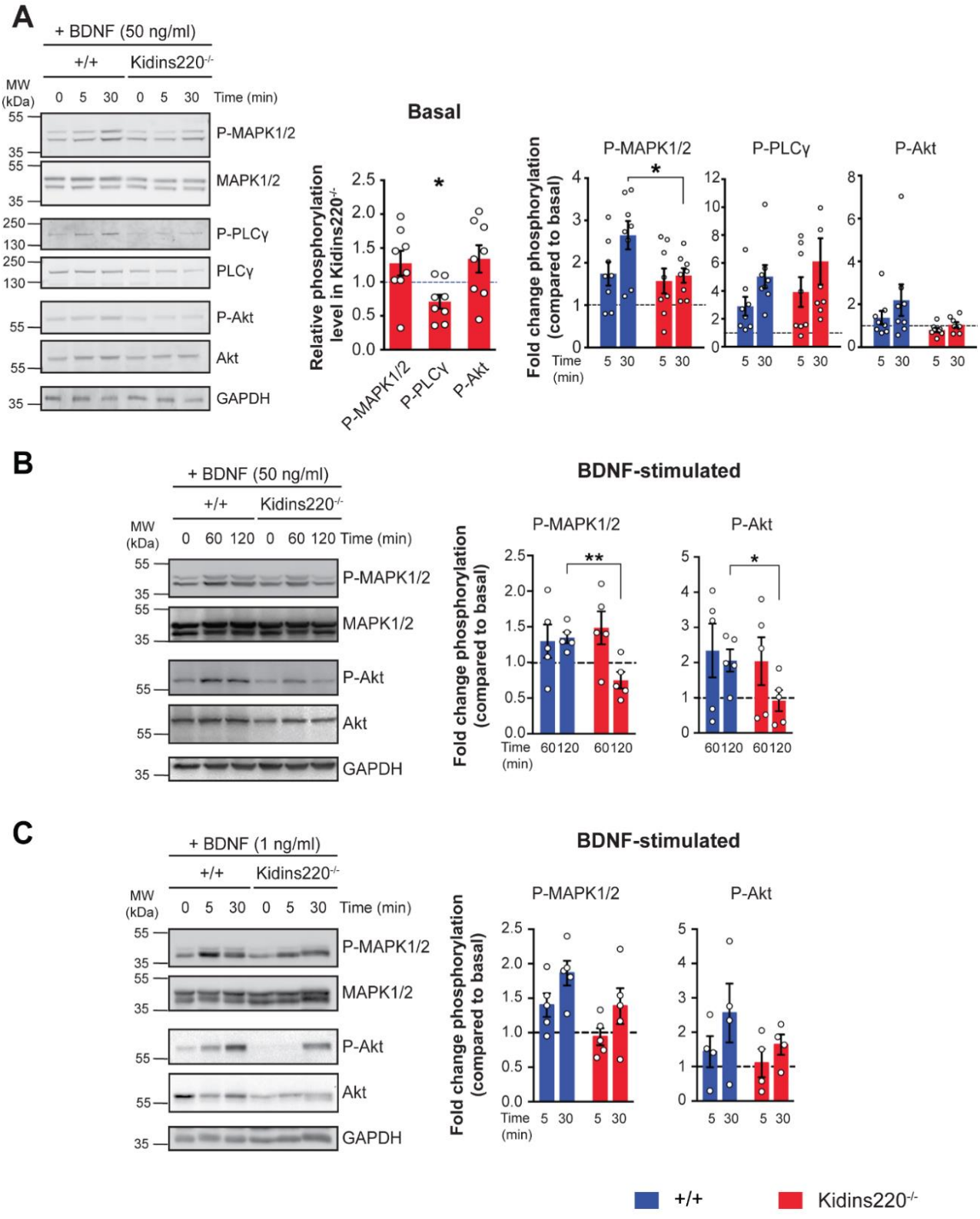

Figure 10 TrkB-dependent BDNF signaling is impaired in Kidins220$^{-/-}$ embryonic astrocytes. (A,B) Wild-type and Kidins220$^{-/-}$ astrocyte cultures were treated with 50 ng/ml BDNF for 5, 30 (A), 60 and 120 min (B) or left untreated. Wild type and Kidins220$^{-/-}$ embryonic astrocyte cultures were treated with 1 ng/ml BDNF for 5 and 30 min or left untreated (C). Lysates were analyzed for phosphorylated MAPK1/2 (Thr202/Tyr204; P-MAPK1/2), PLCγ (Tyr783; P-PLCγ) and Akt (Ser473; P-Akt). Membranes were subsequently stripped and re-probed for the total amount of the same protein. Representative immunoblots are shown on the left. Phosphorylation of MAPK1/2, PLCγ and Akt in lysates of untreated wild-type and Kidins220$^{-/-}$ cells (basal levels)

are plotted in panel A (middle graph). The intensity of bands from Kidins220$^{-/-}$ samples was normalized to that of corresponding wild-type samples within the same nitrocellulose membrane. Time dependence of MAPK1/2, PLCγ and Akt phosphorylation upon stimulation with BDNF of wild-type and Kidins220$^{-/-}$ astrocytes is plotted on the right. Graphs show the fold-change of MAPK1/2, PLCγ and Akt activation compared to phosphorylation levels in untreated samples for each genotype, set to 1 (dashed line in all graphs). The fold-change activation was calculated as follows: we first calculated the phospho:total intensity ratio for each sample, and subsequently divided the phospho:total ratio of every treated sample by the phospho:total ratio of the untreated (control) sample within the same membrane. For MAPK, we calculated the sum of MAPK1 and MAPK2 immunoreactivity. *P<0.05, unpaired Student's t-test, n=8 for both wild-type and Kidins220$^{-/-}$ cultures. For all experiments, GAPDH was used as a loading control. PLCγ did not show any reliable activation at 1 ng/ml BDNF concentration (not shown). *p<0.05, **p<0.01, unpaired Student's t-test, n=8 in (A), n=5 in (B) and n=4-5 in (C) for both wild type and Kidins220$^{-/-}$ cultures. Values are expressed as means ± S.E.M.

c. Expression of full-length TrkB is reduced in postnatal wild-type astrocytes

It has been described that astrocytes undergo important physiological changes from the embryonic development to the postnatal period, accompanied by variations in the expression pattern of several signaling proteins [126]. For this reason, we decided to compare the expression levels of full-length and truncated TrkB receptors in wild-type embryonic and postnatal preparations. We found a specific reduction of the full-length isoform in postnatal cultures that led also to a decrease in the ratio of TrkB:TrkB-T1 with respect to the embryonic cells (**Figure 11A**). In contrast, p75^{NTR} expression did not change with the developmental stage (**Figure 11B**).

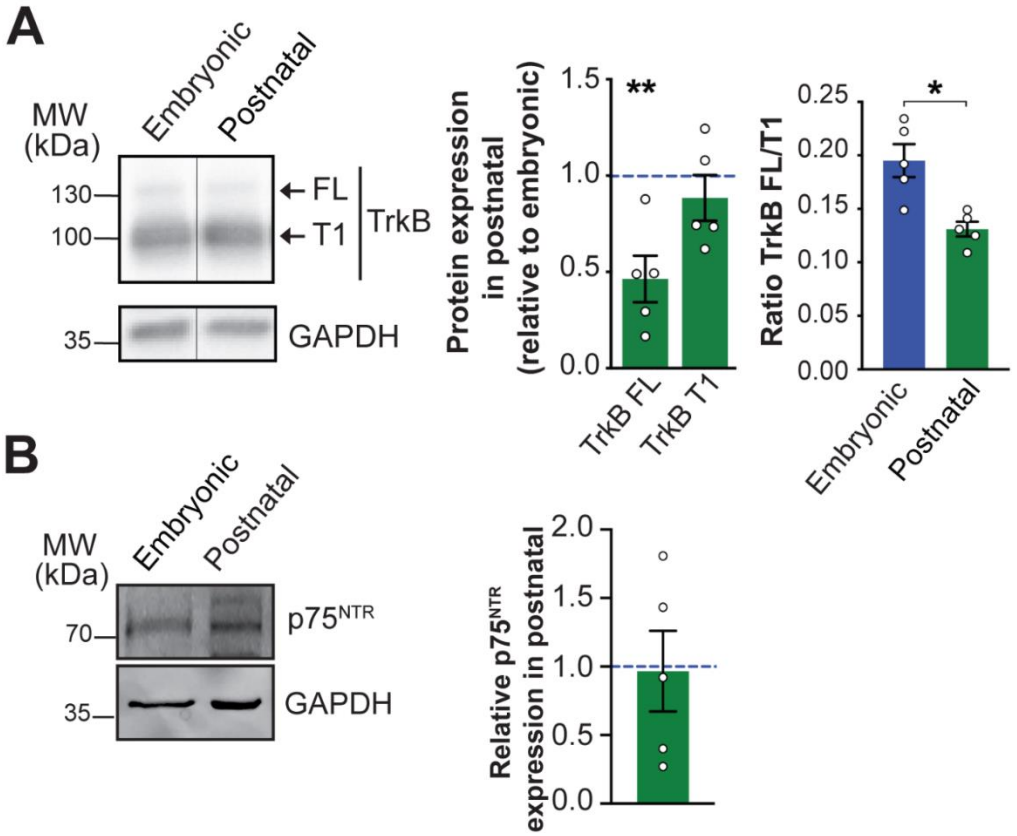

Figure 11 Expression of full-length TrkB is reduced in postnatal astrocytes. (A) Protein extracts from wild-type embryonic and postnatal cultures were analyzed by western blotting using anti-TrkB antibodies (A) and anti-p75^{NTR} antibodies (B). A representative immunoblot is shown on the left; quantification of immunoreactive bands is plotted on the right. Intensity of bands from postnatal samples was normalized to the corresponding bands from wild-type embryonic samples within the same nitrocellulose membrane. *P<0.05, **P<0.01, one sample Student's t-test, n=5 wild-type embryonic and postnatal cultures. Values are expressed as the means ± S.E.M. in all panels.

We also verify if, upon BDNF stimulation, the expression level of the main proteins involved in the neurotrophin downstream pathways were affected during development. Wild-type postnatal cultures exposed to 50 ng/ml BDNF showed an appreciable increase of phosphorylated Akt and MAPK1/2, although the fold-increase of P-MAPK1/2 was less than that observed in embryonic cultures (1.2-fold versus 2.5-fold at 30 min; compare **Figure 12A** and **Figure 10A**). This could be due to the reduced full-length TrkB expression. Using a lower BDNF concentration (1 ng/ml) we obtained a similar trend (**Figure 12B**).

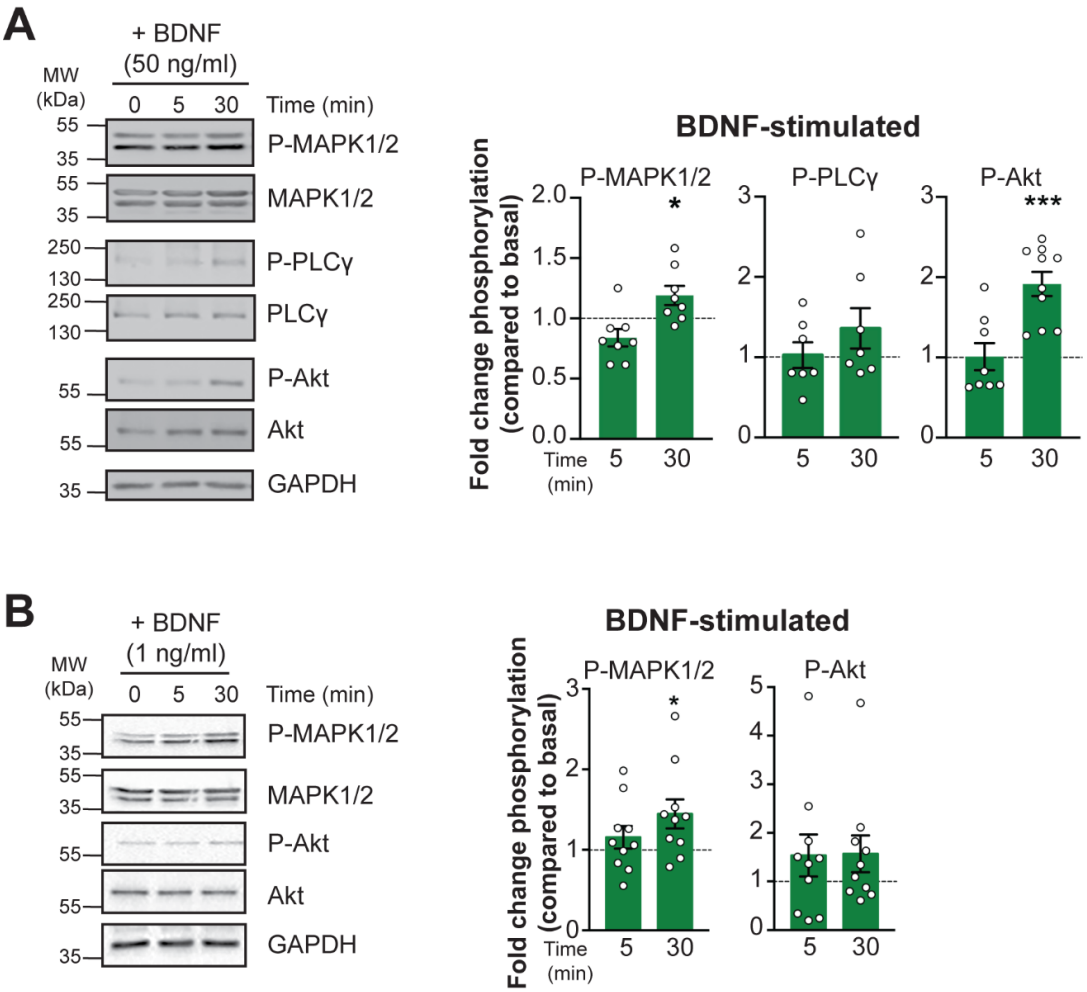

Figure 12 Activation of signaling pathways upon administration of BDNF in wild type postnatal astrocytes. Postnatal wild-type astrocyte cultures were treated with 50 ng/ml (A) or 1 ng/ml (B) BDNF for 5 or 30 min, or left untreated (0). Protein extracts from wild type embryonic and postnatal astrocytes were analyzed for phosphorylated MAPK1/2 (Thr202/Tyr204; P-MAPK1/2), Akt (Ser473; P-Akt) and PLCγ (Tyr783; P-PLCγ). Membranes were subsequently stripped and re-probed for the total amount of the same protein. Representative immunoblots are shown of the left. Time dependence of MAPK1/2, PLCγ and Akt phosphorylation in response to BDNF in wild-type postnatal astrocytes is shown on the right. Graphs express the fold change of MAPK1/2, PLCγ and Akt activation compared to phosphorylation levels in untreated samples, set to 1 (dashed line in all graphs). *p<0.05, one sample Student's *t*-test compared to baseline, n=7–8 independent cultures (A) and n=10 (B) independent cultures. Values are expressed as means ± S.E.M.

Contribution: All the experiments were performed by Dr. Jaudon and Ms. Albini.

d. Kidins220 controls expression levels of both TrkB and TrkB-T1 but is dispensable for activation of BDNF-dependent kinase pathways in postnatal astrocytes

In order to investigate if Kidins220 ablation affect the BDNF pathway in postnatal astrocytes, primary Kidins220$^{lox/lox}$ cultures were infected with lentiviruses expressing either the active form of Cre recombinase to induce depletion of Kidins220 or a functionally inactive form of Cre (ΔCre) as control ([120]; see Materials and Methods for details). We refer to these cultures as Kidins220-depleted (Kidins220$^{lox/lox\text{-}Cre}$) and control

(Kidins220$^{lox/lox-\Delta Cre}$) cultures. Kidins220$^{lox/lox-Cre}$ showed reduced levels of full-length and truncated TrkB compared to the Kidins220$^{lox/lox-\Delta Cre}$ astrocytes. The TrkB:TrkB-T1 ratio (**Figure 13A**) and the levels of p75^{NTR} were unchanged in the absence of Kidins220 (**Figure 13B**). Both results are in full agreement with those obtained on embryonic cultures. We then investigated if the absence of Kidins220 affects also the main proteins involved in the BDNF signaling. The basal expression levels of MAPK1/2, PLCγ and Akt were not affected by depletion of Kidins220 (**Figure 13C**).

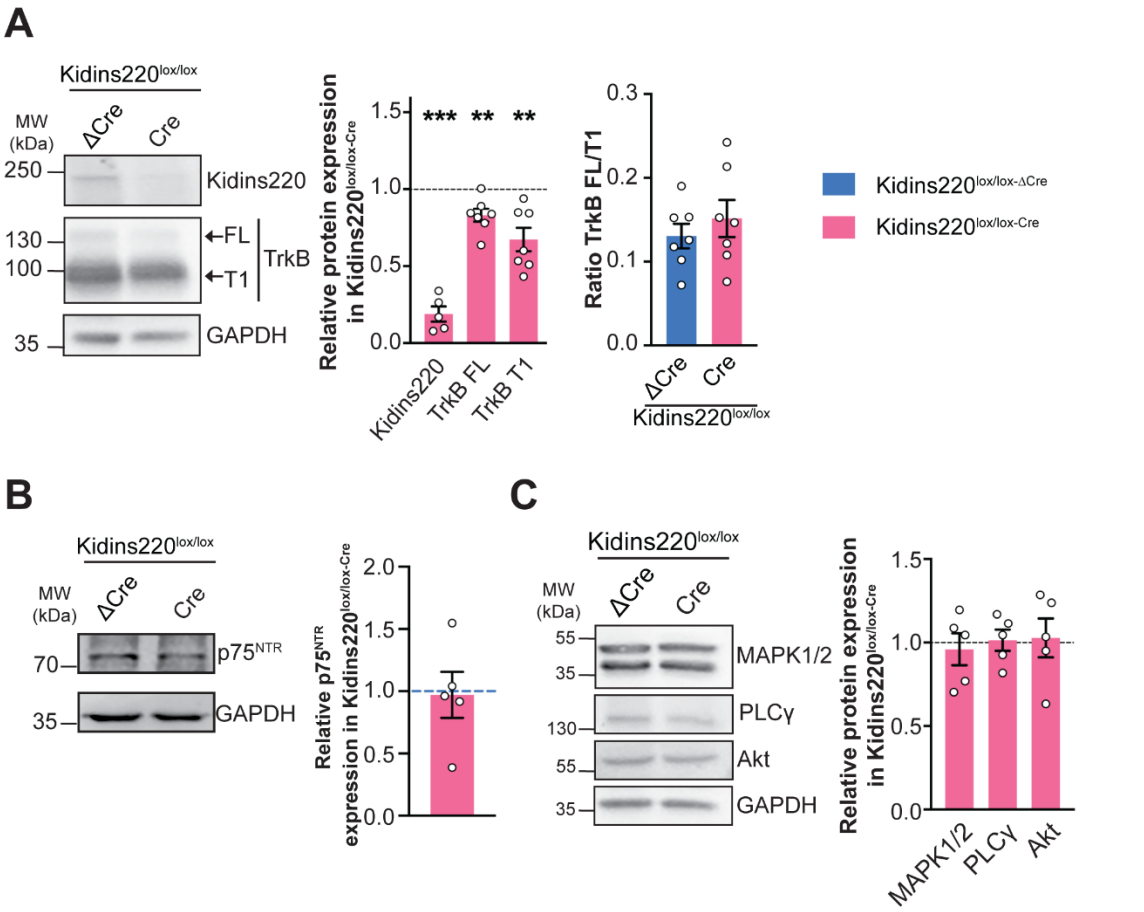

Figure 13 Removal of Kidins220 in postnatal astrocyte cultures affects the expression of both TrkB isoforms. Protein extracts from Kidins220$^{lox/lox}$ P0-P1 astrocyte cultures infected with lentiviruses encoding catalytically dead (ΔCre) or active Cre recombinase were analyzed by western blotting using anti-Kidins220 and anti-TrkB antibodies (A), anti-p75^{NTR} (B) and anti-MAPK1/2, anti-PLCγ and anti-Akt antibodies (C). Representative immunoblots are shown on the left; quantification of immunoreactive bands is plotted on the right. The intensity of bands from Kidins220$^{lox/lox-Cre}$ samples was normalized to the corresponding bands from Kidins220$^{lox/lox-\Delta Cre}$ samples within the same nitrocellulose membrane. **P<0.01, ***P<0.001, one sample Student's t-test, n=5-7 Kidins220$^{lox/lox}$ cultures. Values are expressed as the means ± S.E.M. in all panels.

Contribution: All the experiments were performed by Dr. Jaudon and Ms. Albini.

Moreover, in contrast to the data obtained in embryonic cultures, removal of Kidins220 in postnatal cultures did not affect activation of BDNF-induced phosphorylation of MAPK1/2, PLCγ and Akt (**Figure 14**).

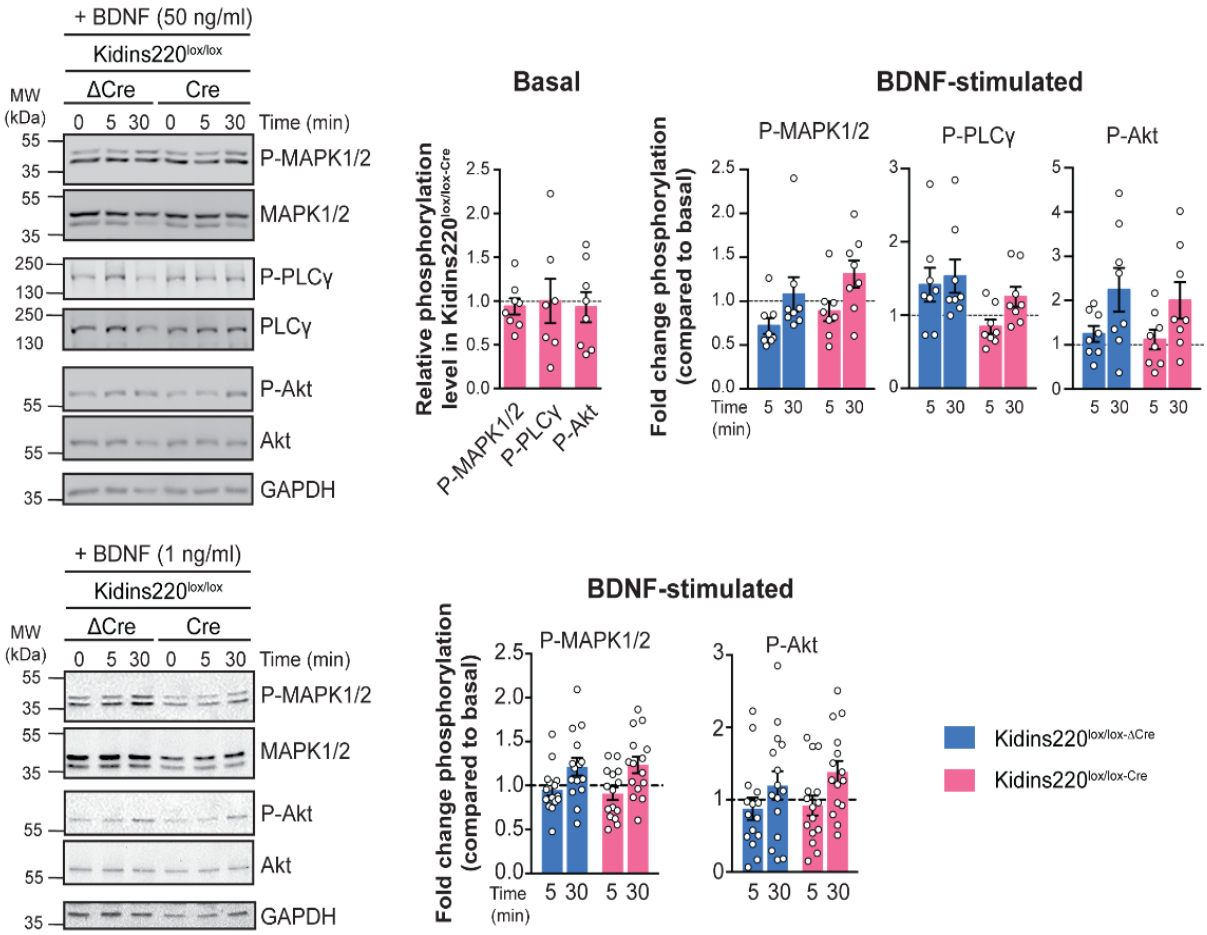

Figure 14 Activation of signaling pathways upon administration of BDNF in Kidins220-deficient postnatal astrocytes. Kidins220$^{lox/lox\text{-}Cre}$ and Kidins220$^{lox/lox\text{-}\Delta Cre}$ astrocyte cultures were treated with 50 ng/ml (A) or 1 ng/ml (B) BDNF for 5, 30 min or left untreated. Lysates were analyzed for phosphorylated MAPK1/2 (Thr202/Tyr204; P-MAPK1/2), Akt (Ser473; P-Akt) and PLCγ (Tyr783; P-PLCγ). Membranes were subsequently stripped and re-probed for the total amount of the same protein. The left panel shows representative immunoblots. The middle panel shows the quantification of basal levels of P-MAPK1/2, P-PLCγ and P-Akt in untreated lysates. The right panel shows the fold change of phosphorylation for P-MAPK1/2, P-PLCγ and P-Akt upon BDNF stimulation in Kidins220$^{lox/lox\text{-}Cre}$ and Kidins220$^{lox/lox\text{-}\Delta Cre}$ astrocytes compared to levels of phosphorylation in untreated samples for each genotype, set to 1 (dashed line in all graphs). The fold-change of phosphorylation was calculated as described in **Figure 10**. For MAPK, we report the sum of MAPK1 and MAPK2 immunoreactivity. P>0.05, unpaired Student's t-test, n=8 independent Kidins220$^{lox/lox}$ cultures. Values are expressed as the means ± S.E.M. in all panels.

Contribution: All the experiments were performed by Dr. Jaudon and Ms. Albini.

Altogether, these data show:

- reduced protein levels of full-length TrkB and reduced activation of kinase pathways upon exposure to BDNF in wild-type postnatal astrocytes compared to embryonic cells;
- a further reduction of both TrkB and TrkB-T1 levels in the absence of Kidins220. However the limited activation of kinase pathways induced by BDNF was not impacted upon depletion of Kidins220.

e. Depletion of Kidins220 impairs BDNF-induced $[Ca^{2+}]_i$ transients in postnatal astrocytes

We subsequently investigated the role played by Kidins220 in BDNF-induced $[Ca^{2+}]_i$ signaling by monitoring BDNF-induced $[Ca^{2+}]_i$ transients in astrocytes [25]. In embryonic cultures, very few cells responded to BDNF stimulation (9.8% for +/+ and 7.4% for Kidins220$^{-/-}$, **Figure 15A**) and responsive cells displayed modest $[Ca^{2+}]_i$ variations (**Figure 15B-C**). In contrast, around 30-35% of cells in postnatal cultures responded to BDNF with sizable $[Ca^{2+}]_i$ peaks (**Figure 15D-F**). Whereas the percentage of responding cells was not affected by Kidins220 depletion **(Figure 15D**), the average amplitude of the BDNF-induced $[Ca^{2+}]_i$ transients was significantly reduced in absence of Kidins220 (**Figure 15E** and **F**; # $p < 0.05$ genotype effect). To investigate the contribution of the different isoforms of TrkB in this process, we repeated the same experiments in the presence of either the tyrosine kinase blocker K-252a [116] to inhibit specifically the full-length TrkB isoform, or the TrkB antagonist ANA-12 [127] to block both full-length and truncated TrkB receptors. Pre-incubation of the cells with K-252a did not affect the percentage of BDNF-responding cells (**Figure 15D**, shaded). However, the amplitude of the observed $[Ca^{2+}]_i$ influx was reduced independently of the presence of Kidins220 (**Figure 15F** and **G**; genotype effect: p=0.0120 (#); K-252a treatment effect: 0,004 (**); treatment x genotype interaction: p=0.3987, see legend for more details), suggesting that the BDNF-induced $[Ca^{2+}]_i$ variations involved full-length TrkB receptors. BDNF-stimulation in presence of ANA-12 did not induce any response, confirming that the residual signal was attributable to TrkB-T1 activation (**Figure 15H**). Furthermore, the observed response was completely dependent on PLCγ activity, as shown by the absence of BDNF-induced $[Ca^{2+}]_i$ transients in the presence of the specific PLCγ inhibitor U73122 (**Figure 15I**).

Altogether, these data show that BDNF induces modest $[Ca^{2+}]_i$ events in embryonic astrocytes, while appreciable $[Ca^{2+}]_i$ responses are elicited in postnatal cells. Postnatal $[Ca^{2+}]_i$ transients are fully dependent on TrkB receptors, as shown by their complete inhibition in the presence of ANA-12. Interestingly, part of this response is mediated by the full-length receptor, as shown by the partial reduction of amplitude in the presence of K-252a. Moreover, our results show that Kidins220 plays an active role in this process, as in its absence the amplitude of $[Ca^{2+}]_i$ events is reduced.

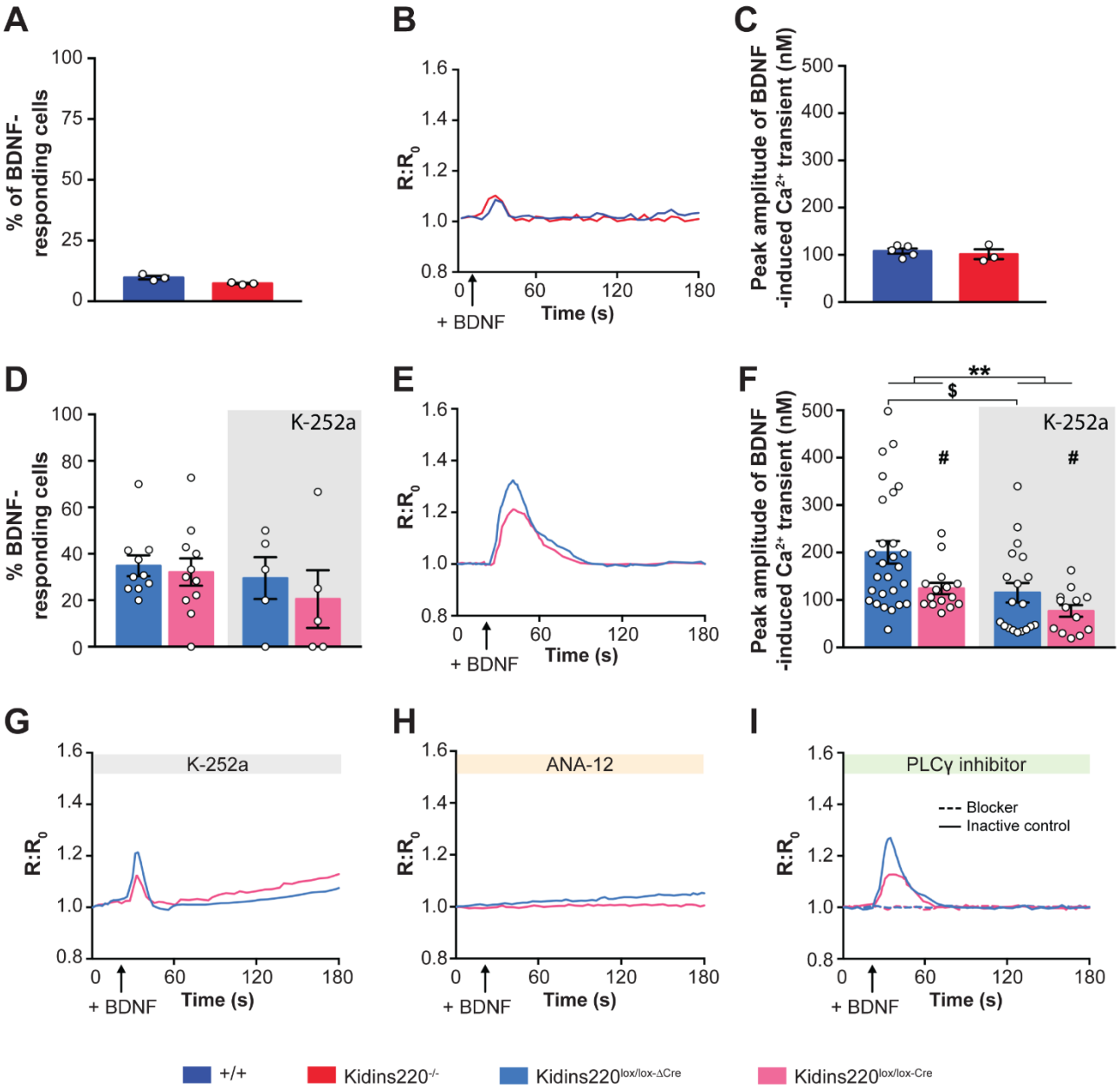

Figure 15 Depletion of Kidins220 in postnatal cultures impairs BDNF-induced Ca^{2+} transients. (A–C) BDNF-induced $[Ca^{2+}]_i$ transients in embryonic wild-type (+/+) and Kidins220$^{-/-}$ astrocytes. Percentage of cells displaying Ca^{2+} transients in response to BDNF (20 ng/ml) stimulation. n=3 for both wild-type and Kidins220$^{-/-}$ cultures (A). $[Ca^{2+}]_i$ transients were defined when R:R0≥0.025. Time-course of $[Ca^{2+}]_i$ transients (B) and peak amplitude (C) of BDNF-evoked Ca^{2+} levels in wild-type and Kidins220$^{-/-}$ astrocytes. (D–I) BDNF-induced $[Ca^{2+}]_i$ transients in postnatal Kidins220$^{lox/lox\text{-}Cre}$ and

Kidins220$^{lox/lox-\Delta Cre}$ astrocytes. Percentage of cells displaying $[Ca^{2+}]_i$ transients in response to BDNF (20 ng/ml) stimulation in the presence or absence of the tyrosine kinase blocker K-252a (D). n=5 and 10 Kidins220$^{lox/lox}$ cultures with and without K-252a, respectively. Time-course of Ca^{2+} transients (E) and peak amplitude (F) of BDNF-evoked Ca^{2+} influx in Kidins220$^{lox/lox-Cre}$ and Kidins220$^{lox/lox-\Delta Cre}$ astrocytes in the absence or presence of K-252a. Two-way ANOVA followed by Tukey's multiple comparison test; $ P=0,0152 treated versus untreated Kidins220$^{lox/lox-\Delta Cre}$ [genotype effect: F(1, 70)=6.656, #P=0.0120; K-252a treatment effect: F(1, 70)=8.837, **P=0,004; treatment×genotype interaction: F(1, 70)=0.7211, P=0.3987], n=27 and 15 cells from six independent cultures for Kidins220$^{lox/lox-\Delta Cre}$ and Kidins220$^{lox/lox-Cre}$ cells in the absence of K-252a, and n=19 and 13 from six independent cultures for Kidins220$^{lox/lox-\Delta Cre}$ and Kidins220$^{lox/lox-Cre}$ cells in the presence of K-252a. Time-course of $[Ca^{2+}]_i$ transients evoked by BDNF in Kidins220$^{lox/lox-\Delta Cre}$ and Kidins220$^{lox/lox-Cre}$ astrocytes in the presence of the TrkB receptor kinase inhibitor K-252a (G), the pan-TrkB antagonist ANA-12 (H), the active PLCγ inhibitor U73122 (dashed lines) or its inactive analogue U73343 (solid lines) (I). Values are expressed as the means ± S.E.M. in all panels.
Contribution: Experiments in panels A-C were performed by Dr. Jaudon; experiments in panel D-I were performed by Ms. Albini.

f. BDNF stimuli promote gene transcription in postnatal astrocyte cells

To clarify the functional effects of BDNF signaling in astroglia, we analyzed the transcriptional profile of cultures treated with 1 ng/ml BDNF for three days. We focused on four genes whose expression is crucial for astrocytes physiology i.e., the excitatory amino acid transporter 2 (Slc1a2, hereafter referred to as GLT-1), the ATP sensitive inward rectifier potassium channel 10 (Kcnj10, hereafter referred to as Kir4.1), aquaporin 4 (Aqp4) and gap junction alpha-1 protein (Gja1, hereafter referred to as Cnx43) (**Figure 16A**). Whereas the expression of the genes encoding GLT-1, Kir4 or Cnx43 was insensitive to BDNF, at least within the time frame of our experiment, transcription of Aqp4 was selectively reduced upon prolonged stimulation (72 h) with BDNF (*P=0.0153, treatment effect). Although Kidins220 deficiency did not alter the transcription response to BDNF, it selectively and markedly reduced the Kir4.1 expression independently of BDNF (##P=0.0067, genotype effect), at both the RNA and protein level, the latter confirmed by western blot analysis (**Figure 16B**).

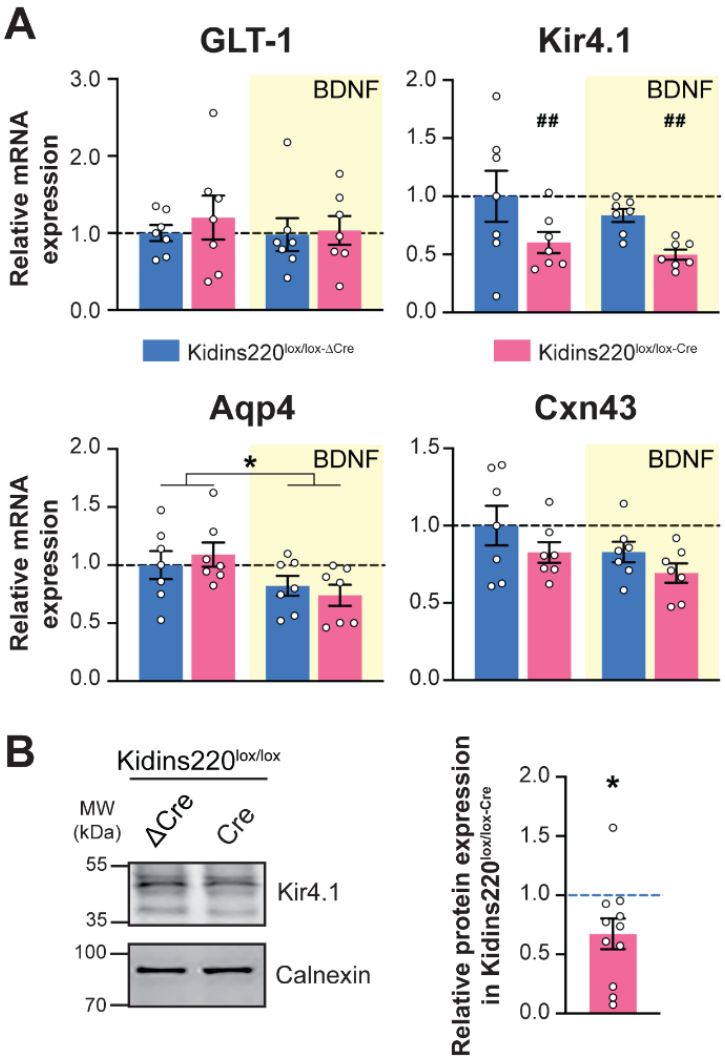

Figure 16 Transcription of genes encoding Aqp4 or Kir4.1 is reduced in response to prolonged treatment with BDNF or Kidins220 deficiency, respectively, in postnatal astrocytes. (A) mRNA expression profile of Slc1a2 (GLT-1), Kcnj10 (Kir4.1), Aqp4 and Gja1 (Cnx43) in postnatal Kidins220$^{lox/lox-\Delta Cre}$ and Kidins220$^{lox/lox-Cre}$ astrocytes treated or not with BDNF (1 ng/ml) for 72 h (see Materials and Methods). mRNA levels in the various samples were normalized to respective levels in untreated Kidins220$^{lox/lox-\Delta Cre}$ samples within the same RT-qPCR plate. Two-way ANOVA followed by Tukey's multiple comparison test. *P<0.05 versus untreated, ##P<0.01 versus Kidins220$^{lox/lox-\Delta Cre}$. GLT-1: Genotype effect: F (1, 24)=0.3813, P=0.5427; BDNF treatment effect: F(1, 24)=0.2042, P=0.6554; treatment×genotype interaction: F(1, 24)=0.1262, P=0.7255. Kir4.1: Genotype effect: F (1, 24)=8.817, ##P=0.0067; BDNF treatment effect: F(1, 24)=1.179, P=0.2883; treatment×genotype interaction: F(1,24)=0.06038, P=0.8080. Aqp4: Genotype effect: F (1, 24) =0.002003, P=0.9647; BDNF treatment effect: F(1, 24)=6.817, *P=0.0153; treatment×genotype interaction: F(1, 24)=0.7202, P=0.4045. Cnx43: Genotype effect: F(1, 24)=3.302, P=0.0817; BDNF treatment effect: F(1, 24)=3.183, P=0.0870; treatment×genotype interaction: F(1, 24)=0.04637, P=0.8313. n=7 independent Kidins220$^{lox/lox}$ cultures. (B) Protein extracts from Kidins220$^{lox/lox}$ P0-P1 astrocyte cultures infected with lentiviruses encoding catalytically dead (ΔCre) or active Cre recombinase were analyzed by western blotting using anti-Kir4.1 antibodies and anti-calnexin antibodies as loading control. A representative immunoblot is shown on the left; quantification of immunoreactive bands is on the right. The band intensity from Kidins220$^{lox/lox-Cre}$ samples was normalized to corresponding band intensity from Kidins220$^{lox/lox-\Delta Cre}$ samples within the same nitrocellulose membrane. *P<0.05, one sample Student's t-test, n=11 Kidins220$^{lox/lox}$ cultures. Values are expressed as the means ± S.E.M. in all panels.

These data suggest that:

- prolonged exposure to BDNF alters the expression of specific astrocyte genes;
- Kidins220 plays a role in the maintenance of astrocyte homeostasis and K^+ buffering function by modulating the expression of Kir4.1.

g. Glycolytic metabolism increases in astrocytes during development and is modulated by Kidins220 at the embryonic stage

One of the main functions of astrocytes is to provide neurons with metabolic support, both under physiological conditions and in situations of high energetic demand. Amongst the numerous astrocyte-derived molecules involved in this process, lactate plays a prominent role both as a metabolic and as a signaling molecule [128]. To assess the levels of glycolytic versus oxidative phosphorylation metabolism, we quantified the amount of lactate in the medium of embryonic and postnatal astrocytes, in the presence and absence of Kidins220 (**Figure 17**). Interestingly, we found that the production of lactate in wild-type postnatal cells is increased compared with that in embryonic cells, suggesting a predominant glycolytic mechanism. Remarkably, Kidins220$^{-/-}$ embryonic cells produce three times more lactate compared to wild-type astrocytes, suggesting impaired mitochondrial metabolism , whereas at the postnatal stage lactate levels in Kidins220-depleted cells are comparable to those in wildtype cultures.

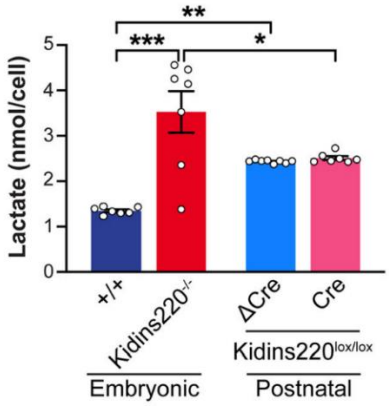

Figure 17 Kidins220 contributes to cell metabolism and BDNF signaling in astrocytes. (A) Lactate concentration (nmol/cell) was measured in culture medium harvested from confluent cultures of embryonic wild-type (+/+) and Kidins220$^{-/-}$ astrocytes (Embryonic, left), and postnatal Kidins220$^{lox/lox\text{-}\Delta Cre}$ and Kidins220$^{lox/lox\text{-}Cre}$ astrocytes (Postnatal, right). Two-way ANOVA followed by Tukey's multiple comparisons test, *P<0.05, **P<0.01, ***P<0.001. Genotype effect: F(1, 25)=25,57, P<0.001; developmental stage effect: F(1, 25)=0.02569, P=0.87; genotype×developmental stage interaction: F(1, 25)=22,37, P<0.001. n=7-8 cultures. Values are expressed as the means ± S.E.M.

Altogether, these data show that the astrocytic metabolism changes during development by way of increasing the glycolytic power, and reveal a novel and previously unknown role of Kidins220 in cell energy metabolism.

5.2. Investigating the role of Kidins220 *in vivo*

a. Generation of animals bearing the CaMKII-Cre driven, forebrain-specific deletion of Kidins220

The conditional knockout of Kidins220 (cKO) was achieved as described in Materials and Methods. The mentioned four experimental groups are: cKO ($Kidins220^{lox/lox;+/Cre}$) and WT ($Kidins220^{+/+;+/Cre}$); lox/lox ($Kidins220^{lox/lox}$) and +/+ ($Kidins220^{+/+}$). Analyzing the mice born during the last 4 years we observed that +/+, +/lox and lox/lox were born at the expected mendelian ratios. Differently, cKO mice are less than expected (**Figure 18**).

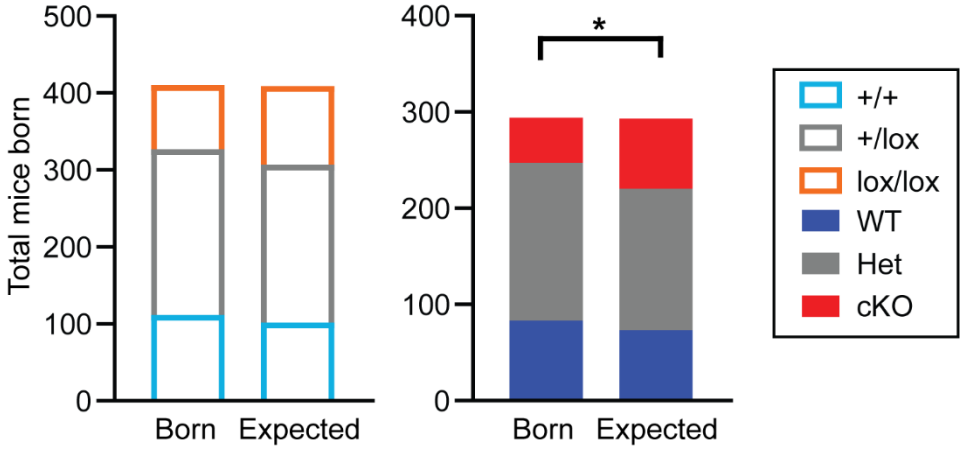

Figure 18 Kidins220 ablation affects the mendelian ratio. Comparison between actual and expected birth for all the genotypes. All the genotypes follow the mendelian ratio except the cKO mice, which are less than expected. $Kidins220^{lox/lox}$ (lox/lox, orange), $Kidins220^{lox/+}$ (+/lox, grey), and $Kidins220^{+/+}$ (+/+, light blue) (*left*), $Kidins220^{lox/lox;\ Cre/+}$ (cKO, red), $Kidins220^{lox/+;Cre/+}$ (Het, grey), and $Kidins220^{+/+;Cre/+}$ (WT, blue) (*right*). Chi-square test (*p<0.05).

Kidins220 expression was evaluated in brain areas of cKO and lox/lox animals by western blot analysis at 3 months. First of all, Kidins220 expression was comparable in the two control groups (**Figure 19A**): as expected, the presence of the Cre enzyme did not affect Kidins220 expression in the WT group. Instead, the presence of only the full-length isoform in the lox/lox group caused a significant reduction in the protein levels. In fact when we analyzed the lox/lox group we observed around 50% reduction in Kidins220 protein amount compared to the corresponding controls (+/+)(**Figure 19B**). When cKO and lox/lox samples were compared directly on the same membrane, we confirmed the specificity of the Cre enzyme. In fact we obtained a significant reduction of Kidins220 expression both in the

cortex and hippocampus of cKO samples while in the cerebellum, where the transgene is not expressed, protein levels are comparable with those of the lox/lox mice (**Figure 19C**). A second, lower band was also found in some samples, which could correspond to some post-translation modification like, for example, glycosylation.

A complete ablation of the protein is not expected, since the activation of the CaMKII promoter is restricted to excitatory neurons, leaving Kidins220 expression unaffected in inhibitory neurons and glial cells, where the protein is also present [114, 119]. Altogether, these data show that:

- the forebrain-specific knockout of Kidins220 was successfully achieved, obtaining viable animals;
- the alteration of Kidins220 splicing pattern causes a global reduction of the protein expression level.

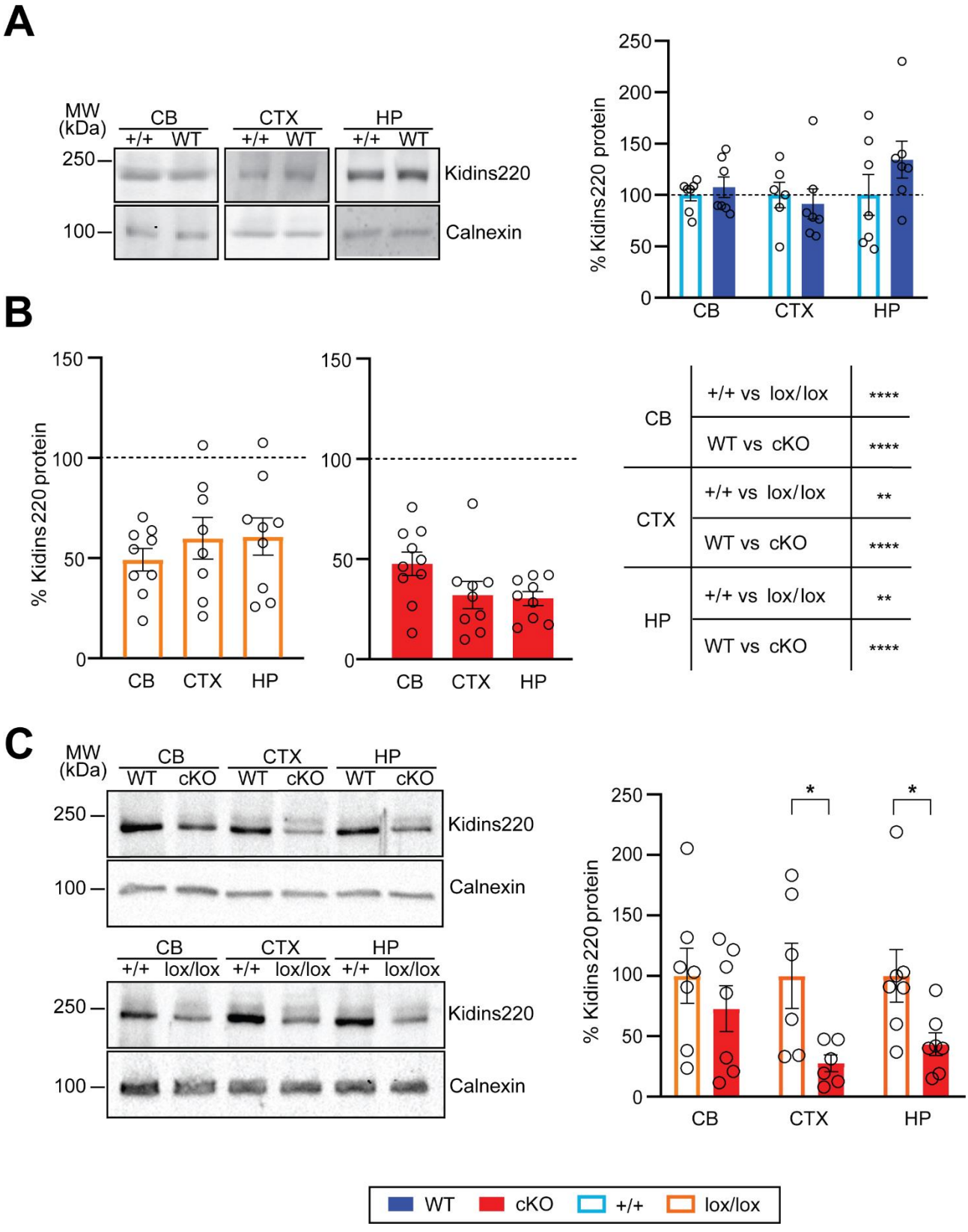

Figure 19 Generation of animals bearing the CaMKII-driven, forebrain-specific deletion of Kidins220. Animals were sacrificed at 3M. Brains were dissected into cerebellum (CB), cortex (CTX) and hippocampus (HP), lysed and analyzed by western blotting with anti-Kidins220 and anti-calnexin antibodies to verify equal loading. (A) *Left:* representative immunoblots for +/+ and WT animals. *Right*:quantification of immuno reactive bands for WT, compared to the +/+ samples within the same nitrocellulose membrane, set to 100%. No

difference in Kidins220 expression were detected between the two genotypes. Unpaired Student's *t*-test; p>0.05, n = 6-7 for +/+ and WT. (B) *Left*: Quantification of immunoreactive bands for lox/lox (orange) and cKO (red), compared to the corresponding control samples (dashed lines) set to 100%. *Right*: the intensity of the bands from lox/lox and cKO samples were normalized to the intensity of bands of their respective controls within the same nitrocellulose membrane and differences were tested by one sample Student's t-test; significance levels are reported in the table. N: Cerebellum: lox/lox 9, cKO 10; Cortex: lox/lox 8, cKO 9; Hippocampus: lox/lox 9, cKO 9. **p<0.01, ***p<0.001; ****p<0.0001. (C) *Left:* representative immunoblots for WT and cKO animals (*top*), +/+ and lox/lox animals (*bottom*) are shown. *Right*: The comparison of Kidins220 expression levels in lox/lox and cKO brain lysates ran on the same nitrocellulose membrane shows a significant reduction of Kidins220 protein in the cortex and hippocampus of cKO mice compared to lox/lox, while in the cerebellum expression levels are comparable. Unpaired Student's t-test, *p<0.05; n: Cerebellum: lox/lox 7, cKO 7; Cortex: lox/lox 6, cKO 6; Hippocampus: lox/lox 7, cKO 7. Normalized values are plotted as mean ± S.E.M. and individual values are represented with circles.

b. Altered spine development in hippocampal neurons of cKO mice

As described in the preliminary results, Kidins220 ablation affects the development of the neurons of both the motor cortex and the dentate gyrus. Since we observed longer and more complex dendritic ramifications in cKO granule neurons [93], we wondered if also the spine density can be altered. We performed the Golgi-Cox staining and we discovered that the increased complexity of the dendritic ramification observed in cKO granule neurons was accompanied by a reduction of the spine density (**Figure 20**).

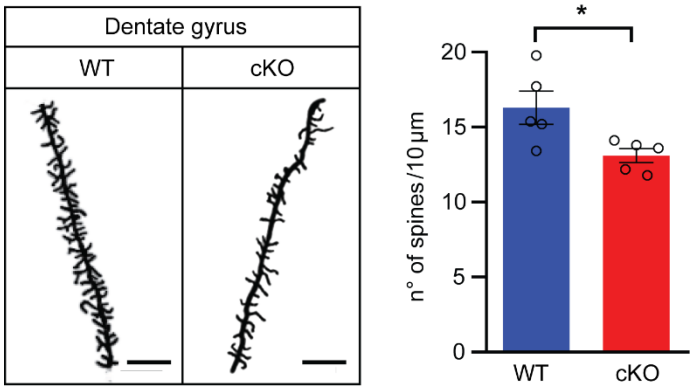

Figure 20 Kidins220 cKO mice display reduced spine density in the dentate gyrus of the hippocampus. Brains were dissected from 3M-old cKO and WT animals and the dentate gyrus of the hippocampus was processed for Golgi-Cox staining. *Left:* representative images; scale bar: 5 µm. *Right*: quantification of the number of spines/10 µm-dendrite stretch shows a significant reduction in cKO animals compared to WT (unpaired Student's *t*-test, *p<0.05; n=5 animals per genotype. At least 18 dendrites from 6 different cells per animal were analysed. Circles indicate the average number of spines for each animal). All data are expressed as means ± S.E.M.

We wondered if the altered neuron development observed in the cKO was due to the full ablation of Kidins220 or could be due to the absence of the isoforms. For this reason, we quantified by Sholl analysis the dendritic branching in the sensory and motor cortices and in the dentate gyrus of the hippocampus of +/+ and lox/lox mice, showing no differences in dendrite arborization in all the areas analyzed (**Figure 21**).

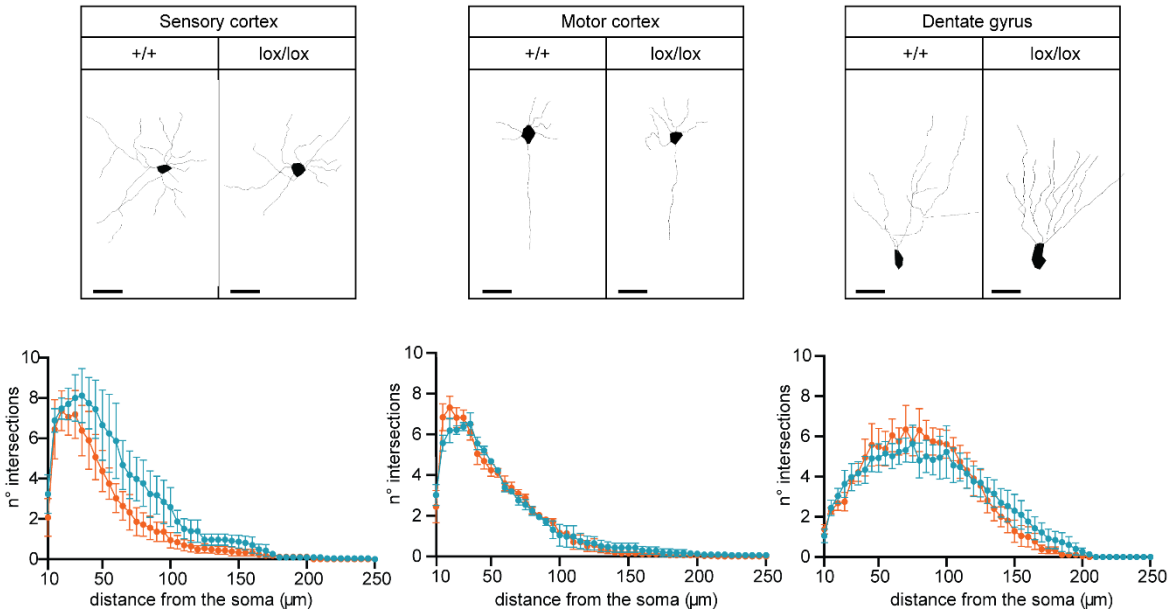

Figure 21 Kidins220 lox/lox mice do not display altered dendritic branching in the cortex and dentate gyrus. Lox/lox (orange) and +/+ (light blue) animals at 3M of age were perfused, brains were dissected and processed for Golgi-Cox staining. *Upper panel*: representative images; scale bar, 100 µm. *Lower panel*: No differences in dendritic arborization was observed in the motor and sensory cortex, and in the granule cells of the hippocampus (RM-ANOVA/Holm-Šídák's multiple comparisons test. $p>0.05$; n=3 animals per genotype from 3 separate litters. 3-10 cells were analysed per animal). All data are expressed as means ± S.E.M.

Contribution: Experiments were performed by Ms. Albini and Ms. Alicja Krawczun-Rygmaczewska.

These data show that in the adult brain, Kidins220 is involved in the maintenance of spine development of selected neuronal populations.

c. TrkB-dependent BDNF signaling is altered in Kidins220 cKO mice

The role played by Kidins220 in the regulation of neurotrophin signaling is well described [68, 69, 129]. To determine whether neurotrophin signaling was altered in our mouse lines, we first quantified the amount of the two main BDNF receptors TrkB and $p75^{NTR}$ in various brain areas of adult cKO and lox/lox animals and respective controls by western blot analysis. We found a reduction of full-length and truncated TrkB in the hippocampus of cKO and lox/lox mice and an increase

of the same receptors in the cKO cerebellum, while they remain constant in the cortex of all genotypes. p75^{NTR} expression was not affected by Kidins220 altered expression in all the samples analysed **(Figure 22A,B)**. The same analysis was performed on amygdala lysates, showing no differences in the expression levels of TrkB and p75^{NTR} receptors (**Figure 22C**).

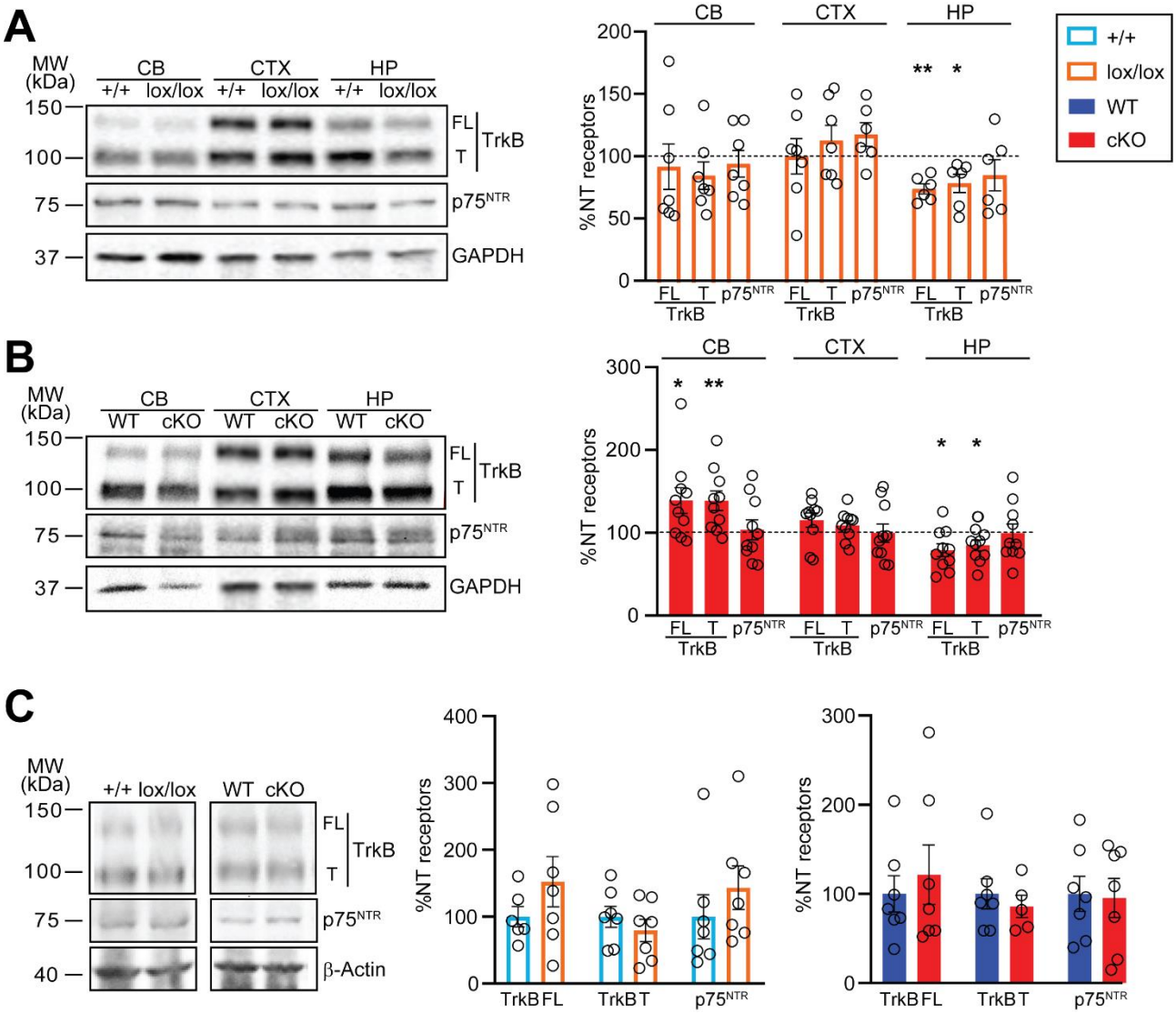

Figure 22 TrkB levels are reduced in the hippocampus of lox/lox and cKO mice. A,B. Cerebellum (CB), cortex (CTX), hippocampus (HP) and amygdalas of animals at 3M of age were lysed and analysed by western blotting with anti-TrkB and p75^{NTR} antibodies. *Left*: representative immunoblots for +/+ and lox/lox (A) and WT and cKO (B) animals are shown as indicated. *Right*: quantification of immunoreactive bands for lox/lox (orange) and cKO (red), compared to the corresponding control samples, set to 100% (dashed lines). Full length and truncated TrkB levels are significantly reduced in the hippocampus of lox/lox and cKO mice, and increased in the cerebellum of cKO mice. The expression of p75^{NTR} was not altered in any sample analysed. The intensity of the bands from lox/lox (orange) and cKO (red) samples were normalized to the corresponding ones from +/+ and WT samples within the same nitrocellulose membrane, respectively. One-sample Student's t-test, * p<0.05, **p<0.01 n =6-7 for +/+ and lox/lox; n=10 for WT, cKO. (C) TrkB and p75^{NTR} receptor levels in the amygdala are not affected in the absence of Kidins220. *Left*: representative immunoblots for +/+ and lox/lox, WT and cKO animals, as

indicated. *Right*: quantification of immunoreactive bands for the various genotypes. Unpaired Student's t-test, p>0.05, n =5-7 for all genotypes. In all panels, values are plotted as mean ± S.E.M, and individual values are represented with circles.

We then measured the concentration of BDNF in cortical, hippocampal, striatal and cerebellar lysates of cKO and lox/lox mice by ELISA, showing no differences in all the analysed structures compared with the corresponding controls (**Figure 23**).

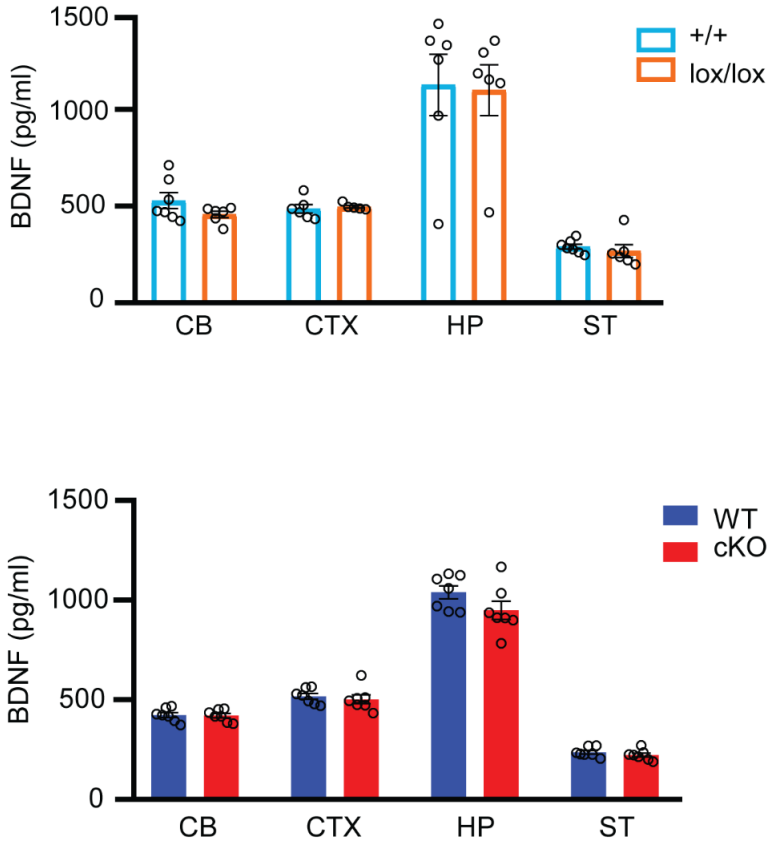

Figure 23 BDNF levels are comparable in the brain of +/+, lox/lox, WT and cKO mice. An ELISA assay was performed on lysates from cortex, hippocampus, cerebellum and striatum in lox/lox compared to +/+ (A) and in cKO compared to WT (B). Unpaired Student's t-test; p>0.05, n=6-7. +/+ (light blue), lox/lox (orange), WT (blue) and cKO (red). Pg/ml of protein are plotted as mean ± S.E.M and individual values are represented with circles.

We subsequently quantified the amount of phosphorylated TrkB (pTrkB) in hippocampal and cortical lysates through ELISA and interestingly, while no differences in pTrkB were detected in lox/lox samples compared to +/+, cKO animals showed markedly decreased pTrkB in the cortex, while the amount of pTrkB in the hippocampus was comparable to WT (**Figure 24A**).

Given the stronger phenotype observed in cKO mice, we restricted our subsequent analysis to cKO animals and asked whether BDNF/TrkB-dependent signaling was affected by the lack of Kidins220. Basal phosphorylation levels of MAPK1/2 and Akt were also assessed, showing a clear increase in basal pAkt in cKO cortical tissue (**Figure 24B**). To assess the responsiveness of the cKO brain to BDNF stimulation, coronal cortico-hippocampal slices were challenged with 10 ng/ml BDNF for 10 min and the phosphorylation levels of TrkB, MAPK1/2 and Akt were evaluated through ELISA and western blotting, respectively. cKO slices were characterized by reduced basal levels of pTrkB and pMAPK1/2 and increased basal levels of pAkt (**Figure 24C**, *middle*). Upon BDNF stimulation, we observed a significant increase in pTrkB and pAkt in cKO slices, while pMAPK1/2 was comparable to WT (**Figure 24C**, *right*).

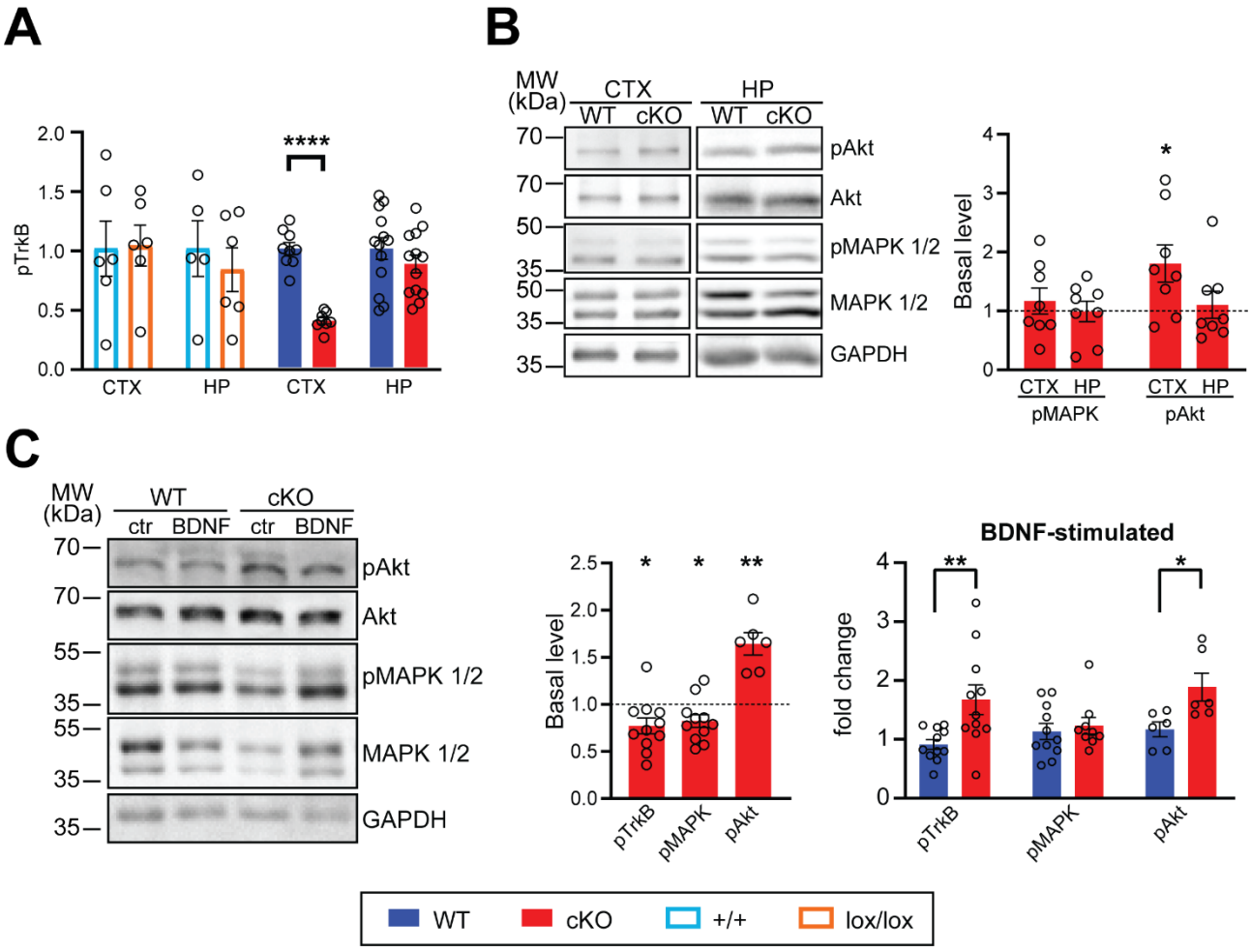

Figure 24. (A) Phosphorylated TrkB levels were analysed by ELISA in the cortex and hippocampus of +/+ and lox/lox, cKO and WT mice. P-TrkB levels were comparable in +/+ and lox/lox samples, while P-TrkB is strongly reduced in the cKO cortex. Values of lox/lox and cKO samples were normalized to values from +/+ and WT samples within

the same ELISA plate. Unpaired Student's *t*-test, ****p<0.001 n = 5-6 for +/+ and lox/lox; n = 9-13 for WT and cKO. (B) *Left*: representative immunoblots for WT and cKO animals. *Right: p*hosphorylated MAPK1/2 and Akt levels were analysed by western blotting in the cortex and hippocampus of cKO and WT mice. P-MAPK1/2 levels are similar in both genotypes while P-Akt is selectively increased in the cortex of cKO animals. One sample Student's *t*-test, *p<0.05, n=9-11 for pTrkB and pMAPK1/2, n=6 for pAkt. (C) WT and cKO coronal cortico-hippocampal slices were treated with 10 ng/ml BDNF for 10 min or left untreated. After treatment, slices were lysed and analysed for phosphorylated MAPK1/2 (Thr202/Tyr204) and Akt by western blotting, and for phosphorylated TrkB by ELISA. *Left*: for the western blot analysis, membranes were probed for phospho-MAPK1/2 and phospho-Akt, subsequently stripped and re-probed for the total amount of the same protein. *Middle*: Comparison of basal levels of phosphorylated TrkB, MAPK1/2 and Akt in untreated lysates. Values of cKO samples were normalized to the corresponding values from WT samples within the same nitrocellulose membrane or ELISA plate. One-sample Student's *t*-test, *p<0.05, **p<0.01. *Right*: fold change of TrkB, MAPK1/2 and Akt phosphorylation upon BDNF stimulation. Values of phosphorylated proteins were first normalized to the total amount of protein, and subsequently to the untreated samples. Student's unpaired *t*-test, *p<0.05, **p<0.05, n=6-11 animals per genotype. In all panels, values are plotted as mean ± S.E.M, and individual values are represented with circles.

Contribution: Experiments in panel A-B were performed by Ms. Albini, experiments in panel C were performed by Dr. Jaudon and by Ms. Albini.

Altogether, these experiments show that in the absence of Kidins220 the BDNF-TrkB system is affected at multiple levels: cKO mice are characterized by reduced TrkB expression in the hippocampus and reduced pTrkB levels in the cortex, as well as by altered activation of Akt under basal conditions and upon BDNF stimuli.

d. Partial rescue of the anxiety-like phenotype of Kidins220 cKO mice by boosting BDNF signaling

Given the well-established involvement of the BDNF/TrkB system in the circuits underlying anxiety [52, 130-132], we sought to rescue the reduced anxiety observed in the open field test by chronic administration of 7,8-DHF, a known agonist of BDNF signaling [133]. cKO mice receiving DHF showed a reduction of the time spent in the centre in last 10 min of the test (**Figure 25A**), so that their performance became indistinguishable from WT mice subjected to the same treatment, indicating that chronic activation of BDNF signaling is able to rescue, at least partially, the low-anxiety phenotype of cKO animals. The treatment is not affecting the activity of the mice independently of the genotype, as shown by the total distance travelled by the four experimental groups (**Figure 25B**). The pharmacological rescue experiments indicate that alterations in BDNF signaling

system underlie at least partially the low-anxiety phenotype shown by these animals.

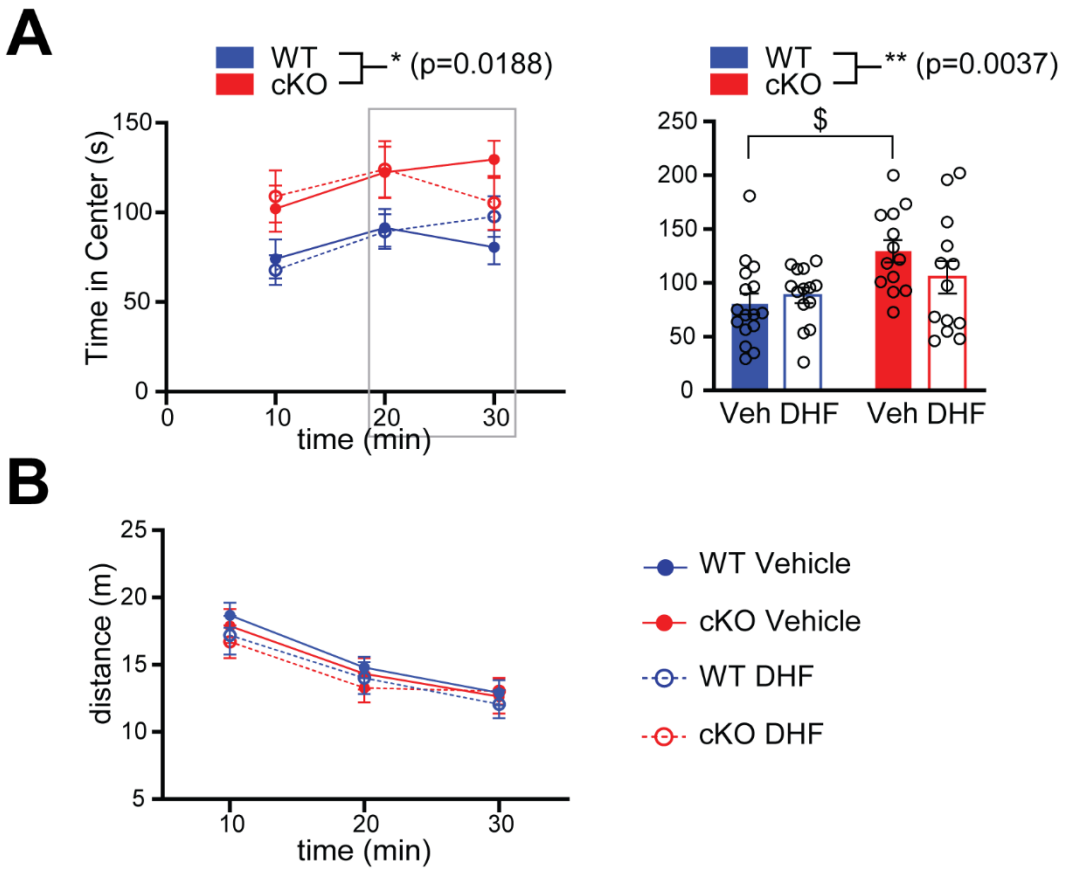

Figure 25 The BDNF agonist 7,8-DHF partially rescues the reduced anxiety levels of cKO mice. A. WT and cKO mice that received DHF or vehicle in the drinking water for 4 weeks were tested in the open field test. The experiment was performed and quantified as in Figure 5A. *Left*: cKO mice spent more time in the center of the arena, confirming the reduced anxiety phenotype ($F_{3, 53}$ = 3.623; *p<0.05 genotype effect, RM-ANOVA). *Right*: the bar graph shows the time spent in the center by the four experimental groups in the last 10 min of the test. Vehicle-treated cKO mice spent significantly more time in the center compared to WT animals ($F_{1, 52}$ = 9,250; **p<0.01 genotype effect, *p<0.05 two-way ANOVA/Holm-Šídák's multiple comparisons test), while no difference was detected between the DHF-treated groups. B. The distance travelled was comparable across genotypes ($F_{3, 51}$ = 0,2802; p>0.05 genotype effect, RM-ANOVA). WT Vehicle n=16; WT DHF n=15; cKO Vehicle n=13; cKO DHF n=13. In all panels, values are plotted as mean ± S.E.M, and individual values are represented with circles.

6. Discussion

Kidins220 is a scaffold protein commonly expressed in all cells of the central nervous system in a development-dependent manner. Most of the information about the role of Kidins220 in regulating brain activity was obtained using primary neurons from KO embryos or from adult heterozygous mice. Consequently, this leads to several questions that so far have not been addressed: which is the effect of Kidins220 total ablation on glial cells? Does Kidins220 removal at later developmental phases affect mouse growth and nervous circuit formation? To tackle these points, in this project we deeply investigated Kidins220 role in astrocytes, the most abundant cells present in the brain, and in an adult mouse model where Kidins220 ablation is limited to the excitatory neurons of the forebrain starting two weeks after birth.

6.1. Role of Kidins220 in mouse astrocytes

In 2018, Dallerac and colleagues described in detail that, during the development from the embryonic to the postnatal stage, glial cells are subjected to changes in several physiological processes, such as protein expression and the corresponding pathways [126]. For this reason, we studied the role of Kidins220 in both embryonic and postnatal astrocytes. We demonstrate that, in Kidins220$^{-/-}$ embryonic astrocytes, TrkB protein expression is strongly reduced, accompanied by a decrease of the downstream proteins PLCγ under basal conditions and phosphorylated MAPK under BDNF stimulation. Interestingly, the downregulation of phosphorylated MAPK is reported after 30 minutes of BDNF stimulation. After 1 h, it reaches comparable levels to those observed in wildtype astrocytes, and 2 h after BDNF administration MAPK activation is significantly reduced reaching even lower levels compared to the basal ones. Consistently, AKT expression also shows the same impairment at long timepoints. These data are in line with the well described role of Kidins220 as key regulator of the TrkB-dependent BDNF pathway, in particular sustaining the MAPK signaling [68, 69] and suggest that Kidins220 absence does not prevent the capability of astrocytes to respond to BDNF stimulation but affects its timing and kinetics.

It is largely reported that astrocytes mostly express one of the TrkB isoforms, the truncated one (TrkB-T) [134, 135], and there is limited evidence of TrkB full length expression [111, 113]. Interestingly, we were able to detect both TrkB isoforms in embryonic astrocytes, as well as in postnatal astrocytes, and we wondered if the pathways activated by the two

receptors are different between these developmental time points. We demonstrate that in our wildtype astrocytes the activation of downstream pathways is due to the phosphorylation of full length TrkB upon BDNF stimulation, further supporting the evidence of its expression in the astrocytes. We also observed that in wildtype postnatal astrocytes the expression of full length TrkB was significantly reduced compared to that observed in embryonic astrocytes, supporting the idea that TrkB phosphorylation plays a more prominent role during astrocytes' embryonic stage compared to its contribution to astrocyte physiology after birth [113]. Instead, the expression of TrkB-T does not change in the different developmental stages, so that the ratio between the two isoforms is altered in the postnatal astrocytes, favoring TrkB-T over full-length TrkB, further supporting that the main intracellular pathways activated in postnatal astrocytes upon BDNF stimulation are those initiated by TrkB-T. Nevertheless, we observed that pathways downstream of TrkB full length (both pMAPK and pAKT) are significantly activated at 30 minutes even if this receptor isoform is less expressed. This reinforces the hypothesis that the signaling cascades downstream to TrkB full length are active during the embryonic life of astrocytes but, if required, can be reactivated during later phases. In fact, it is largely reported that under several pathological conditions (i.e. injury, chronic diseases and tumors) astrocytes re-express the full-length TrkB receptor [136-141] and in this way re-activate all the developmental programs and BDNF-TrkB dependent pathways [142, 143].

It is important to highlight that we observed a high variability in the phosphorylation of the main BDNF downstream proteins in postnatal astrocytes when Kidins220 is removed. The full length TrkB expression in postnatal astrocytes lacking Kidins220 is reduced compared to the controls, however cells that do express TrkB may do so at different levels, suggesting cell heterogeneity even within the same genotype.

These results support the idea that the BDNF-dependent, kinase-based signaling cascades are activated principally in embryonic cultures, where the lack of Kidins220 indeed has a bigger impact compared to the postnatal astrocytes.

Looking at this evidence, we wondered if the removal of Kidins220 could also affect the postnatal astrocytes' response to BDNF. Interestingly, TrkB receptor expression is impaired also in postnatal Kidins220$^{lox/lox}$ astrocytes where Kidins220 expression was reduced through Cre infection, without any alteration in the TrkB/TrkB-T ratio, neither in the

expression of downstream proteins and of the co-receptor $p75^{NTR}$. In addition to the alteration of BDNF downstream pathways, in 2019 Jaudon and colleagues reported that embryonic Kidins220$^{-/-}$ astrocytes display an overall reduction in Ca^{2+} channel expression (in particular purinergic channels) and in ATP secretion. The disruption in Ca^{2+} homeostasis and in ATP production generate an unsuitable environment for neurons. The authors demonstrated that wildtype neurons grown onto embryonic Kidins220$^{-/-}$ astrocytes showed an alteration in the mean firing frequency at lower injected currents (<150 pA) and a consequent reduction of the rheobase associated with an impairment in arborization [114]. Given the importance of Ca^{2+} waves in astrocyte-to-astrocyte communication and in gliotransmitter release that regulates neuron firing, we can assert that the alteration of Ca^{2+} homeostasis in Kidins220$^{-/-}$ embryonic astrocytes directly affects neuronal activity by altering proper neuronal maturation and firing properties. In addition, the authors grew wildtype primary neurons in a Kidins220$^{-/-}$ astrocyte conditioned medium. Interestingly, neurons presented again an impairment in the firing rate, but at higher injected currents (>200 pA). In this specific case, neurons were incapable to withstand sustained action potential occurrence. The alteration in firing frequency could be associated with the strong reduction in ATP secretion by Kidins220$^{-/-}$ astrocytes. Curiously, Kidins220$^{-/-}$ neurons, when cultured alone, do not show any alteration in short-term plasticity [116] suggesting that the overall detrimental phenotype is determined by the combination of both astrocyte and neuron alterations.

Our data describe a developmental stage shift in the astrocytes' ability to elicit BDNF-dependent Ca^{2+} transients. In fact, both the number of BDNF-responding cells and the amplitude of Ca^{2+} transients are increased in postnatal astrocytes. Moreover, we showed that the Ca^{2+} transients observed upon BDNF stimulation are directly due to TrkB activation, highlighting that both TrkB isoforms play a key role in this response but confirming that the predominant component is triggered by TrkB-T [25]. Moreover, those transients are fully dependent on PLCγ suggesting that the pathways activated by both receptors converge on SOCE that, as previously described, can be directly altered by Kidins220 ablation [114]. In fact, in astrocytes Ca^{2+}release from intracellular stores lowers intra-ER Ca^{2+}concentration, which in turn activates SOCE, an essential mechanism to maintain Ca^{2+} homeostasis in every cell type, including astrocytes. SOCE controls Ca^{2+}

signaling and gliosecretion in response to extracellular stimuli [144, 145]. Its activation is mediated through transient receptor potential (TRP) channels, a family of ion channels that permeate Ca^{2+} and monovalent cations [103], as well as by the Orai channels [146]. In addition to the altered SOCe mechanisms, in Kidins220$^{-/-}$ astrocytes the expression of the Ca^{2+} channel TRPV4 is altered both at mRNA and protein level. TRPV4 is thermo-, osmo-, and mechano-sensitive [147-149], mediate Ca^{2+} influx in primary astrocytes [150] and promote Ca^{2+}-dependent Ca^{2+} release [151, 152]. In particular TRPV4 is expressed in cortical astrocytes and in complex with AQP4 regulates volume increase/decrease during osmotic shock [150]. Its increased levels in Kidins220$^{-/-}$ astrocytes further support Kidins220 involvement in Ca^{2+} dynamics. Kidins220 role is also fundamental for the magnitude of those transient. In fact, when the scaffold protein is absent, we observe a reduction in the Ca^{2+} transient amplitude.

In Kidins220$^{-/-}$ embryonic astrocytes, transient receptor potential cation channel subfamily V member 4 (TRPV4) is upregulated [114]. Moreover, our transcriptional analysis on postnatal cultures demonstrated that aqp4 mRNA is downregulated by BDNF, in both wild type and Kidins220-downregulated astrocytes. These data suggest that during development, Kidins220 may influence the expression of some fundamental genes, and that in the postnatal stages BDNF is able to modulate astrocyte physiology and their function of maintaining nervous system homeostasis. mRNA analysis highlights also that Kir4.1 transcription is impaired by Kidins220 ablation, which is reflected in lower protein levels. This impairment cannot be rescued through BDNF chronic administration, highlighting that Kidins220 plays a role in the maintenance of astrocyte homeostasis and K^+ buffering function by modulating the expression of Kir4.1 through mechanisms independent of BDNF stimulation. Together with the increased expression of TRPV4 [114], the reduced TrkB activation and the reduction of Kir4.1 expression, we can hypothesize that Kidins220 absence manifests itself with a global stress reaction for astrocytes. Even if data regarding coculture between postnatal astrocytes lacking Kidins220 and wildtype neurons are not at the moment available, we can speculate that the impairment in both Ca^{2+} and K^+ conductance could lead to the same neuronal firing alterations previously reported [114]. Looking at these results, it will be interesting to expand our analysis to check if the expression of other genes targeted by the BDNF is influenced in the absence of Kidins220.

The mechanisms that lead to altered gene expression in the absence of Kidins220 are not presently known, but we speculate that the long-term activation of BDNF-dependent signaling pathways may be chronically altered, thus leading to altered gene expression.

Last but not least, our data also support the hypothesis that in the absence of Kidins220, astrocytes undergo a metabolism shift towards a more predominant glycolytic mechanism. Remarkably, Kidins220$^{-/-}$ embryonic cells produce three times more lactate compared to wildtype astrocytes, suggesting impaired mitochondrial metabolism, whereas at the postnatal stage lactate levels are comparable in both astrocyte genotypes. This hypothesis is also supported by significant reduction in the extracellular ATP concentration observed in the same KO astrocytes compared to the controls [114].

6.2. Role of Kidins220 in the adult mouse brain

Our mouse line is the first animal model in which the effects of Kidins220 absence can be investigated in the adult. In these animals, Kidins220 absence is limited to the excitatory neurons of the forebrain but despite this limited ablation, cKO animals displayed several functional deficits.

In our cKO model, neurons in the cortex and the hippocampus show altered dendritic morphology accompanied by a reduction in the spine density of the granule cells of the dentate gyrus, which are both dependent on the BDNF/TrkB system [47, 153, 154]. In Kidins220$^{lox/lox}$ mice, in which only Kidins220 full length is expressed, cortical neuron arborization is not altered, suggesting that the full-length isoform is the main responsible for maintaining dendritic morphology. However, the lack of splicing isoforms affects TrkB expression in the hippocampus, where the levels of both TrkB isoforms are reduced, indicating that the correct isoform pattern of Kidins220 may have a role in modulating TrkB availability and the consequent BDNF response. The reduced TrkB expression observed in the hippocampus of the Kidins220$^{lox/lox}$ mice is also present in cKO animals, where we also observed an increased expression of the same receptors in the cerebellum. The same reduction of TrkB expression in Kidins220$^{lox/lox}$ and cKO mice suggest that it is due to the absence of some isoforms while the increased level observed in the cerebellum can be link to compensatory mechanisms in response to the reduction of TrkB in the hippocampus and to reduced activation of this receptor in the cortex. In fact, cerebellar development relies on BDNF-TrkB [47, 155-157] and in

our mice the cerebellum is not targeted by the CaMKII promoter. Overall, our data suggest that, within the hippocampus, Kidins220 modulates TrkB levels and its full-length isoform is involved in this process to control dendritic arborization and spine stability. The role of Kidins220 isoforms in plasticity and memory is still not understood, but alterations of neurotrophic signaling may play a role, especially considering the role of Kidins220 isoforms in the cellular response to neurotrophins [78].

The brain circuits underlying anxiety are well known and include the medial prefrontal cortex and hippocampus [158], while BDNF involvement in anxiety is debated [159]. Mutant mouse lines with reduced levels of BDNF show increased [19, 52] or unaltered [131] anxiety, and increasing BDNF levels also increases anxiety [132, 160]. In our cKO mice we have observed a lower anxious phenotype. Can the altered anxiety phenotype be linked to impairment in BDNF accumulation or in its signaling pathways? In our mice BDNF levels are unchanged, despite what was previously described in a different mouse model [129]: these mutant animals showed BDNF accumulation in the striatum due to Kidins220 dowregulation. These contrasting results could be due to a non-identical model; indeed, even if two KO models are generated through a very similar strategy [77, 116], they could show different phenotypes. Even if BDNF levels were maintained, we observed a significant reduction in the basal level of pTrkB in the cKO cortex with a concomitant, significant increase in pAKT levels. Moreover, upon acute BDNF stimulation pTrkB reaches higher levels in cKO than in control mice. This altered signaling may be due to compensatory mechanisms in response to the reduced basal activation of TrkB. If we take in account that cKO mice express the same level of TrkB (both FL and Tr), the basal impairment observed in TrkB phosphorylation, as well as the increased activation of the receptor upon BDNF stimulation, are even more remarkable, suggesting this could be due to altered TrkB localization and/or recycling.

It is well described that the Akt signaling cascade controls dendritic arborization and, within the hippocampus, BDNF-dependent Akt activation is required for spine morphogenesis and plasticity [161], while cortical neuron morphogenesis is mainly mediated by Kidins220 dependent AKT pathway [117]. Knowing that no alterations of BDNF and TrkB expression levels are detected in the cKO cortex, which could be the reason of the reduced TrkB activation / overactivation of pAkt observed in cKO mice?

One possibility is altered membrane availability of TrkB receptors. In fact, in order to activate the specific downstream pathways, Trk receptors need to be available on the membrane surface of the cells. In particular, it has been demonstrated that to be competent for signaling, TrkB needs to be localized into lipid microdomains [162]. Kidins220 as well is localized in rafts where it is associated to several proteins [163]. Kidins220 is also known to be an important regulator of the early endosomes fate [71]. In fact, in the absence of Kidins220 endosomes are preferentially directed to the degradative pathway [71]. Since a reduction of TrkB clustering was associated to Kidins220 deficiency [117], it is possible that in its absence, receptors are led to their degradation rather than sorting to the membrane surface. Alternatively, impaired internalization / recycling may cause per se a reduction of downstream pathways activation. In fact it has been described that, if clathrin-mediated endocytosis is impaired, also BDNF-dependent TrkB phosphorylation is impaired [162].

Since the lack of Kidins220 reduces TrkB phosphorylation, a chronic administration of neurotrophins may overcome this defect rescuing not only the biochemical impairment but also its behavioral consequence. The chronic administration of a BDNF mimetic partially rescues the low-anxiety phenotype of cKO animals. The pharmacological rescue experiments indicate that alterations in the BDNF signaling system underlie at least partially the low-anxiety phenotype shown by these animals.

The fine communication between cortex and hippocampus is well described [164, 165], and alterations in one area affect the other. The main findings observed in the cortico-hippocampal area of our cKO mouse model are: (i) reduction of pTrkB only in the cortex; (ii) increase of both basal and BDNF-induced pAKT levels in the cortex; (iii) identical BDNF levels in all the genotypes and in all the areas; (iv) altered neuron morphology in both cortex and hippocampus, accompanied by reduced spine density in the hippocampus; (v) increase level of BDNF receptors in cerebellum.

Kidins220 KO is only in the excitatory neurons, while all the other cells present in the brain, namely inhibitory neurons and glial cells, still express the protein. As reported in 2012 [116], Kidins220$^{-/-}$ neurons manifest a reduction in short-term plasticity upon BDNF administration but no impairment of electrophysiological properties under basal conditions. However, as reported from Jaudon and colleagues [114], if Kidins220$^{-/-}$

astrocytes are co-cultured with wildtype neurons, those neurons show impairment in their basal physiology. With all these information and looking at our data, we can speculate that, when Kidins220 is removed only in one specific cell population, and these cells are cultured separately from all the others (as in our primary neurons / primary astrocyte cultures), the effects produced by the lack of the protein may not manifest themselves in full. However, when Kidins220 KO cells communicate with other cells where the deficit is not present, one cell population can influence the intracellular pathways and physiology of the other, for example, astrocytes may increase the secretion of specific gliotransmitters / growth factors trying to compensate the impairments of neuronal cells. This hypothesis could also explain the unchanged level of BDNF observed in the different brain areas. Thus, we are still far from having a satisfactory understanding of the role of Kidins220 in the complex cross-talk between different neuronal and glial subpopulations *in vivo*. The various deficits observed in our cKO mice could be due to impaired TrkB activation in excitatory neurons. However, it is possible that astrocytes, microglia and/or inhibitory neurons attempt to resolve the observed biochemical and morphological deficits, maybe through hyperactivation of the BDNF downstream pathways that normally modulate dendritic morphology and spine maturation.

All together our *in vitro* and *in vivo* results further deepen the link between Kidins220 and BDNF, highlighting that Kidins220 affects neural cell physiology differently in the various cell types and at different developmental stages. Importantly, even small alterations in Kidins220 expression levels/splice isoforms may cause important deficits, which is relevant in the increasing number of pathogenic mutations identified in the KIDINS220 gene. Some questions about Kidins220 function are still open and will be the object of future studies; in particular its role in metabolism regulation and how its mutations are involved in human pathologies.

6.3. Ongoing experiments and future perspectives

a. Transgenic mice show deficits in social interaction

Our data show that cKO mice have reduced anxiety levels that can partially be rescued through administration of a BDNF mimetic. What we still do not know is if this less anxious behavior can affect also their ability to socialize and, more in general, to interact with other mice. Knowing the link between Kidins220 and some psychological diseases [89, 166], it will be interesting to investigate this social aspect. It will be interesting to perform some other behavioral experiments as the novel mouse recognition test, to evaluate not only if our mice interact, but also if the long term olfactory memory is impaired. This experiment has also one other important feature: the stimulus mice used for the test can, by themselves, interact and induce interest in the tested mice allowing us to better understand also the kind of interaction that our mice manifest with not-familiar animals. Moreover, some experiments performed on cKO mice showed an impairment in the social odor recognition (Almacellas-Barbanoj, unpublished data), suggesting that their olfactory ability is intact but they are not able to discriminate social vs non social smells. Interestingly, this is a phenotype observed in oxytocin-deficient mice. Over the last years oxytocin has increasingly been selected as possible target for the social deficits observed in psychiatric disorders like autism and schizophrenia [167]. In this respect, it is important to underline that many proteins involved in the oxytocin signaling are common also to the BDNF pathway. Therefore, it is possible that the impairments in BDNF pathways observed in the absence of Kidins220 impact also on the oxytocin pathway, producing the altered social phenotype manifested by our mutant mice. If our hypothesis is true, then mice with reduced oxytocin signaling should be insensitive to Kidins220 modulation.

We plan to perform some molecular and biochemical studies to elucidate the link between social behavior, BDNF and the oxytocin pathways when Kidins220 is not expressed. It is important to remember that the direct and precise evaluation of this hormone is very difficult as it can be altered by several external factors. For this reason, we will focalize our attention on some downstream proteins, in particular on the transcription factor c-fos, which is activated upon MAPK phosphorylation. In order to better understand if and how the oxytocin pathway is impaired in our cKO mouse model upon social stimuli, we plan to investigate c-fos gene and protein expression and to perform a series of histochemical

studies in order to assess which brain areas are activated after the social stimulus. We will also assess if the basal level of oxytocin receptor is altered in our mice. It would be also very interesting to evaluate through immunohistochemistry the activation of TrkB and its main downstream proteins in animals exposed to social stimuli, in order to evaluate if there are differences and which type of cells are involved (i.e., neurons, astrocytes, microglia).

Answering to those questions will further increase the knowledge about Kidins220, linking the protein to another pathway crucial for nervous system physiology, such as that of oxytocin. These answers may also lay the foundation for a better understanding of the impaired social abilities observed in psychiatric disorders and in this way may be helpful in the identification of possible markers and targets to easy and early identify, diagnose and maybe one day treat these diseases.

7. Bibliography

1. Levi-Montalcini, R. and V. Hamburger, A diffusible agent of mouse sarcoma, producing hyperplasia of sympathetic ganglia and hyperneurotization of viscera in the chick embryo. Journal of Experimental Zoology, 1953. **123**(2): p. 233-287.
2. Barde, Y.A., D. Edgar, and H. Thoenen, Purification of a new neurotrophic factor from mammalian brain. EMBO J, 1982. **1**(5): p. 549-53.
3. Leibrock, J., et al., Molecular cloning and expression of brain-derived neurotrophic factor. Nature, 1989. **341**(6238): p. 149-52.
4. Hohn, A., et al., Identification and characterization of a novel member of the nerve growth factor/brain-derived neurotrophic factor family. Nature, 1990. **344**(6264): p. 339-41.
5. Jones, K.R. and L.F. Reichardt, Molecular cloning of a human gene that is a member of the nerve growth factor family. Proceedings of the National Academy of Sciences, 1990. **87**(20): p. 8060-8064.
6. Maisonpierre, P.C., et al., Neurotrophin-3: a neurotrophic factor related to NGF and BDNF. Science, 1990. **247**(4949 Pt 1): p. 1446-51.
7. Rosenthal, A., et al., Primary structure and biological activity of a novel human neurotrophic factor. Neuron, 1990. **4**(5): p. 767-73.
8. Seidah, N.G., et al., Cellular processing of the neurotrophin precursors of NT3 and BDNF by the mammalian proprotein convertases. FEBS Lett, 1996. **379**(3): p. 247-50.
9. Lee, R., et al., Regulation of cell survival by secreted proneurotrophins. Science, 2001. **294**(5548): p. 1945-8.
10. Krishnan, V. and E.J. Nestler, The molecular neurobiology of depression. Nature, 2008. **455**(7215): p. 894-902.
11. Psychiatric, G.C.C.C., et al., Genomewide association studies: history, rationale, and prospects for psychiatric disorders. Am J Psychiatry, 2009. **166**(5): p. 540-56.
12. Gauthier, L.R., et al., Huntingtin controls neurotrophic support and survival of neurons by enhancing BDNF vesicular transport along microtubules. Cell, 2004. **118**(1): p. 127-38.
13. Ventriglia, M., et al., Association between the BDNF 196 A/G polymorphism and sporadic Alzheimer's disease. Mol Psychiatry, 2002. **7**(2): p. 136-7.

14. Kaisho, Y., et al., Regional expression of the nerve growth factor gene family in rat brain during development. Biochemical and Biophysical Research Communications, 1991. **174**(1): p. 379-385.
15. Katoh-Semba, R., et al., Distribution of brain-derived neurotrophic factor in rats and its changes with development in the brain. Journal of Neurochemistry, 1997. **69**(1): p. 34-42.
16. Tongiorgi, E., M. Righi, and A. Cattaneo, Activity-dependent dendritic targeting of BDNF and TrkB mRNAs in hippocampal neurons. J Neurosci, 1997. **17**(24): p. 9492-505.
17. Maisonpierre, P.C., et al., Human and rat brain-derived neurotrophic factor and neurotrophin-3: gene structures, distributions, and chromosomal localizations. Genomics, 1991. **10**(3): p. 558-68.
18. Fukuchi, M. and M. Tsuda, Involvement of the 3'-untranslated region of the brain-derived neurotrophic factor gene in activity-dependent mRNA stabilization. J Neurochem, 2010. **115**(5): p. 1222-33.
19. Chen, Z.Y., et al., Variant brain-derived neurotrophic factor (BDNF) (Met66) alters the intracellular trafficking and activity-dependent secretion of wild-type BDNF in neurosecretory cells and cortical neurons. J Neurosci, 2004. **24**(18): p. 4401-11.
20. Chang, H.M., et al., Neurotrophins and glial cell line-derived neurotrophic factor in the ovary: physiological and pathophysiological implications. Hum Reprod Update, 2019. **25**(2): p. 224-242.
21. Wiesmann, C., et al., Crystal structure of nerve growth factor in complex with the ligand-binding domain of the TrkA receptor. Nature, 1999. **401**(6749): p. 184-8.
22. Ultsch, M.H., et al., Crystal structures of the neurotrophin-binding domain of TrkA, TrkB and TrkC. J Mol Biol, 1999. **290**(1): p. 149-59.
23. Twiss, J.L., J.H. Chang, and N.C. Schanen, Pathophysiological mechanisms for actions of the neurotrophins. Brain Pathol, 2006. **16**(4): p. 320-32.
24. Huang, E.J. and L.F. Reichardt, Trk receptors: roles in neuronal signal transduction. Annu Rev Biochem, 2003. **72**: p. 609-42.
25. Rose, C.R., et al., Truncated TrkB-T1 mediates neurotrophin-evoked calcium signalling in glia cells. Nature, 2003. **426**(6962): p. 74-8.

26. Carim-Todd, L., et al., Endogenous truncated TrkB.T1 receptor regulates neuronal complexity and TrkB kinase receptor function in vivo. J Neurosci, 2009. **29**(3): p. 678-85.
27. Bhattacharyya, A., et al., High-resolution imaging demonstrates dynein-based vesicular transport of activated Trk receptors. J Neurobiol, 2002. **51**(4): p. 302-12.
28. Grimes, M.L., et al., Endocytosis of activated TrkA: evidence that nerve growth factor induces formation of signaling endosomes. J Neurosci, 1996. **16**(24): p. 7950-64.
29. Grimes, M.L., E. Beattie, and W.C. Mobley, A signaling organelle containing the nerve growth factor-activated receptor tyrosine kinase, TrkA. Proc Natl Acad Sci U S A, 1997. **94**(18): p. 9909-14.
30. Hendry, I.A., et al., The retrograde axonal transport of nerve growth factor. Brain Res, 1974. **68**(1): p. 103-21.
31. Howe, C.L., et al., NGF signaling from clathrin-coated vesicles: evidence that signaling endosomes serve as a platform for the Ras-MAPK pathway. Neuron, 2001. **32**(5): p. 801-14.
32. Yano, H., et al., Association of Trk neurotrophin receptors with components of the cytoplasmic dynein motor. J Neurosci, 2001. **21**(3): p. RC125.
33. Dalla Costa, I., et al., The functional organization of axonal mRNA transport and translation. Nat Rev Neurosci, 2021. **22**(2): p. 77-91.
34. Teng, K.K., et al., Understanding proneurotrophin actions: Recent advances and challenges. Dev Neurobiol, 2010. **70**(5): p. 350-9.
35. Hempstead, B.L., et al., High-affinity NGF binding requires coexpression of the trk proto-oncogene and the low-affinity NGF receptor. Nature, 1991. **350**(6320): p. 678-83.
36. Nykjaer, A., et al., Sortilin is essential for proNGF-induced neuronal cell death. Nature, 2004. **427**(6977): p. 843-8.
37. Baldwin, A.N. and E.M. Shooter, Zone mapping of the binding domain of the rat low affinity nerve growth factor receptor by the introduction of novel N-glycosylation sites. J Biol Chem, 1995. **270**(9): p. 4594-602.
38. Bothwell, M., Functional interactions of neurotrophins and neurotrophin receptors. Annu Rev Neurosci, 1995. **18**: p. 223-53.
39. Chao, M.V. and B.L. Hempstead, p75 and Trk: a two-receptor system. Trends Neurosci, 1995. **18**(7): p. 321-6.

40. Chapman, B.S., A region of the 75 kDa neurotrophin receptor homologous to the death domains of TNFR-I and Fas. FEBS Lett, 1995. **374**(2): p. 216-20.
41. Chapman, B.S. and I.D. Kuntz, Modeled structure of the 75-kDa neurotrophin receptor. Protein Sci, 1995. **4**(9): p. 1696-707.
42. Feinstein, E., et al., The death domain: a module shared by proteins with diverse cellular functions. Trends Biochem Sci, 1995. **20**(9): p. 342-4.
43. Nykjaer, A., T.E. Willnow, and C.M. Petersen, p75NTR--live or let die. Curr Opin Neurobiol, 2005. **15**(1): p. 49-57.
44. Teng, H.K., et al., ProBDNF induces neuronal apoptosis via activation of a receptor complex of p75NTR and sortilin. J Neurosci, 2005. **25**(22): p. 5455-63.
45. Longo, F.M. and S.M. Massa, Small-molecule modulation of neurotrophin receptors: a strategy for the treatment of neurological disease. Nat Rev Drug Discov, 2013. **12**(7): p. 507-25.
46. Alcantara, S., et al., TrkB signaling is required for postnatal survival of CNS neurons and protects hippocampal and motor neurons from axotomy-induced cell death. J Neurosci, 1997. **17**(10): p. 3623-33.
47. Minichiello, L. and R. Klein, TrkB and TrkC neurotrophin receptors cooperate in promoting survival of hippocampal and cerebellar granule neurons. Genes Dev, 1996. **10**(22): p. 2849-58.
48. Klein, R., et al., The trk proto-oncogene encodes a receptor for nerve growth factor. Cell, 1991. **65**(1): p. 189-97.
49. Chan, J.P., et al., Examination of behavioral deficits triggered by targeting Bdnf in fetal or postnatal brains of mice. Neuroscience, 2006. **142**(1): p. 49-58.
50. Chan, J.P., et al., Depletion of central BDNF in mice impedes terminal differentiation of new granule neurons in the adult hippocampus. Mol Cell Neurosci, 2008. **39**(3): p. 372-83.
51. Monteggia, L.M., Elucidating the role of brain-derived neurotrophic factor in the brain. Am J Psychiatry, 2007. **164**(12): p. 1790.
52. Rios, M., et al., Conditional deletion of brain-derived neurotrophic factor in the postnatal brain leads to obesity and hyperactivity. Mol Endocrinol, 2001. **15**(10): p. 1748-57.

53. Wu, C., et al., Expression profile of nerve growth factor after muscle incision in the rat. Anesthesiology, 2009. **110**(1): p. 140-9.
54. Saarelainen, T., et al., Transgenic mice overexpressing truncated trkB neurotrophin receptors in neurons show increased susceptibility to cortical injury after focal cerebral ischemia. Mol Cell Neurosci, 2000. **16**(2): p. 87-96.
55. Koponen, E., et al., Transgenic mice overexpressing the full-length neurotrophin receptor trkB exhibit increased activation of the trkB-PLCgamma pathway, reduced anxiety, and facilitated learning. Mol Cell Neurosci, 2004. **26**(1): p. 166-81.
56. Cattaneo, E., et al., Loss of normal huntingtin function: new developments in Huntington's disease research. Trends Neurosci, 2001. **24**(3): p. 182-8.
57. Casey, B.J., et al., Brain-derived neurotrophic factor as a model system for examining gene by environment interactions across development. Neuroscience, 2009. **164**(1): p. 108-20.
58. Skeldal, S., et al., Proteolytic processing of the p75 neurotrophin receptor: A prerequisite for signalling?: Neuronal life, growth and death signalling are crucially regulated by intra-membrane proteolysis and trafficking of p75(NTR). Bioessays, 2011. **33**(8): p. 614-25.
59. Esposito, D., et al., The cytoplasmic and transmembrane domains of the p75 and Trk A receptors regulate high affinity binding to nerve growth factor. J Biol Chem, 2001. **276**(35): p. 32687-95.
60. Baldwin, A.S., Regulation of cell death and autophagy by IKK and NF-kappaB: critical mechanisms in immune function and cancer. Immunol Rev, 2012. **246**(1): p. 327-45.
61. Iglesias, T., et al., Identification and cloning of Kidins220, a novel neuronal substrate of protein kinase D. J Biol Chem, 2000. **275**(51): p. 40048-56.
62. Kong, H., et al., An evolutionarily conserved transmembrane protein that is a novel downstream target of neurotrophin and ephrin receptors. J Neurosci, 2001. **21**(1): p. 176-85.
63. Neubrand, V.E., et al., Kidins220/ARMS as a functional mediator of multiple receptor signalling pathways. J Cell Sci, 2012. **125**(Pt 8): p. 1845-54.

64. Li, J., A. Mahajan, and M.D. Tsai, Ankyrin repeat: a unique motif mediating protein-protein interactions. Biochemistry, 2006. **45**(51): p. 15168-78.

65. Neubrand, V.E., et al., Kidins220/ARMS regulates Rac1-dependent neurite outgrowth by direct interaction with the RhoGEF Trio. J Cell Sci, 2010. **123**(Pt 12): p. 2111-23.

66. Higuero, A.M., et al., Kidins220/ARMS modulates the activity of microtubule-regulating proteins and controls neuronal polarity and development. J Biol Chem, 2010. **285**(2): p. 1343-57.

67. Arevalo, J.C., et al., The ARMS/Kidins220 scaffold protein modulates synaptic transmission. Mol Cell Neurosci, 2010. **45**(2): p. 92-100.

68. Arevalo, J.C., et al., A unique pathway for sustained neurotrophin signaling through an ankyrin-rich membrane-spanning protein. EMBO J, 2004. **23**(12): p. 2358-68.

69. Arevalo, J.C., et al., Identification of a switch in neurotrophin signaling by selective tyrosine phosphorylation. J Biol Chem, 2006. **281**(2): p. 1001-7.

70. Guo, W., G. Nagappan, and B. Lu, Differential effects of transient and sustained activation of BDNF-TrkB signaling. Dev Neurobiol, 2018. **78**(7): p. 647-659.

71. Hisata, S., et al., Rap1-PDZ-GEF1 interacts with a neurotrophin receptor at late endosomes, leading to sustained activation of Rap1 and ERK and neurite outgrowth. J Cell Biol, 2007. **178**(5): p. 843-60.

72. Bracale, A., et al., Kidins220/ARMS is transported by a kinesin-1-based mechanism likely to be involved in neuronal differentiation. Mol Biol Cell, 2007. **18**(1): p. 142-52.

73. Luo, S., et al., {alpha}-Syntrophin regulates ARMS localization at the neuromuscular junction and enhances EphA4 signaling in an ARMS-dependent manner. J Cell Biol, 2005. **169**(5): p. 813-24.

74. Andreazzoli, M., et al., Kidins220/ARMS interacts with Pdzrn3, a protein containing multiple binding domains. Biochimie, 2012. **94**(9): p. 2054-7.

75. Lopez-Menendez, C., et al., Kidins220/ARMS downregulation by excitotoxic activation of NMDARs reveals its involvement in neuronal survival and death pathways. J Cell Sci, 2009. **122**(Pt 19): p. 3554-65.

76. Steinberg, F., et al., A global analysis of SNX27-retromer assembly and cargo specificity reveals a function in glucose and metal ion transport. Nat Cell Biol, 2013. **15**(5): p. 461-71.
77. Wu, S.H., et al., Ankyrin Repeat-rich Membrane Spanning/Kidins220 protein regulates dendritic branching and spine stability in vivo. Dev Neurobiol, 2009. **69**(9): p. 547-57.
78. Schmieg, N., et al., Novel Kidins220/ARMS Splice Isoforms: Potential Specific Regulators of Neuronal and Cardiovascular Development. PLoS One, 2015. **10**(6): p. e0129944.
79. Josifova, D.J., et al., Heterozygous KIDINS220/ARMS nonsense variants cause spastic paraplegia, intellectual disability, nystagmus, and obesity. Hum Mol Genet, 2016. **25**(11): p. 2158-2167.
80. Chang, M.S., J.C. Arevalo, and M.V. Chao, Ternary complex with Trk, p75, and an ankyrin-rich membrane spanning protein. J Neurosci Res, 2004. **78**(2): p. 186-92.
81. Cai, S., et al., Kidins220 and tumour development: Insights into a complexity of cross-talk among signalling pathways (Review). Int J Mol Med, 2017. **40**(4): p. 965-971.
82. Liao, Y.H., et al., Upregulated ankyrin repeat-rich membrane spanning protein contributes to tumour progression in cutaneous melanoma. Br J Cancer, 2011. **104**(6): p. 982-8.
83. Rogers, D.A. and N.F. Schor, Kidins220/ARMS is expressed in neuroblastoma tumors and stabilizes neurotrophic signaling in a human neuroblastoma cell line. Pediatr Res, 2013. **74**(5): p. 517-24.
84. Carvalho, D., et al., The prognostic role of intragenic copy number breakpoints and identification of novel fusion genes in paediatric high grade glioma. Acta Neuropathol Commun, 2014. **2**: p. 23.
85. Ballatore, C., V.M. Lee, and J.Q. Trojanowski, Tau-mediated neurodegeneration in Alzheimer's disease and related disorders. Nat Rev Neurosci, 2007. **8**(9): p. 663-72.
86. Lopez-Menendez, C., et al., Kidins220 accumulates with tau in human Alzheimer's disease and related models: modulation of its calpain-processing by GSK3beta/PP1 imbalance. Hum Mol Genet, 2013. **22**(3): p. 466-82.

87. Kazdoba, T.M., P.T. Leach, and J.N. Crawley, Behavioral phenotypes of genetic mouse models of autism. Genes Brain Behav, 2016. **15**(1): p. 7-26.
88. Manchia, M. and V. Fanos, Targeting aggression in severe mental illness: The predictive role of genetic, epigenetic, and metabolomic markers. Prog Neuropsychopharmacol Biol Psychiatry, 2017. **77**: p. 32-41.
89. Kranz, T.M., et al., Rare variants in the neurotrophin signaling pathway implicated in schizophrenia risk. Schizophr Res, 2015. **168**(1-2): p. 421-8.
90. Kushima, I., et al., Comparative Analyses of Copy-Number Variation in Autism Spectrum Disorder and Schizophrenia Reveal Etiological Overlap and Biological Insights. Cell Rep, 2018. **24**(11): p. 2838-2856.
91. Borrie, S.C., et al., Cognitive Dysfunctions in Intellectual Disabilities: The Contributions of the Ras-MAPK and PI3K-AKT-mTOR Pathways. Annu Rev Genomics Hum Genet, 2017. **18**: p. 115-142.
92. del Puerto, A., et al., Kidins220 deficiency causes ventriculomegaly via SNX27-retromer-dependent AQP4 degradation. Molecular Psychiatry, 2021.
93. Almacellas-Barbanoj, A., et al., Kidins220/ARMS modulates brain morphology and anxiety-like traits in adult mice. Cell Death Discov, 2022. **8**(1): p. 58.
94. Ghosh, S. and C. Bouchard, Convergence between biological, behavioural and genetic determinants of obesity. Nat Rev Genet, 2017. **18**(12): p. 731-748.
95. Zhang, K., et al., SINO Syndrome Causative KIDINS220/ARMS Gene Regulates Adipocyte Differentiation. Front Cell Dev Biol, 2021. **9**: p. 619475.
96. Mero, I.L., et al., Homozygous KIDINS220 loss-of-function variants in fetuses with cerebral ventriculomegaly and limb contractures. Hum Mol Genet, 2017. **26**(19): p. 3792-3796.
97. Kim, Y., J. Park, and Y.K. Choi, The Role of Astrocytes in the Central Nervous System Focused on BK Channel and Heme Oxygenase Metabolites: A Review. Antioxidants (Basel), 2019. **8**(5).
98. Semyanov, A. and A. Verkhratsky, Astrocytic processes: from tripartite synapses to the active milieu. Trends Neurosci, 2021. **44**(10): p. 781-792.
99. Pellerin, L., et al., Activity-dependent regulation of energy metabolism by astrocytes: an update. Glia, 2007. **55**(12): p. 1251-62.

100. Bonvento, G. and J.P. Bolanos, Astrocyte-neuron metabolic cooperation shapes brain activity. Cell Metab, 2021. **33**(8): p. 1546-1564.

101. Eroglu, C. and B.A. Barres, Regulation of synaptic connectivity by glia. Nature, 2010. **468**(7321): p. 223-31.

102. Verkhratsky, A., V. Untiet, and C.R. Rose, Ionic signalling in astroglia beyond calcium. J Physiol, 2020. **598**(9): p. 1655-1670.

103. Ben Achour, S., et al., Is astrocyte calcium signaling relevant for synaptic plasticity? Neuron Glia Biol, 2010. **6**(3): p. 147-55.

104. Gueguinou, M., et al., KCa and Ca(2+) channels: the complex thought. Biochim Biophys Acta, 2014. **1843**(10): p. 2322-33.

105. Brini, M., et al., Neuronal calcium signaling: function and dysfunction. Cell Mol Life Sci, 2014. **71**(15): p. 2787-814.

106. Zorec, R., et al., Astroglial excitability and gliotransmission: an appraisal of Ca2+ as a signalling route. ASN Neuro, 2012. **4**(2).

107. Zafra, F., et al., Regulation of brain-derived neurotrophic factor and nerve growth factor mRNA in primary cultures of hippocampal neurons and astrocytes. J Neurosci, 1992. **12**(12): p. 4793-9.

108. Alderson, R.F., et al., Truncated TrkB mediates the endocytosis and release of BDNF and neurotrophin-4/5 by rat astrocytes and schwann cells in vitro. Brain Res, 2000. **871**(2): p. 210-22.

109. Kinboshi, M., et al., Inhibition of Inwardly Rectifying Potassium (Kir) 4.1 Channels Facilitates Brain-Derived Neurotrophic Factor (BDNF) Expression in Astrocytes. Front Mol Neurosci, 2017. **10**: p. 408.

110. Saba, J., et al., Astrocytes from cortex and striatum show differential responses to mitochondrial toxin and BDNF: implications for protection of striatal neurons expressing mutant huntingtin. J Neuroinflammation, 2020. **17**(1): p. 290.

111. Condorelli, D.F., et al., Neurotrophins and their trk receptors in cultured cells of the glial lineage and in white matter of the central nervous system. J Mol Neurosci, 1995. **6**(4): p. 237-48.

112. Liebl, D.J., et al., Regulation of Trk receptors following contusion of the rat spinal cord. Exp Neurol, 2001. **167**(1): p. 15-26.

113. Climent, E., et al., Astrocytes in culture express the full-length Trk-B receptor and respond to brain derived neurotrophic factor by changing intracellular calcium levels: effect of ethanol exposure in rats. Neurosci Lett, 2000. **288**(1): p. 53-6.

114. Jaudon, F., et al., Kidins220/ARMS controls astrocyte calcium signaling and neuron-astrocyte communication. Cell Death Differ, 2019.

115. Cesca, F., et al., Kidins220/ARMS is an essential modulator of cardiovascular and nervous system development. Cell Death Dis, 2011. **2**: p. e226.

116. Cesca, F., et al., Kidins220/ARMS mediates the integration of the neurotrophin and VEGF pathways in the vascular and nervous systems. Cell Death Differ, 2012. **19**(2): p. 194-208.

117. Chen, Y., et al., Ankyrin repeat-rich membrane spanning protein (kidins220) is required for neurotrophin and ephrin receptor-dependent dendrite development. J Neurosci, 2012. **32**(24): p. 8263-9.

118. Li, Q., et al., High neural activity accelerates the decline of cognitive plasticity with age in Caenorhabditis elegans. Elife, 2020. **9**.

119. Scholz-Starke, J., et al., Kidins220/ARMS is a novel modulator of short-term synaptic plasticity in hippocampal GABAergic neurons. PLoS One, 2012. **7**(4): p. e35785.

120. Kaeser, P.S., et al., RIM proteins tether Ca2+ channels to presynaptic active zones via a direct PDZ-domain interaction. Cell, 2011. **144**(2): p. 282-95.

121. Vandesompele, J., et al., Accurate normalization of real-time quantitative RT-PCR data by geometric averaging of multiple internal control genes. Genome Biol, 2002. **3**(7): p. RESEARCH0034.

122. Grynkiewicz, G., M. Poenie, and R.Y. Tsien, A new generation of Ca2+ indicators with greatly improved fluorescence properties. J Biol Chem, 1985. **260**(6): p. 3440-50.

123. Parrini, M., et al., Aerobic exercise and a BDNF-mimetic therapy rescue learning and memory in a mouse model of Down syndrome. Sci Rep, 2017. **7**(1): p. 16825.

124. Condorelli, D.F., et al., Expression of neurotrophins and their receptors in primary astroglial cultures: induction by cyclic AMP-elevating agents. J Neurochem, 1994. **63**(2): p. 509-16.

125. Hutton, L.A., J. DeVellis, and J.R. Perez-Polo, Expression of p75NGFR trkA, and trkB mRNA in rat C6 glioma and type I astrocyte cultures. Journal of Neuroscience Research, 1992. **32**(3): p. 375-383.

126. Dallerac, G., J. Zapata, and N. Rouach, Versatile control of synaptic circuits by astrocytes: where, when and how? Nat Rev Neurosci, 2018. **19**(12): p. 729-743.

127. Cazorla, M., et al., Identification of a low-molecular weight TrkB antagonist with anxiolytic and antidepressant activity in mice. J Clin Invest, 2011. **121**(5): p. 1846-57.

128. Magistretti, P.J. and I. Allaman, A cellular perspective on brain energy metabolism and functional imaging. Neuron, 2015. **86**(4): p. 883-901.

129. Lopez-Benito, S., et al., Regulation of BDNF Release by ARMS/Kidins220 through Modulation of Synaptotagmin-IV Levels. J Neurosci, 2018. **38**(23): p. 5415-5428.

130. Chen, Z.Y., et al., Genetic variant BDNF (Val66Met) polymorphism alters anxiety-related behavior. Science, 2006. **314**(5796): p. 140-3.

131. Gorski, J.A., et al., Learning deficits in forebrain-restricted brain-derived neurotrophic factor mutant mice. Neuroscience, 2003. **121**(2): p. 341-54.

132. Papaleo, F., et al., Working memory deficits, increased anxiety-like traits, and seizure susceptibility in BDNF overexpressing mice. Learn Mem, 2011. **18**(8): p. 534-44.

133. Jang, S.W., et al., A selective TrkB agonist with potent neurotrophic activities by 7,8-dihydroxyflavone. Proc Natl Acad Sci U S A, 2010. **107**(6): p. 2687-92.

134. Fenner, B.M., Truncated TrkB: beyond a dominant negative receptor. Cytokine Growth Factor Rev, 2012. **23**(1-2): p. 15-24.

135. Holt, L.M., et al., Astrocyte morphogenesis is dependent on BDNF signaling via astrocytic TrkB.T1. Elife, 2019. **8**.

136. McKeon, R.J., J. Silver, and T.H. Large, Expression of full-length trkB receptors by reactive astrocytes after chronic CNS injury. Exp Neurol, 1997. **148**(2): p. 558-67.

137. Soontornniyomkij, V., et al., Expression of brain-derived neurotrophic factor protein in activated microglia of human immunodeficiency virus type 1 encephalitis. Neuropathol Appl Neurobiol, 1998. **24**(6): p. 453-60.

138. Stadelmann, C., et al., BDNF and gp145trkB in multiple sclerosis brain lesions: neuroprotective interactions between immune and neuronal cells? Brain, 2002. **125**(Pt 1): p. 75-85.

139. Galli, R., et al., Isolation and characterization of tumorigenic, stem-like neural precursors from human glioblastoma. Cancer Res, 2004. **64**(19): p. 7011-21.
140. Ignatova, T.N., et al., Human cortical glial tumors contain neural stem-like cells expressing astroglial and neuronal markers in vitro. Glia, 2002. **39**(3): p. 193-206.
141. Silver, D.J. and D.A. Steindler, Common astrocytic programs during brain development, injury and cancer. Trends Neurosci, 2009. **32**(6): p. 303-11.
142. Meng, L., et al., Targeting the BDNF/TrkB pathway for the treatment of tumors. Oncol Lett, 2019. **17**(2): p. 2031-2039.
143. Buffo, A., et al., Origin and progeny of reactive gliosis: A source of multipotent cells in the injured brain. Proc Natl Acad Sci U S A, 2008. **105**(9): p. 3581-6.
144. Papanikolaou, M., A. Lewis, and A.M. Butt, Store-operated calcium entry is essential for glial calcium signalling in CNS white matter. Brain Struct Funct, 2017. **222**(7): p. 2993-3005.
145. Gao, X., et al., STIMs and Orai1 regulate cytokine production in spinal astrocytes. J Neuroinflammation, 2016. **13**(1): p. 126.
146. Verkhratsky, A., R.C. Reyes, and V. Parpura, TRP channels coordinate ion signalling in astroglia. Rev Physiol Biochem Pharmacol, 2014. **166**: p. 1-22.
147. Guler, A.D., et al., Heat-evoked activation of the ion channel, TRPV4. J Neurosci, 2002. **22**(15): p. 6408-14.
148. Liedtke, W. and J.M. Friedman, Abnormal osmotic regulation in trpv4-/- mice. Proc Natl Acad Sci U S A, 2003. **100**(23): p. 13698-703.
149. Mizuno, A., et al., Impaired osmotic sensation in mice lacking TRPV4. Am J Physiol Cell Physiol, 2003. **285**(1): p. C96-101.
150. Benfenati, V., et al., Expression and functional characterization of transient receptor potential vanilloid-related channel 4 (TRPV4) in rat cortical astrocytes. Neuroscience, 2007. **148**(4): p. 876-92.
151. Dunn, K.M., et al., TRPV4 channels stimulate Ca2+-induced Ca2+ release in astrocytic endfeet and amplify neurovascular coupling responses. Proc Natl Acad Sci U S A, 2013. **110**(15): p. 6157-62.

152. Benfenati, V. and S. Ferroni, Water transport between CNS compartments: functional and molecular interactions between aquaporins and ion channels. Neuroscience, 2010. **168**(4): p. 926-40.

153. Sun, D., et al., Critical Roles of Embryonic Born Dorsal Dentate Granule Neurons for Activity-Dependent Increases in BDNF, Adult Hippocampal Neurogenesis, and Antianxiety-like Behaviors. Biol Psychiatry, 2021. **89**(6): p. 600-614.

154. Danzer, S.C., et al., Altered morphology of hippocampal dentate granule cell presynaptic and postsynaptic terminals following conditional deletion of TrkB. Hippocampus, 2008. **18**(7): p. 668-78.

155. Carter, A.R., et al., Brain-derived neurotrophic factor modulates cerebellar plasticity and synaptic ultrastructure. J Neurosci, 2002. **22**(4): p. 1316-27.

156. Schwartz, P.M., et al., Abnormal cerebellar development and foliation in BDNF-/- mice reveals a role for neurotrophins in CNS patterning. Neuron, 1997. **19**(2): p. 269-81.

157. Rico, B., B. Xu, and L.F. Reichardt, TrkB receptor signaling is required for establishment of GABAergic synapses in the cerebellum. Nat Neurosci, 2002. **5**(3): p. 225-33.

158. Calhoon, G.G. and K.M. Tye, Resolving the neural circuits of anxiety. Nat Neurosci, 2015. **18**(10): p. 1394-404.

159. Olsen, D., et al., Loss of BDNF or its receptors in three mouse models has unpredictable consequences for anxiety and fear acquisition. Learn Mem, 2013. **20**(9): p. 499-504.

160. Govindarajan, A., et al., Transgenic brain-derived neurotrophic factor expression causes both anxiogenic and antidepressant effects. Proc Natl Acad Sci U S A, 2006. **103**(35): p. 13208-13.

161. Nikoletopoulou, V., et al., Modulation of Autophagy by BDNF Underlies Synaptic Plasticity. Cell Metab, 2017. **26**(1): p. 230-242 e5.

162. Assaife-Lopes, N., et al., Regulation of TrkB receptor translocation to lipid rafts by adenosine A(2A) receptors and its functional implications for BDNF-induced regulation of synaptic plasticity. Purinergic Signal, 2014. **10**(2): p. 251-67.

163. Cabrera-Poch, N., et al., Lipid raft disruption triggers protein kinase C and Src-dependent protein kinase D activation and Kidins220 phosphorylation in neuronal cells. J Biol Chem, 2004. **279**(27): p. 28592-602.

164. Witter, M.P., et al., Cortico-hippocampal communication by way of parallel parahippocampal-subicular pathways. Hippocampus, 2000. **10**(4): p. 398-410.

165. Sirota, A., et al., Communication between neocortex and hippocampus during sleep in rodents. Proc Natl Acad Sci U S A, 2003. **100**(4): p. 2065-9.

166. Pinto, D., et al., Convergence of genes and cellular pathways dysregulated in autism spectrum disorders. Am J Hum Genet, 2014. **94**(5): p. 677-94.

167. Cochran, D.M., et al., The role of oxytocin in psychiatric disorders: a review of biological and therapeutic research findings. Harv Rev Psychiatry, 2013. **21**(5): p. 219-47.

8. Appendix: Published work

Kidins220/ARMS controls astrocyte calcium signaling and neuron-astrocyte communication

Jaudon F., Chiacchiaretta M., **Albini M.**, Ferroni S., Benfenati F., Cesca F.

Cell death and differentiation. October 2019 doi: 10.1038/s41418-019-0431-5

Abstract

Through their ability to modulate synaptic transmission, glial cells are key regulators of neuronal circuit formation and activity. Kidins220/ARMS (kinase-D interacting substrate of 220 kDa/ankyrin repeat-rich membrane spanning) is one of the key effectors of the neurotrophin pathways in neurons where it is required for differentiation, survival, and plasticity. However, its role in glial cells remains largely unknown. Here, we show that ablation of Kidins220 in primary cultured astrocytes induced defects in calcium (Ca^{2+}) signaling that were linked to altered store-operated Ca^{2+} entry and strong overexpression of the transient receptor potential channel TRPV4. Moreover, Kidins220$^{-/-}$ astrocytes were more sensitive to genotoxic stress. We also show that Kidins220 expression in astrocytes is required for the establishment of proper connectivity of cocultured wild-type neurons. Altogether, our data reveal a previously unidentified role for astrocyte expressed Kidins220 in the control of glial Ca^{2+} dynamics, survival/death pathways and astrocyte–neuron communication.

I partecipated to this work during the revision performing some biochemical experiments on embryonic astrocytes.

Neuroinflammation induces synaptic scaling through IL-1β-mediated activation of the transcriptional repressor REST/NRSF

Buffolo F.*, Petrosino V.*, **Albini M.***, Moschetta M., Carlini F., Floss T., Kerlero de Rosbo N., Cesca F., Rocchi A., Uccelli A., Benfenati F.

Cell death and disease. February 2021 doi: 10.1038/s41419-021-03465-6

* These authors contributed equally to this work

Abstract

Neuroinflammation is associated with synapse dysfunction and cognitive decline in patients and animal models. One candidate for translating the inflammatory stress into structural and functional changes in neural networks is the transcriptional repressor RE1-silencing transcription factor (REST) that regulates the expression of a wide cluster of neuron-specific genes during neurogenesis and in mature neurons. To study the cellular and molecular pathways activated under inflammatory conditions mimicking the experimental autoimmune encephalomyelitis (EAE) environment, we analyzed REST activity in neuroblastoma cells and mouse cortical neurons treated with activated T cell or microglia supernatant and distinct pro-inflammatory cytokines. We found that REST is activated by a variety of neuroinflammatory stimuli in both neuroblastoma cells and primary neurons, indicating that a vast transcriptional change is triggered during neuroinflammation. While a dual activation of REST and its dominant-negative splicing isoform REST4 was observed in N2a neuroblastoma cells, primary neurons responded with a pure full-length REST upregulation in the absence of changes in REST4 expression. In both cases, REST upregulation was associated with activation of Wnt signaling and increased nuclear translocation of β-catenin, a well-known intracellular transduction pathway in neuroinflammation. Among single cytokines, IL-1β caused a potent and prompt increase in REST transcription and translation in neurons, which promoted a delayed and strong synaptic downscaling specific for excitatory synapses, with decreased frequency and amplitude of spontaneous synaptic currents, decreased density of excitatory synaptic connections, and decreased frequency of action potential-evoked Ca2+ transients. Most important, the IL-1β effects on excitatory transmission were strictly REST dependent, as conditional deletion of REST completely occluded the effects of IL-1β activation on synaptic transmission and network excitability. Our results demonstrate that REST upregulation

represents a new pathogenic mechanism for the synaptic dysfunctions observed under neuroinflammatory conditions and identify the REST pathway as therapeutic target for EAE and, potentially, for multiple sclerosis.

This paper stemmed from a collaborative project. I contributed to this research performing some of the biochemical experiments on the cell models used (N2a cell line and wildtype primary neurons), the viability and the calcium imaging experiments performed on the primary neurons.

A developmental stage- and Kidins220-dependent switch in astrocyte responsiveness to brain-derived neurotrophic factor

Jaudon F.*, **Albini M.***, Ferroni S., Benfenati F., Cesca F.

Journal of Cell Science August 2021 doi: 10.1242/jcs.258419

* These authors contributed equally to this work

Abstract

Astroglial cells are key to maintain nervous system homeostasis. Neurotrophins are known for their pleiotropic effects on neuronal physiology but also exert complex functions to glial cells. Here, we investigated (i) the signaling competence of mouse embryonic and postnatal primary cortical astrocytes exposed to brain-derived neurotrophic factor (BDNF) and, (ii) the role of kinase D-interacting substrate of 220 kDa (Kidins220), a transmembrane scaffold protein that mediates neurotrophin signaling in neurons. We found a shift from a kinase-based response in embryonic cells to a response predominantly relying on intracellular Ca2+ transients [Ca2+]i within postnatal cultures, associated with a decrease in the synthesis of full length BDNF receptor TrkB, with Kidins220 contributing to the BDNF activated kinase and [Ca2+]i pathways. Finally, Kidins220 participates in the homeostatic function of astrocytes by controlling the expression of the ATP-sensitive inward rectifier potassium channel 10 (Kir4.1) and the metabolic balance of embryonic astrocytes. Overall, our data contribute to the understanding of the complex role played by astrocytes within the central nervous system, and identify Kidins220 as a novel actor in the increasing number of pathologies characterized by astrocytic dysfunctions.

My contribution to this paper is reported in the first part of this thesis.

Kidins220/ARMS Modulates Brain Morphology and Anxiety-Like Traits in Adult Mice

Almacellas-Barbanoj A.*, Albini M.*, Satapathy A.*, Jaudon F., Michetti C., Huang H., Manago' F., Papaleo F., Benfenati F., Cesca F.

Cell Death Discovery, January 2022

* These authors contributed equally to this work

Abstract

Kinase D interacting substrate of 220 kDa (Kidins220), also known as ankyrin repeat-rich membrane spanning (ARMS), is a transmembrane scaffold protein that participates in fundamental aspects of neuronal physiology including cell survival, differentiation and synaptic plasticity. The Kidins220 constitutive knockout line displays developmental defects in the nervous and cardiovascular systems that lead to embryonic lethality, which has so far precluded the study of this protein in the adult. Moreover, Kidins220 mRNA is tightly regulated by alternative splicing, whose impact on nervous system physiology has not yet been addressed in vivo. Here, we have asked to what extent the absence of Kidins220 splicing and the selective knockout of Kidins220 impact on adult brain homeostasis. To answer this question, we used a floxed line that expresses only the full-length, non-spliced Kidins220 mRNA, and a forebrain-specific, CaMKII-Cre driven Kidins220 conditional knockout (cKO) line. Kidins220 cKO brains are characterized by enlarged ventricles in the absence of cell death, and by deficient dendritic arborisation in several cortical regions. The deletion of Kidins220 leads to behavioral changes, such as reduced anxiety-like traits linked to alterations in TrkB-BDNF signaling and sex-dependent alterations of hippocampal-dependent spatial memory. Kidins220 floxed mice present similarly enlarged brain ventricles and increased associative memory. Thus, both the absolute levels of Kidins220 expression and its splicing pattern are required for the correct brain development and related expression of behavioral phenotypes. These findings are relevant in light of the increasing evidence linking mutations in the human KIDINS220 gene to the onset to severe neurodevelopmental disorders.

My contribution to this paper is reported in the second part of this thesis.